Development of Novel pH Sensor Based on Nanoparticle Modified Electrochemical Sensing Platform

by

Irani Akhter

A thesis submitted in partial fulfillment of the requirements for the degree of
Master of Science in Chemistry

Khulna University of Engineering & Technology
Khulna 9203, Bangladesh

April 2017

Declaration

This is to certify that the thesis work entitled "Development of Novel pH Sensor Based On Nanoparticle Modified Electrochemical Sensing Platform" has been carried out by Irani Akhter in the Department of Chemistry, Khulna University of Engineering & Technology, Khulna, Bangladesh. The above thesis work has not been submitted anywhere for the award of any degree or diploma.

Signature of Supervisor

Signature of Candidate

Acknowledgements

All the admirations are for almighty Allah, who helped me in difficulties and gave me enough strength and ability to accomplish this research work.

First and foremost I would like to extend my sincere gratitude to my thesis advisor **Dr. A.B.M. Mamun Jamal**, Assistant Professor, Department of Chemistry, Khulna University of Engineering & Technology.I thank him immensely for his excellent guidance, support and valuable suggestions throughout this endeavor, which nurtured a lot of confidence in me.

I would like to thank Prof. Dr. Md. Abdul Motin, Head, the Department of Chemistry, KUET and the staff of the department for their continuous support during my thesis work.

I would like to give my special thanks to Prof. Dr. Mohammad Abu Yousuf, Department of Chemistry, KUET for his excellent support, laboratory facilities, advice and enthusiasm throughout my M.Sc. I am indeed grateful to all my dear teachers of the Department of Chemistry, KUET who triggered my interest in the subject and was my real inspiration for doing research.

I would like to thanks University Grant Commission and Khulna University of Engineering & Technology for funding my research. I sincerely thank all my labmates and friends for their sincere co-operation and encouragement.

Many thanks to Dr. Kafil M. Rajib, Tyndall National Institute, Ireland for the assistance concerning the XRD and Raman study and SEM-EDX measurement of WO_3 nanoparticles.

Finally, last but not the least I would like to thank my parents and my family members who have always been encouraging me in all aspects of life.

Irani Akhter

Abstract

In biological and environmental applications, pH is an important parameter that needs to monitor in regular basis. Conventionally, the measurement processes take a considerable amount of time involving several calibration steps and handling of fragile electrodes. In this work, we propose a new, robust and reliable way of sensing pH. The sensor has been fabricated based on tungsten oxide nanoparticle modified glassy carbon electrode (WO_3/GCE). WO_3 is a promising material for pH sensor because of its availability, stability, good morphological and structural control of the synthesized nanostructures.

In this work, hydrothermal synthesis method was used for the fabrication of WO_3 nanoparticles. For the fabrication of the pH sensor, the nanoparticles were mixed with Nafion and chitosan before drop coating onto the GCE surface. Scanning electron microscopy (SEM), x-ray diffraction (XRD), energy dispersive x-ray spectroscopy (EDX) and Raman spectroscopy were used to characterize the nanoparticle. Cyclic voltammetry (CV), zero current potentiommetry (OCP) and square wave voltammetry (SWV) were used to monitor the potential shift based on different pH in the buffer solutions. This electrochemical pH sensor showed a sensitivity of 60 $mVpH^{-1}$ and a potential drift of 2.4 – 5.0 % after three hours of continuous use. The sensor showed linearity range of pH 3 -11 and could retain 95% of its initial activity after 1 week of use. The electrode was found to respond both in the presence and absence of oxygen, further expanding the potential applications to include de-oxygenated environments. The WO_3 based sensor showed good sensitivity and long term stability, which would be a potential platform to develop a low cost pH sensor for a wider range of applications.

Contents

		PAGE
Title page		i
Declaration		ii
Certificate of Research		iii
Acknowledgement		iv
Abstract		v
Contents		vi
List of Tables		ix
List of Figures		x
CHAPTER I	Introduction	1 - 33
	1.1 General	1
	1.2 Why pH is important	2
	1.3 What is pH sensor?	3
	1.4 Types of pH sensor	4
	1.4.1 ISFET based pH sensor	4
	1.4.2 pH image sensor	4
	1.4.3 Optical fiber pH sensor	5
	1.4.4 Magnetoelestic pH sensor	5
	1.4.5 Conductimetric pH sensor	5
	1.4.6 cantilever based pH sensor	5
	1.4.7 Glass electrode pH sensor	6
	1.4.8 Potentiometric pH sensor	6
	1.5 Electrochemical sensors	6
	1.5.1 Chemically modified electrodes	8
	1.5.2 General methods of modification of electrodes	9
	1.6 Electrochemical pH sensor	13
	1.7 pH sensor for environmental application	15
	1.8 pH sensor for bio-medical application	17
	1.9 Theoretical Background	18

	1.9.1 Fundamentals of electrochemistry	18
	1.10 Various electro analytical techniques	26
	1.10.1 Cyclic voltammetry	26
	1.10.2 Square-wave voltammetry (SWV)	28
	1.11 Sensor characterization	30
	1.11.1 Scanning electron Microscopy (SEM)	30
	1.11.2 X-ray diffraction (XRD)	32
	1.12 Objectives of the present work	33
CHAPTER II	Literature review	34 - 51
	2.1 Introduction	34
	2.2 Nanoparticle based pH sensor	34
	2.3 Metal / metal oxide based pH sensor	36
	2.4 Electrodes modified with pH sensitive polymers	40
	2.5 Solid state pH sensor	42
	2.6 Potentiometric pH sensor	44
	2.7 Calibration curve	46
	2.8 Analytical performance of the pH sensor	48
CHAPTER III	Experimental	52 - 61
	3.1 Reagent and materials	52
	3.2 Equipments	52
	3.3 Electrochemical Techniques	53
	3.4 Preparation of WO_3 nanocrystal	57
	3.5 Modification of working electrode	57
	3.6 Preparation of pH solutions	58
	3.7 Standardization of the system	58
	3.8 Electrochemical pH measurement	59
	3.9 Removing Dissolved Oxygen from Solution	60
	3.10. Reproducibility and repeatability measurements	60
	3.11 Drift and stability measurements	60
	3.12 Real sample test	61

CHAPTER IV	Results and Discussion	62 - 86
	4.1 Electrochemical setup standardization	62
	4.2 Synthesis of nanoparticle and its physical characterization	65
	4.3 Sensor fabrication	68
	4.4 Electrochemical characterization of WO_3 nanoparticle modified GCE	68
	4.5 Electrochemical characterization of WO_3 nanoparticle modified AuE	69
	4.6 Electrochemical characterization of Bare GCE	72
	4.6.1 Electrochemical characterization of NiO nanoparticle NiO/GCE using SWV	74
	4.6.2 Electrochemical characterization of WO_3 / GCE using SWV	76
	4.6.3 Zero current potentiometric (OCP) sensing and analytical performance of pH sensor	79
	4.7 Electrochemical characterization of WO_3 / GCE in the presence and absence of oxygen	80
	4.8 Real sample test	81
	4.9 Repeatability and reproducibility measurements	84
	4.10 Drift and stability measurements	84
CHAPTER V	Conclusions and Recommendations	87
	References	88

LIST OF TABLES

Table No	Description	Page
2.1	List of pH sensing material	50
4.1	Electrochemical parameters obtained from voltammograms	63
4.2	Comparison of different pH sensors	86

LIST OF FIGURES

Figure No	Description	Page
1.1	pH sensor	4
1.2	Mechanism of electrochemical sensor	7
1.3	Structure of chitosan	12
1.4	Chemical structure of nafion	12
1.5	pH measurement circuit	13
1.6	Schematic representation of the electrical double layer	19
1.7	Movement of charged particles in a potential field	21
1.8	Spontaneous movement of particles	21
1.9	Movement of particles by stirring	22
1.10	Schematic Diagram of a voltammetric cell based on a three electrode system	23
1.11	Gold disk working electrode	24
1.12	Ag/Agcl reference electrode	24
1.13	Platinum electrode	25
1.14	A potentiostat with circuit diagram of a three-electrode system	26
1.15	Cyclic voltammetry input waveform	28
1.16	Typical Cyclic Voltammogram response for a reversible redox couple	28
1.17	(a) Potential form in square-wave voltammetry: Esw, potential amplitude; dE, potential step; t, duration of a single pulse. The current is sampled twice in each pulse, in the time period between two arrows at the inset; (b) resulting simulated voltammogram in square-wave voltammetry: If, forward current, Ib, backward current, Inet, net current.	30
1.18	Different types of signals produced when high-energy electron impinges on a material	31
1.19	Schematic diagram of a SEM	32
3.1	Cyclic Voltammogram response for a reversible redox couple	55

3.2	Potential form in square-wave voltammetry.	56
3.3	Schematic diagram of Modification of working electrode.	57
3.4	Electrochemical experimental setup	59
4.1	Cyclic voltammograms of ferricyanide GCE were performed at concentration of 2mM of ferricyanide 0.1 M KNO_3 as supporting electrolyte, different scan rate 20, 40, 60, 80, 100, 120, 140, 160 mV/s.	62
4.2	The anodic and the cathodic peak heights as function of the square root of the scanning rate for platinum electrode.	64
4.3	SEM images of WO_3 nanoparticles at different magnifications	66
4.4	XRD patterns of WO_3 nanoparticles	66
4.5	EDX images of WO_3 nanoparticles	67
4.6	Raman spectra of WO_3 nanoparticles	67
4.7	Schematic diagram of stepwise fabrication of the pH sensor	68
4.8	CVs detailing the effect of scan rate (60 –160) mV / s using WO_3/GCE at 0.1M PBS	69
4.9	CVs of 0.1 M different pH value in the presence of WO_3/GCE (scan rate 0 .05 mV / s)	70
4.10	SWV of 0.1 M buffer at different pH values in the presence of WO_3 / GCE (scan rate 0.05 mV / s)	71
4.11	pH sensitivity measured from pH 3 to 11 using AuE/WO_3.	71
4.12	CVs of 0.1 M buffer at different pH values on bare GCE (scan rate 0.05 mV / s)	72
4.13	SWV of 0.1 M buffer at different pH values (3-11) on bare GCE (scan rate 0 .05mV / s).	72
4.14	pH sensitivity measured from pH 3 to 11 at Bare GCE.	73
4.15	CVs of 0.1 M buffer at different pH values in the presence of NiO/GCE (scan rate .05 mV / s).	74
4.16	SWV of 0.1 M at different pH values (3-11) in presence of NiO/GCE (scan rate 0 .05 mV / s).	74
4.17	pH sensitivity measured from pH 3 to 11 using NiO /GCE	75
4.18	Cyclic voltammetry of 0.1 M buffer at different pH values (3-11)	77

	in the presence of WO_3/GCE (scan rate 0 .05 mV / s).	
4.19	SWV of 0.1 M buffer at different pH values (3-11) in the presence of WO_3/GCE (scan rate 0 .05 mV / s).	77
4.20	pH sensitivity measured with standard deviation from pH 3 to 11 using WO_3/GCE	78
4.21	Zero current potentiometry (OCP) of 0.1 M buffer at different pH values in the presence of WO_3/GCE	79
4.22	pH sensitivity measured from pH 3 to 11 using WO_3/GCE.	79
4.23	CVs showing the response of the WO_3 immobilized layer to the presence and absence of oxygen in pH 6 PBS buffer.	80
4.24	Electrochemical signal (SWV) obtained in "real" unbuffered samples for malt vinegar using WO_3/GCE.	81
4.25	Electrochemical signal (SWV) obtained in "real" unbuffered samples for malt vinegar using WO_3/GCE.	82
4.26	Electrochemical signal (OCP) obtained in "real" unbuffered samples for malt vinegar using WO_3/GCE.	82
4.27	Electrochemical signal (OCP) obtained in "real" unbuffered samples for antacid using WO_3/GCE.	83
4.28	Repeatability and reproducibility test of three WO_3 NPs pH sensor electrodes at various pH buffer solutions.	84
4.29	Electrode drift of WO_3 nanoparticle immobilized on the GCE; potential readings of pH 5, 7 and 9, signals have been taken every 30 min over period of 3 hours**.**	85

Chapter I

Introduction

1.1. General

Analytical chemistry is the science of obtaining, processing, and communicating information about the composition and structure of matter. In other words, it is the art and science of determining what matter is and how much of it exists. This is divided into two parts. First one, qualitative analysis that gives the indication of the identity of the chemical species in the sample and the second one, quantitative analysis that determines the amount of certain components in the substance.

The area of chemistry that deals with the inter conversion of electrical energy and chemical energy is called electrochemistry. The area of analytical chemistry that includes the analytical methods which study an analyte by measuring the potential (volts) and / or current (amperes) in an electrochemical cell containing the analyte is called electro analytical chemistry. These methods are divided into several categories like potentiometry, coulometry, voltammetry etc [1].

Today, electroanalytical chemistry can play a vital role in nanotechnologies. Nanotechnologies are now poised to revolution the electronic, chemical, industries and biomedical. There are many interesting areas in nanotechnology [2, 3]. One of the most important aspects in this field is the preparation and development of nonmaterial's, such as nanoparticles [4–8]. Nanoparticles can be made with different materials as small as 1 nm. Nanoparticles are useful in biochemical analysis, such as in sensors and biomarkers. In the past twenty years, the development of studies on chemical sensors and biosensors was very rapid [9]. One of the most widely studied sensors, the pH sensor, was focused on because, in biological and environmental applications, pH is an important parameter that needs to monitor regularly [10]. Conventionally, the measurement processes take a considerable amount of time involving several calibration steps and handling of fragile electrodes. Various metal oxide based potentiometric pH sensors have drawn much attention in past decades due to their stability against dissolutions, and independence from cationic

interferences [11, 12]. Among the oxide materials being studied, WO_3 is found to be a promising material for pH sensor because of its availability, stability, good morphological and structural control of the synthesized nanostructures, and reversible change of conductivity, high sensitivity, selectivity, biocompatibility and act as good catalyst [13]. In 1987, Wrighton et al. [14] reported WO_3 based pH sensor, where a micro electrochemical transistor was operating either electrically or chemically by changing the gate voltage or the pH of the solution respectively. Nevertheless the use of WO_3 with high surface area was mainly reported for gas sensor applications. Recently Lidia et al. [15] has reported WO_3 based pH sensor, where gold electrode has been used as working electrode with a linearity of pH 5-9, sensitivity of 56 mV/pH. Also, in 2013, Jamal et al. [16] has reported gold nanowire array based pH sensor with better sensitivity compare to the GCE.

In this work, a facile, stable and sensitive pH sensor is fabricated by synthesizing WO_3 nanoparticle using hydrothermal method, and drop cast the nanoparticle along with chitosan and nafion onto the GCE. The sensing abilities of the electrode were investigated in terms of static and dynamic properties such as calibration, sensitivity, time response, stability as well as oxygenated and deoxygenated environment. This method allowed the fabrication suitable for mass production and cost effective; and will open up the door to fabricate a miniaturized carbon based sensing platform which would be suitable both in clinical and environmental applications.

1.2. Why pH is important

pH has great importance in laboratory measurements because a lot of chemical and biological processes are dependent on pH.

- It is essential to measure pH to find the chemical characteristics of a substance. Both the speed or rate of chemical reactions and the solubility of chemicals or biomolecules are dependent on pH. So controlling pH is very important in order to optimize the desired reaction or to prevent unwanted reactions.
- The pH value of rivers, lakes and oceans depends on the type of plants and animals living there. The wastewater from factories changes the pH value of water so we can detect the presence of dangerous chemicals inside water.

- Process industries deals with pH measurements like food industries, drugs, textiles, semiconductors, cements etc.

What is pH

pH is the combination of two words, p for power and H for hydrogen [17]. In an aqueous solution, the equilibrium exists between water, alkali (OH^-) and acid H^+

$$H_2O \leftrightarrow H^+ + OH^-$$

pH is the acidity or basicity of the material. The pH value can be written as mathematically.

$$pH= -\log\alpha\ H^+$$

so the pH value is the negative logarithm activity of hydrogen ions [17]. pH is used to mention the degree of basicity or acidity of an aqueous solution at a given temperature. The term acidity shows that the pH reflects the amount of hydrogen ions and not the concentration of hydrogen ions. Normally the pH range is from 1-14. If the pH value is from 1-6 then the solution is acidic, if the pH value is 7 then the solution is neutral and if the pH value is from 8-14 then the solution is basic.

1.3. What is pH sensor

pH is the unit of measure for the acidity of a solution in a process. Product quality depends on pH and Emerson Process Management has a sensor for your needs, whether it is a general application, poisoning, coating, high temperature, low conductivity, or sanitary. pH sensors measure the level of pH in sample solutions by measuring the activity of the hydrogen ions in the solutions. This activity is compared to pure water (a neutral solution) using a pH scale of 0 to 14 to determine the acidity or alkalinity of the sample solutions.

Figure 1.1: pH sensor

1.4. Types of pH sensor

1.4.1. ISFET based pH sensors

ISFET stands for ion sensitive field effect transistor. ISFET sensor is based on new technology and is an alternative to glass electrode. The working principle is based on the fact that the drain current is an indicator of pH in the solution in which the ISFET is immersed. ISFET is glass-less and can be small sized due to its fabrication technology and is inexpensive device as compared to glass electrode. It can be battery powered and pocket sized pH measurement system [17]. ISFET devices are compatible with CMOS processes and can be realized with microelectronic technology. ISFET devices are used to measure the wide range of pH from basic to acidic solutions. ISFET devices in general use Si_3N_4 and Al_2O_3 as gate insulators.

1.4.2. pH image sensors

pH image sensors are used in various real time and chemical industrial applications. They are used to take two dimensional distributions and dynamic images of chemical variations. pH image sensor work on the charge transfer technique. CMOS (Complementary metal oxide semiconductor) circuit process technology can be used to fabricate pH image sensors. pH image sensors may have great importance in medical, biological and chemical industrial applications.

1.4.3. Optical fiber pH sensors

Optical fiber sensors have many advantages over other glass electrode methods for the measurement of pH like they have fast response and effects of ionic concentrations are negligible. Optical fiber pH sensors are based on color change principle of sensing polymer.

1.4.4. Magnetoelestic pH sensors

Magnetoelastic pH sensor is based on the principle of an efficient conversion between magnetic and elastic energies and vice versa. By changing the electric field in a coil, a magnetic field is induced, which cause vibration in a magnetoelastic ribbon like senor. Magnetoelastic pH sensor consists of two coils (drive coil and pickup coil), magnetoelastic substrate, pH sensitive material deposited on substrate [18].

1.4.5. Conductimetric pH sensors

A conductimetric pH sensor is based on the measurement of the conductivity of a pH-responsive hydrogel and other materials. It is constructed by coating planar interdigitated electrode arrays with a photolithographically patterned hydrogel membrane [19]. The hydrogel sensing layer swells or shrinks to a hydration determined by the pH of a solution in which it is immersed. Sensing layer must respond to analyte of interest and produce a measureable change in the electrical properties.

1.4.6. Cantilever based pH sensors

Cantilever based pH sensor is a useful technique to measure the pH of aqueous solution. It is based on a cantilever attached with a piezoresistive. Aqueous solution enters from inlet tube and cause the swelling or shrinking of the hydrogel depending upon the pH. When the pH of the solution changes, hydrogel swells or shrinks which cause the deformation of the cantilever. So by changing the shape of hydrogel, cantilever bend and this change is converted into the voltage with the help of piezoresistive. In this way the pH of the aqueous solution is measured.

1.4.7. Glass electrode pH sensors

pH of the solution is very difficult to measure directly. So the measurement of pH is done by comparing the potential of the solutions of known H ions with the solution of unknown H ions. The solution with known H^+ ions is called reference solution. The potential between these two solutions is measured by using two cells. One is called reference half cell and the other is called sensing half cell.

1.4.8. Potentiometric pH sensors

In potentiometric sensors the signal is measured as potential difference (voltage) between the working electrode and the reference electrode. The working electrode's potential depends on the concentration of the analyte in the gas or solution phase. The reference electrode is needed to provide a defined reference potential. Potentiometric pH sensors consist of for example Pt/PtO_2, W/W_2O_3, Pb/PbO_2, Ir/IrO_2 etc [17]. pH sensitive material is applied on the working electrode and when the voltage is changed between the working electrode and reference electrode, that potential difference is measured. In this way the change in the pH can be measured. Theses sensors are very efficient over a wide pH range, at high temperature and pressure. The response time of these sensors are also fast as compared to other sensors.

1.5. Electrochemical Sensors

Electrochemical Sensors are the devices, which are composed of an active sensing material with a signal transducer. The role of these two important components in sensors is to transmit the signal without any amplification from a selective compound or from a change in a reaction. These devices produce any one of the signals as electrical, thermal or optical output signals which could be converted into digital signals for further processing. One of the ways of classifying sensors is done based on these output signals. Among these, electrochemical sensors have more advantage over the others because; in these, the electrodes can sense the materials which are present within the host without doing any damage to the host system. On the other hand, sensors can be broadly classified in to two categories as chemical sensors and biosensors. The biosensors can be defined in terms of

sensing aspects, where these sensors can sense biochemical compounds such as biological proteins, nucleotides and even tissues [20].

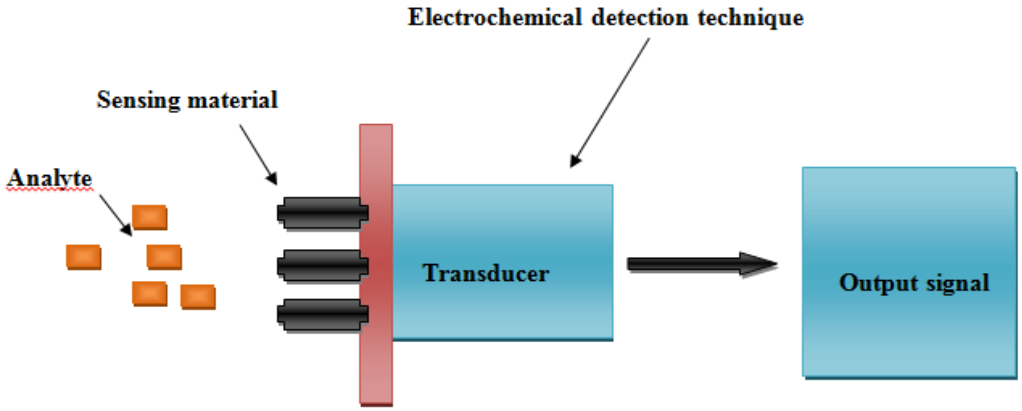

Figure 1.2: Mechanism of electrochemical sensor.

Depending on the exact mode of signal transduction, electrochemical sensors can use a range of modes of detection such as potentiometric, voltammetric and conductimetric. Each principle requires a specific design of the electrochemical cell. Potentiometric sensors are very attractive for field operations because of their high selectivity, simplicity and low cost. They are, however, less sensitive and often slower than their voltammetric counterparts. Examples of transduction techniques include:

- ***Potentiometric*** – The measurement of the potential at zero current. The potential is proportional to the logarithm of the concentration of the substance being determined.

- ***Voltammetric*** **–** Increasing or decrease the potential that is applied to a cell until the oxidation or reduction of the analyte occurs. This generates a rise in current that is proportional to the concentration of the electroactive potential. Once the desired stable oxidation/reduction potential is known, stepping the potential directly to that value and observing the current is known as amperometry.

- ***Conductiometric*** – Observing changes in electrical conductivity of the solution. [21]

The selection and development of an active material is a challenge. The active sensing materials may be of any kind as whichever acts as a catalyst for sensing a particular analyte or a set of analyte. The recent development in the nanotechnology has paved the way for large number of new materials and devices of desirable properties which have useful functions for numerous electrochemical sensor and biosensor applications [22].

Basically by creating nanostructure, it is possible to control the fundamental properties of materials even without changing their chemical composition. In this way the attractive world of low dimensional systems, together with the current tendencies on the fabrication of functional nanostructured arrays could play a key role in the new trends of nanotechnology [23-25].

Further, the nanostructures can be used for both efficient transport of electrons and optical excitation, and these two factors make them critical to the function and integration of nanoscale devices [26-28]. In fact, nano systems are the smallest dimension structures that can be used for efficient transport of electrons and are thus critical to the function and integration of these nanoscale devices.

1.5.1. Chemically modified electrodes

Immobilisation of chemical microstrutures onto electrode surfaces has been a major growth area in electrochemistry in recent years. Chemically modified electrodes (CME) result from a deliberate immobilization of a modifier agent onto the electrode surface though chemical reactions, chemisorption, composite formation or polymer coating. Compared to conventional electrodes, greater control of electrode characteristics and reactivity is achieved by surface modificaton, since the immobilization transfers the physicochemical properties of the modifier to the electrode surface. The interest in this area is motivated by the many potential applications of such a system. Examples include development of electrocatalytic systems with high chemical selectivity and activity, coating of semiconducting electrodes with photo sensitizing and anticorrosive properties,

electrochromic displays, micro electrochemical devices for the field of molecular electronics and electrochemical sensors. The main benefits to analytical applications include acceleration of electron transfer reactions, preferential accumulation, or selective membrane permeation and interferent exclusion [29].

One of the common approaches for incorporating a modifier onto the surface has been coverage with an appropriate polymer film. Most polymers are applied to electrode surfaces by a combination of adsorptive attraction and low solubility in the electrolyte solution, using preformed polymers or electrochemical polymerisation. An early approach in the use of pre-formed polymers was their use as anchoring groups for coordinating metal complexes to pyrolytic graphite electrodes [30]. Examples include poly (4-vinylpyridine) (PVP), poly (vinylferrocene) (PVF), poly (p-nitro styrene), metal polymers and others, used as redox monomers in polymer modification schemes after synthetic procedures [31]. The advantages of preconcentrating CME were obtained by coating the electrode surface with a thin film of an ion exchange polymer [32]. The strategy of coating an anion exchange polymer onto an electrode surface is similar to the stripping voltammetric method principle. These techniques solid electrodes coated with a thin layer of an ion exchange polymer, which allows the quick pre-concentration and simultaneous amperometric detection of an ion redox analyte.

Differents types of inorganic films, such as metal oxide, clay, zeolite, and metal ferrocyanide, can also be formed on electrode surfaces. These films are of interest because they frequently show well-defined structures, are thermally and chemically stable, and are usually inexpensive and readily available [33].

1.5.2. General methods of modification of electrodes

The concept of chemically modified electrodes (CMEs) is one of the exciting developments in the field of electroanalytical chemistry. Many different strategies have been employed for the modification of the electrode surface. The motivations behind the modifications of the electrode surface are: (i) improved electrocatalysis, (ii) freedom from surface fouling and (iii) prevention of undesirable reactions competing kinetically with the desired electrode process [34]. The increasing demand for it has led to the development of

a rapid, simple and non-separation method for the simultaneous determination of isomers where the CMEs have emerged as an efficient and versatile approach, and have attracted considerable attention over the past decades due to its advantages in terms of reduced costs, automatic and fast analysis, high sensitivity and selectivity [35-39]. There are numerous techniques that may be used to modify electrode surfaces. Among various CMEs, polymer-modified electrodes (PMEs) are promising approach to determination. Some modification processes are-

Covalent Bonding: This method employs a linking agent (e.g. an organosilane) to covalently attach one of several monomolecular layers of the chemical modifier to the electrode surface [37].

Drop-Dry Coating (or solvent evaporation): A few drops of the polymer, modifier or catalyst solution are dropped onto the electrode surface and left to stand to allow the solvent to dry out.

Dry-Dip Coating: The electrode is immersed in a solution of the polymer, modifier or catalyst for a period sufficient for spontaneous film formation to occur by adsorption. The electrode is then removed from solution and the solvent is allowed to dry out [35].

Composite: The chemical modifier is simply mixed with an electrode matrix material, as in the case of an electron-transfer mediator (electro catalyst) combined with the carbon particles (plus binder) of a carbon paste electrode. Alternatively, intercalation matrices such as certain Langmuir-Blodgett films, zeolites, clays and molecular sieves can be used to contain the modifier [39].

Spin-Coating (or Spin-Casting): also called spin casting, a droplet of a dilute solution of the polymer is applied to the surface of a rotating electrode. Excess solution is spun off the surface and the remaining thin polymer film is allowed to dry. Multiple layers are applied in the same way until the desired thickness is obtained. This procedure typically produces pinhole-free thin films for example; oxide xerogel film electrodes prepared by spin-coating a viscous gel on an indium oxide substrate [35].

Electrodeposition: In this technique the electrode is immersed in a concentrated solution ($\sim 10^{-3}$ $molL^{-1}$) of the polymer, modifier or catalyst followed by repetitive voltammetry scans. The first and second scans are similar, subsequent scans decrease with the peak current. For example, electrochemical deposition of poly (o-toluidine) on activated carbon fiber [39].

Electropolymerisation: A solution of monomer is oxidized or reduced to an activated form that polymerizes to form a polymer film directly on the electrode surface. This procedure results in few pinholes since polymerization would be accentuated at exposed (pinhole) sites at the electrode surface. Unless the polymer film itself is redox active, electrode passivation occurs and further film growth is prevented.

In this technique the electrode is immersed in a polymer, modifier or catalyst solution and layers of the electropolimerized material builds on the electrode surface. Generally, the peak current increases with each voltammetry scan such that there is a noticeable difference between the first and final scans indicating the presence of the polymerized material. For example, electro polymerization of aniline on platinum electrode perturbations.

Chitosan: Chitosan is a derivative of chitin, which is one of the world's most plentiful organic resources and is derived from the shells of crustaceans. It is a linear polyaminosaccharaide composed of randomly distributed β-(1, 4)-linked D-glucosamine and N-acetyl-D-glucosamine groups. Due to its structure, chitosan possesses good adhesion and cheapness properties; therefore it has been used as an immobilization matrix. Although it has poor electrical conductivity, but it usually has been combined with carbon nanotubes, redox mediator and metal nanoparticles [40].

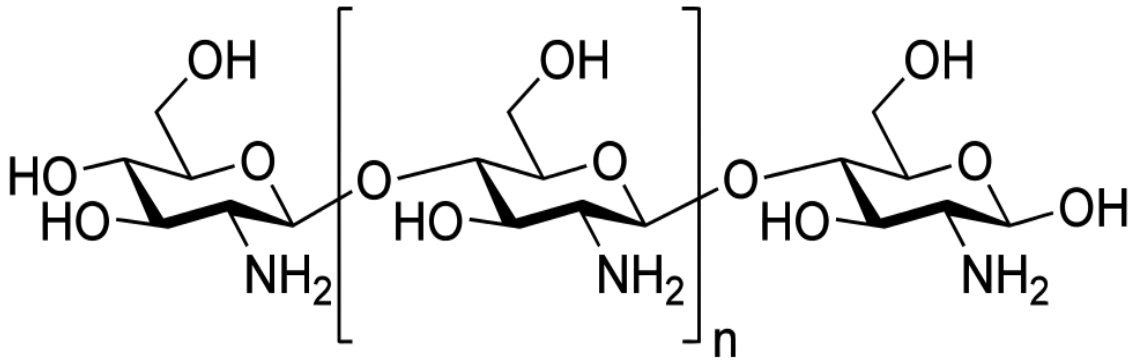

Figure 1.3: Structure of Chitosan.

Chitosan is soluble in aqueous acidic media at pH < 6.5. When dissolved, it bears a high positive charge on its amino groups. Chitosan has gel-forming properties as a result of its ability to adhere to negatively charged surfaces and aggregate polyanionic compounds.

Nafion: Nafion is a sulfonatedtetrafuorethylene copolymer. Because of its tetrafuorethylene (Teflon) backbone, Nafion possesses excellent thermal and mechanical stability. The combination with sulfonic acid group results in its highly cationconductive property. Nafion membrane coated on the electrodes can prevent interference mainly via two mechanisms: firstly its complex polymer structure (with small pores) only allows small molecules to pass through; and secondly its positive charge limits the diffusion of anionic components such as AA across the membrane. To obtain a Nafion coated surface, the electrodes are dipped in Nafion polymer solution and then dried.

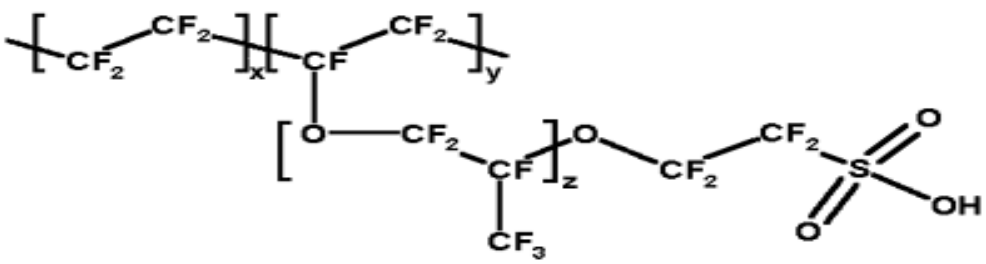

Figure 1.4: Structure of nafion

Nafion can be used to generate composite films, coat electrodes, or repair damaged membranes [41]. Nafion especially interesting is its demonstration in biocompatibility.

1.6. Electrochemical pH sensor

A pH sensor consists of two primary parts:

• **Measuring electrode:** The measuring electrode is sometimes called the glass electrode, and is also referred to as a membrane or active electrode.
• **Reference electrode:** The reference electrode is also referred to as a standard electrode.

The pH measurement is comprised of two half-cell, or electrode, potentials. One half-cell is the pH sensitive glass measuring electrode and the other is the reference electrode. Just as the two half-cell potentials of a battery are required to complete a circuit so does a pH sensor.
The mathematical expression for this is:

$$E = E_m - E_r$$

where:
Em = the electrode potential of the measuring electrode
Er = the electrode potential of the reference electrode

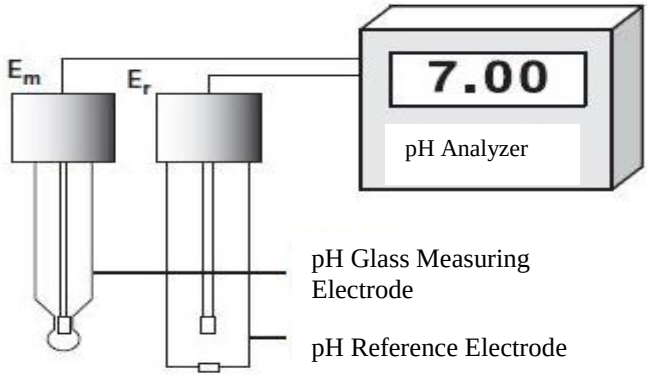

Figure 1.5: pH Measurement Circuit

This type of measurement, in millivolts, is called a potentiometric measurement. Since voltage-measuring devices only determine differences in potentials, there is no method for determining the potential of a single electrode. A galvanic measurement circuit is formed by connecting the measuring electrode (half-cell potential) and the reference electrode (half-cell potential) to the signal input of the measuring device. At the reference electrode, there is a solid/solution interface, where a chemical reaction takes place. This enables an electrical current to flow through the measuring device, the pH meter, which allows the reading to be made. Since the current that passes through the half-cells and the solution being measured is extremely small, the pH meter must have high internal impedance, so it does not "drag down" the millivolt potential produced by the electrodes. This low current flow ensures that the chemical characteristic of the solution being measured remains unaltered.

A galvanic potential is formed when charge exchanges occur at the phase boundaries of the glass measuring electrode. In effect, the pH sensor assembly forms a galvanic cell using two metal conductors lead wires of the measuring and reference electrodes interconnected through their respective electrolyte solutions and the media. Since phase boundaries cannot be measured individually and there are always more than two phase boundaries present, the pH meter measures the overall potential. The overall potentialiscomprised of the following elements:

• Metal lead-out wire of the measuring electrode
• Electrolyte of the measuring electrode
• Diffusion potentials at solid/solution interfaces
• Electrolyte of the reference electrode
• Metal lead-out wire of the reference electrode

The measuring and reference electrodes can be in one of two forms: two physically separate electrodes, known as an electrode pair; or the electrodes can be joined together in a single glass body assembly known as a combination electrode. The electrode pair and combination electrode styles originated many years ago and continue to be widely used today. In the 1970s, a different style pH sensor was developed and patented specifically for continuous on-line measurement applications. This pH sensor uses a differential electrode technique that employs two pH glass measuring electrodes. One electrode is used as the active or measuring electrode, and the other is used as part of a reference assembly. The reference assembly consists of a pH glass measuring electrode immersed in a 7 pH buffer

solution which is mechanically isolated from the solution being measured by a double junction "salt bridge". These two half-cell potentials are then referenced to a third ground electrode. The differential electrode technique is expressed as:

$$E_{out} = [(E_m - E_g) - (E_r - E_g)]$$

where:
Em = measuring electrode voltage
Er = reference electrode assembly voltage
Eg = solution ground electrode voltage
After canceling the Eg term:

Other major components of the differential pH sensor include the sensor cable, a temperature compensation device, electrolyte solutions, and reference junctions. Based on field-proven results, the differential electrode technique has shown marked advantages over conventional electrode pairs and combination electrodes. The double junction salt bridge (part of the reference assembly) makes it extremely difficult for an appreciable amount of the solution being measured to migrate into the inner chamber. Since the inner chamber is filled with a buffer, a 100 to 1 dilution would only represent a change in measured pH of 0.05 pH units. Similar dilutions to the conventional reference electrode used in electrode pairs or combination electrodes could cause shifts of up to 2.0 pH units.
Another advantage of the differential electrode technique is the third "ground electrode." Since ground loop currents will pass through only this electrode, and not through the reference electrode, the overall pH signal output is unaffected by the ground loop potential.

1.7. pH sensor for environmental application

Keeping the water in our lakes, rivers, and streams clean requires monitoring of water quality at many points as it gradually makes its way from its source to our oceans. Over the years ever increasing environmental concerns and regulations have heightened the need for increased diligence and tighter restrictions on wastewater quality. Control of water pollution was once concerned mainly with treating wastewater before it was discharged from a manufacturing facility into the nation's waterways. Today, in many cases, there are

restrictions on wastewater that is discharged to city sewer systems or to other publicly owned treatment facilities. Many jurisdictions even restrict or regulate the runoff of storm water affecting not only industrial and commercial land, but also residential properties as well.

In its simplest form, water pollution management requires impoundment of storm water runoff for a special field period of time before being discharged. Normally, a few simple tests such as pH and suspended solids must be checked to verify compliance before release. If water is used in any way prior to discharge, then the monitoring requirements can expand significantly. For example, if the water is used for once-through cooling, testing may include temperature, pH, total dissolved solids (TDS), chemical oxygen demand (COD), and biochemical oxygen demand (BOD), to name a few.

Once water is used in a process, some form of treatment is often required before it can be discharged to a public waterway. If wastewater is discharged to a city sewer or publicly owned facility, and treatment is required, the quality is often measured and the cost is based not only on the quantity discharged, but also the amount of treatment required. As a minimum requirement suspended solids must be removed. Such removal is often accomplished by filtering or using clarifiers. Monitoring consists of measuring total suspended solids (TSS) or turbidity.

If inorganic materials have been introduced into the water, their concentration must be reduced to an acceptable level. Inorganics, such as heavy metals, typically are removed by raising the pH to form insoluble metal oxides or metal hydroxides. The precipitated contaminants are filtered or settled out. Afterward, the pH must be adjusted back into a "normal" range, which often requires continuous monitoring of pH.

Organic materials by far require the most extensive treatment. Many different methods have been devised to convert soluble organic compounds into insoluble inorganic matter. Most of these involve some form of biological oxidation treatment. Bacteria are used to metabolize the organic materials into carbon dioxide and solids, which can be easily removed. To insure that these processes work smoothly and efficiently requires regular monitoring of the health of the biological organisms. The level of food (organic material), nutrients (nitrogen and phosphorous), dissolved oxygen, and pH are some of the

parameters that must be controlled. After bio-oxidation the wastewater is filtered or clarified. Often the final effluent is treated with an oxidizing compound such as chlorine to kill any remaining bacterial agents, but any excess oxidant normally must be removed prior to discharge. Oxidation Reduction Potential (ORP)/Redox is ideal for monitoring the level of oxidants before and after removal. The final effluent stream must be monitored to make sure it meets all regulatory requirements.

The monitoring of wastewater pollution does not end there. Scientists are continuously testing water in streams, ground water, lakes, lagoons, and other bodies of water to determine if and what effects any remaining contamination is having on the receiving waters and its associated aquatic life. Measurements may include pH, conductivity, TDS, temperature, dissolved oxygen, TSS and organic levels (COD and BOD).

Environmental testing is not limited to monitoring of wastewater systems. Control of air emissions often includes gas-cleaning systems that involve the use of water. Wet scrubbers and wet electrostatic precipitators are included in this group. A flue gas desulfurization (FGD) system is one type of wet scrubber that uses slurry of lime, limestone, or other caustic material to react with sulfur compounds in the flue gas. The key to reliable operation of these units is proper monitoring of solids levels and pH. After use, the water in these systems must be treated or added to other wastewater from the plant, where it is treated by one of the methods previously discussed.

With proper monitoring, systems that maintain cleaner air and water can be operated efficiently and effectively. Such operation will go a long way toward maintaining a cleaner environment for us and future generations.

1.8. pH sensor for bio-medical applications:

In biomedical field, main applications of pH sensor are as follows:

1. Detecting the information of clinical chemistry. In the field of medical clinic and basic research, the biology's information needs to be detected to ensure the present state of given biology. For example, before operating on a patient, a doctor needs to know the pH in the body. Under this condition, clinic thermometer and pH sensor has to be employed to help doctor quickly detect pH in the body.

2. Continuously monitoring some parameters of biology outside and inside. In biomedical field, heart pH has to be monitored continuously by heart pH sensor for a few days after operation.

3. Control. In medicine, people usually utilize some parameter detected by biomedical sensor to control or adjust physiological course of body. In the food industry, biomedical sensor could be utilized to measure some enzyme and its concentration to control the process of fabricating food and to analyze the nutritional ingredient of food. Of course, biomedical sensor such as P^H sensor could be also employed to detect our atmosphere and condition to improve our living situation.

1.9. Theoretical Background

1.9.1. Fundamentals of Electrochemistry

Faradic currents: Faradic current is the sum of all type of currents that are generated due to the electrochemical reaction of analyte in the cell. It is called faradic because it obeys faradays laws of electrolysis. Examples of faradic currents include diffusion current which is the term of interest in polarographic analysis. Kinetic currents are part of the faradic current where it should be clear that reactions should be rapid but of lower rate than the diffusion of the analyte. Kinetic currents are sensitive to changes in temperature with just small contribution to the faradic current. Most of the faradic current thus originates from the diffusion current.

Non Faradic Currents: These do not obey faraday's laws of electrolysis and are thus of no analytical value. The most important contribution to non-faradic currents originates from what is called capacitive current. This capacitive current results from the double layer which is formed between the charged mercury drop and the counter ions at the solution interface. Another contribution comes from migration current which results from electrostatic attraction of analyte ions by the oppositely charged mercury drop. Addition of supporting electrolyte of enough concentration will make this term close to zero.

Charging currents and the Electrical Double Layer: The application of a potential to the electrode surface causes ions near the electrode surface to migrate towards or away from the electrode depending on the respective charge of the electrode and the ions. This forms an electrical double layer, comprised of the electrical charge at the surface of the electrode and the charge of the ions in the solution near the electrode. This double layer leads to the generation of a non-faradaic charging current. Whenever a charged solid surface is placed in any solution, the ions, carrying charge opposite to that carried by the surface, cluster around the solid surface. These sheet of ionic charge adjacent to the charged solid surface and the charged surface constitute a double layer. The electrical double layer is an array of charged particles and orientated dipoles. It is composed of two layers; the layer closest to the electrode is known as the inner Helmholtz plane (IHP) and the outer Helmholtz plane (OHP) (Figure 1.6). The planes were discovered by Hermann von Helmholtz in 1853. The IHP is composed of solvent molecules and specifically adsorbed ions, whilst the OHP represents the imagined out er layer closest to the electrode that passes through the centre of solvated ions, but is separated by the molecules at the IHP. These layers are both held at the surface of the electrode. The behavior of the interface between the electrode and the solution is similar to that of a capacitor.

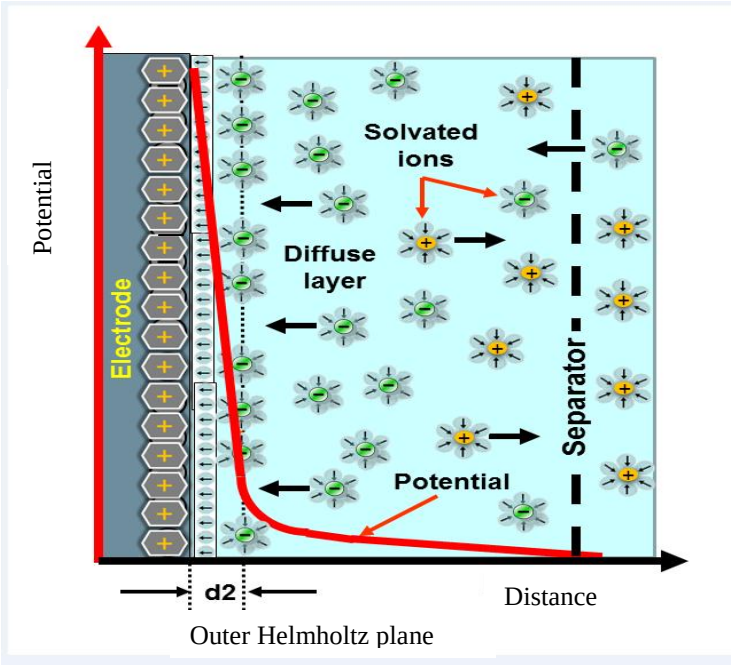

Figure 1.6: Schematic representation of the electrical double layer [42].

Beyond the double layer, is a diffuse layer of scattered ions that extent into the bulk solution. These ions are ordered relative to the columbic forces acting upon them and the random motion of the solution by thermal motion. The balance of the electrostatic forces on ions at the surface of the electrode, which are repelled or attracted dependent on their charge, is counterbalanced by the random motion of the diffuse layer. This causes a non-uniform distribution of ions near the electrode surface. As a result, the field strength of the potential applied to the electrode diminishes rapidly, thereby causing the double layer to be extremely thin at 10 – 20 nanometers in thickness. It is also essential to use a high electrolyte concentration, typically a 100 fold greater than that of the analyte, as this concentrates the charge at the Helmholtz planes, therefore ensuring that diffusion is the dominant mechanism for mass transport [43].

Mass transfer process in voltammetry: The movement of the electro-active substance through solution is called mass transfer at the electrode surface. In electrochemical systems, three modes of mass transport are generally considered which a substance may be carried to the electrode surface from bulk solution including diffusion, convection and migration. Any of these or more than one might be operating in a given experiment which is depended on the experimental conditions.

In general, there are three types of mass transfer processes:

- Migration
- Diffusion
- Convection

Migration: Migration is the movement of ions through a solution as a result of electrostatic attraction between the ions and the electrodes. It is the primary cause of mass transfer in the bulk of the solution in a cell. This motion of charged particle through solution, induced by the charges on the electrodes is called migration. This charge movement constitutes a current. This current is called migration current. The larger the number of different kinds of ions in a given solution, the smaller is the fraction of the total charge that is carried by a particular species. Electrolysis is carried out with a large excess of inert electrolyte in the solution so the current of electrons through the external circuit

can be balanced by the passage of ions through the solution between the electrodes, and a minimal amount of the electroactive species will be transported by migration. Migration is the movement of charged species due to a potential gradient. In voltammetric experiments, migration is undesirable but can be eliminated by the addition of a large excess of supporting electrolytes in the electrolysis solution. The effect of migration is applied zero by a factor of fifty to hundred ions excess of an inert supporting electrolyte.

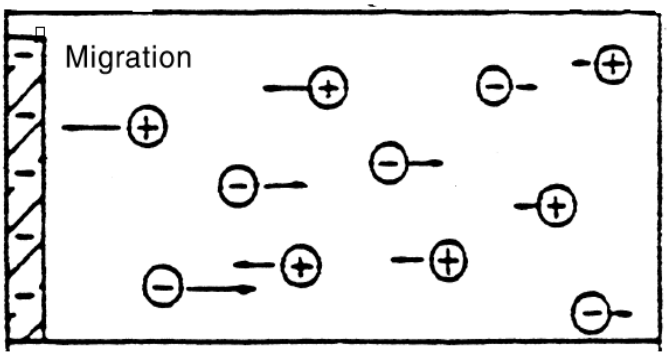

Figure 1.7: Movement of charged particles in a potential field [43].

Diffusion: Diffusion refers to the process by which molecules intermingle as a result of their kinetic energy of random motion. Whereas a concentration difference between two regions of a solution, ions or molecules move from the more concentrated region to the dilute and leads to a disappearance of the concentration difference.

The one kind of mode of mass transfer is diffusion to an electrode surface in an electrochemical cell. The rate of diffusion is directly proportional to the concentration difference. When the potential is applied, the cations are reduced at the electrode surface and the concentration is decreased at the surface film. Hence a concentration gradient is produced. Finally, the result is that the rates of diffusion current become larger.

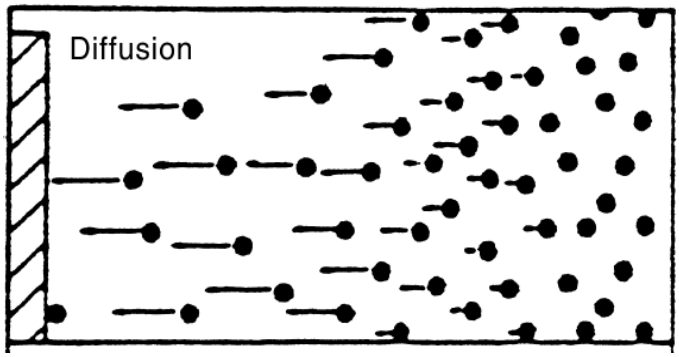

Figure 1.8: Spontaneous movement of particles [43].

Convection: By mechanical way reactants can also be transferred to or from an electrode. Thus forced convection is the movement of a substance through solution by stirring or agitation. This will tend to decrease the thickness of the diffuse layer at an electrode surface and thus decrease concentration polarization. Natural convection resulting from temperature or density differences also contributes to the transport of species to and from the electrode. At the same time a type of current is produced. This current is called convection current. Removing the stirring and heating can eliminate this current. Convection is a far more efficient means of mass transport than diffusion.

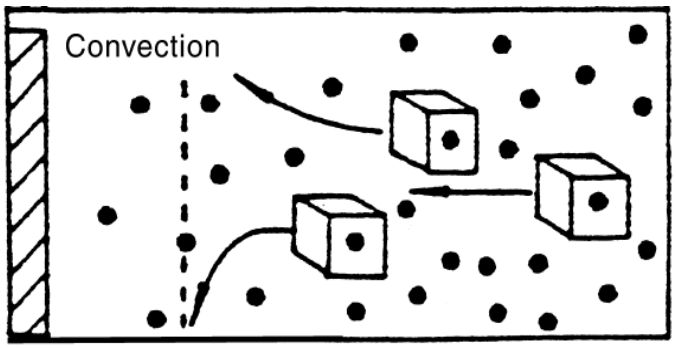

Figure 1.9 : Movement of particles by stirring [43].

Electrochemical setup

Electrochemical Cell: An electrochemical cell is a device that capable of either generating electrical energy from chemical reaction or facilitating chemical reactions through the

introduction of electrical energy. An electrochemical cell consists two half-cells. Each half-cell consists of an electrode and an analyte. An electrode is an electrical conductor used to make contact with a non-metallic part of a circuit (eg. a semiconductor, an electrolyte or a vacuum).An electrolyte is a substance that ionizes when dissolved in suitable ionizing solvent. This can conduct electricity in solution. This can be organic, inorganic or organometallic compounds.

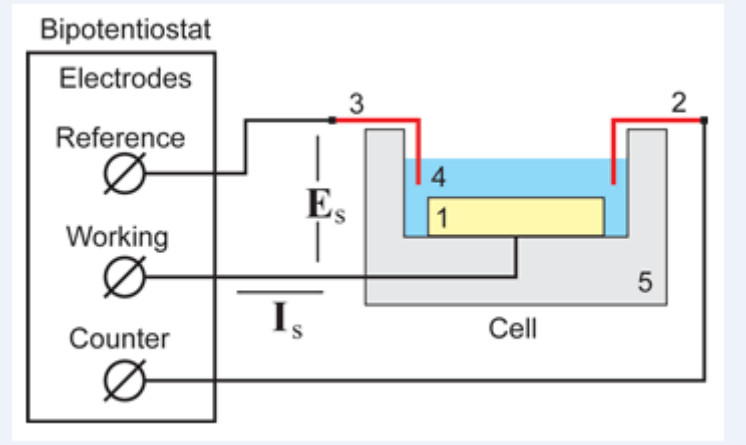

Figure 1.10: Schematic Diagram of a voltammetric cell based on a three electrode system. CE: counter electrode, WE: Working electrode, RE: Reference electrode. This is an example of a three electrode cell.

Electrodes: An electrode is an electrical conductor used to make contact with a nonmetallic part of a circuit (e.g. a semiconductor, an electrolyte or a vacuum). Types of electrode

- Working electrode
- Reference electrode
- Counter electrode

Working Electrode (WE): Working electrode (WE) is one which electrochemical reaction occurs. The working electrode makes contact with the analyte and transfer charge to and from the analyte. The working electrode must be made of a material that is stable in the electrolyte medium utilized during the experiment, e.g.: carbon. This is to ensure that the electrode does not corrode or become fouled, thereby altering the surface area, and to prevent other compounds reducing in the potential range of interest. Working electrodes

should have high surface reproducibility with a uniform distribution of potential across the surface to prevent IR drop. The background current within the potential region of interest should be low. The cost, availability and toxicity of the material should also be considered.

Figure 1.11: gold disk working electrode.

Reference Electrode: A reference electrode acts as a half-cell which has a stable and accurately maintained potential which is used a reference for the measurement of voltage applied by the counter electrode (CE). It is potentiometric and thus has zero current flowing through it. The potentiostat compensates if a difference in voltage is detected between the AE and WE and adjusts the output accordingly until the difference is zero, this action is known as feedback [44]. An example of a commonly used reference electrode the silver-silver chloride (Ag/AgCl). For applications such as chromo amperometry where small currents are flowing for short time periods, two electrode systems may be used, where the counter electrode assumes the role of RE and WE. Since current flowing through the reference electrode may alter its stability over time, three electrode systems with a counter electrode are often utilized in experimental situations, and for square-wave voltammetric applications over prolonged time periods.

Figure 1.12: Ag/AgCl reference electrode

Counter Electrode: It is also called auxiliary electrode, is used to balance the electric current that is expected to flow through the working electrode. The CE is composed of an inert material such as carbon or platinum.

Figure 1.13: Platinum electrode [45].

Potentiostat: The instrument used to control the potential difference applied across the electrochemical cell is called a potentiostat. A potentiostat adjusts the voltage difference between the anode and the cathode in order to maintain a constant working electrode potential. A potential is applied to the working electrode, resulting in a flow of charge towards the counter electrode. A potential drop (iR) is caused by the electrolyte conductivity, the distance between the electrodes, the magnitude of the current and resistance across the electrode material. If the iR drop is uncompensated, the reaction will

no longer operate at the desired potential, and the reaction may cease. The reference electrode monitors the potential at the working electrode and feeds the value back to the opamp. If a difference in potential is observed between the RE and WE, the potential applied to the CE is altered to compensate. A second op-amp is used as a current-voltage converter to measure the flow of current, with a resistor used to output the voltage per unit current.

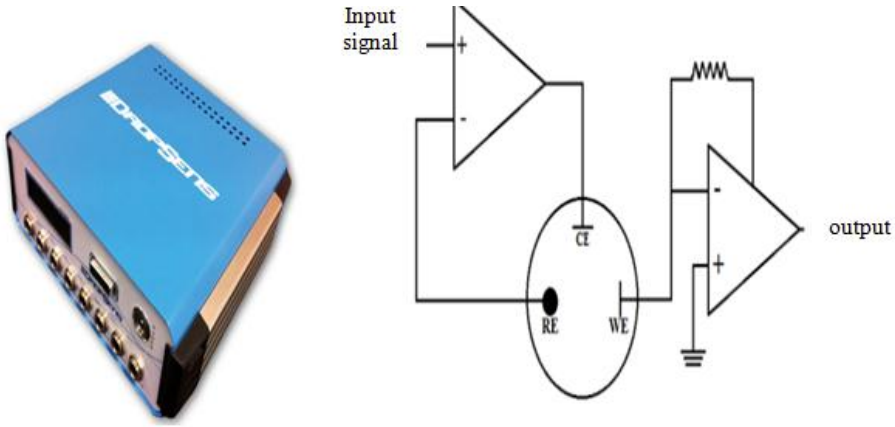

Figure 1.14: A potentiostat with circuit diagram of a three-electrode system.

1.10. Various electrochemical techniques

1.10.1. Cyclic voltammetry (CV)

Cyclic voltammetry is one of the most exploited techniques in electrochemical studies. Its primary advantage comes from the fact that it gives insight into both the half-reactions taking place at the working electrode, providing at the same time information about the chemical or physical phenomena coupled to the studied electrochemical reaction . Hence cyclic voltammetry is often considered as electrochemical spectroscopy. Although its usage is relatively minimal in quantitative food analysis, it is important to elaborate the principles of cyclic voltammetry, since every electroanalytical study almost inevitably commences with this technique. In cyclic voltammetry, starting from an initial potential Ei, a staircase (Figure 1.15) potential sweep (or linear sweep in older potentiostat) is applied to the working electrode. After reaching a switching potential Ef, the sweep is reversed

and the potential returns to its initial value. The main instrumental parameter in the cyclic voltammetry is the scan rate (v¼dE=t), since it controls the timescale of the voltammetric experiment. The useful scan rates range from 1 to 1000 mV=s, although scan rates of over 10 V=s are technically achievable. The instrumental output in cyclic voltammetric techniques is a current–potential curve, a cyclic voltammogram (Figure 1.16). The main features of the cyclic voltammogram are the cathodic and anodic peak potentials, the cathodic and anodic peak currents, and the formal (or half-peak) potential. While the half-peak potential (defined simply as a median between the cathodic and the anodic peak potentials) provides mainly thermodynamics information, the magnitudes of the peak currents reveal the kinetics involved in the electrochemical reaction. The shape of the cyclic voltammogram gives information about the type of the electrode reaction, the number of electrons involved in the elementary step of electrochemical transformation, as well as about the additional phenomena coupled to the electrochemical reaction of interest, like those for coupled chemical reactions or adsorption and crystallization. If the electron transfer process is much faster than the kinetics of the mass transport processes (diffusion), then the electrode reaction is electrochemically reversible. In this case, the peak separation DEp is defined as follows:

$$\Delta E_{\mathrm{p}} = |E_{\mathrm{p,c}} - E_{\mathrm{p,a}}| = 2.303\frac{RT}{nF}$$

For example, in a simple reversible and diffusion-controlled electrochemical reaction, where one electron is exchanged in an elementary act, the peak separation should be about 59 mV (at 258C). Moreover, the peak potential separation should not vary by increasing the scan rate, while both cathodic and anodic peak currents should be a linear function of the square root of the scan rate. Every breach of these criteria means deflection of the electrochemical reversibility, caused either by the slow electron transfer (quasi-reversibility or irreversibility) or by additional involvement of the electroactive species in chemical reactions or adsorption phenomena. For an electrochemically reversible reaction, the concentration of the electroactive species is linked to the peak current Ip by the Randles–Sev¯cik expression [46] , and at 258C it reads as follows:

$$I_p = 2.69 \times 10^5 \, n^{3/2} A c_0 \sqrt{Dv}$$

where

A is the active electrode surface area

c0 is the initial concentration of the electroactive species in the solution

D is its diffusion coefficient

n is the number of the electrons exchanged

v is the scan rate

This equation enables exploration of cyclic voltammetry for quantitative determination purposes.

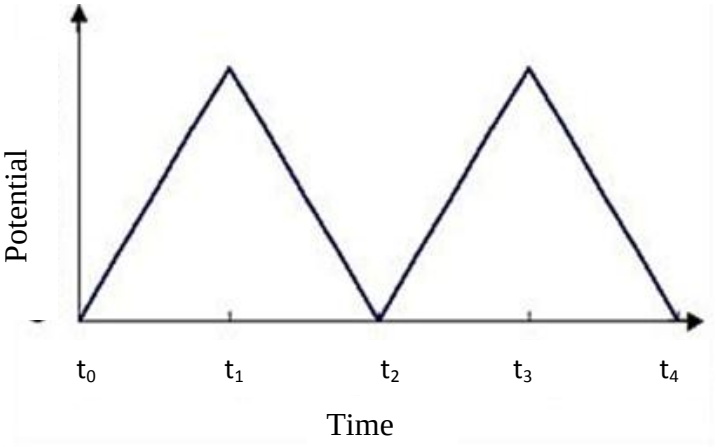

Figure 1.15: Cyclic voltammetry input waveform.

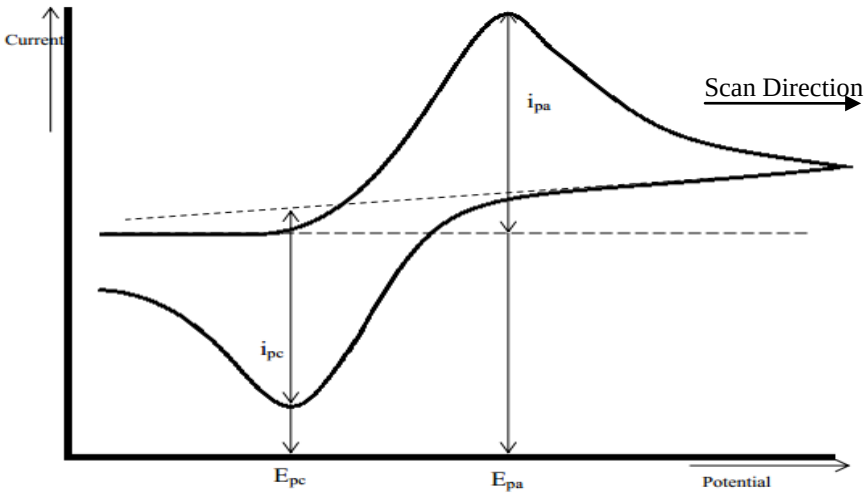

Figure 1.16: Typical Cyclic Voltammogram response for a reversible redox couple.

1.10.2. Square-wave voltammetry (SWV)

Square-wave voltammetry (SWV) is the most advanced and the most sophisticated technique in the family of pulse voltammetric techniques [47]. The potential form in SWV consists of symmetrical square-wave pulses with constant amplitude ESW, which are superimposed on a staircase-wave form (Figure 1.17.a). The potential in SWV changes for a constant potential step dE. The current in this technique is measured twice at the end of each half cycle. The currents measured at the end of oxidation half cycles give the oxidative (forward) current component, while the currents measured at reduction half cycles give the reduction (backward) current component (Figure 1.17.b). The net current in SWV is obtained as a subtraction between the forward and the backward currents. However, since the reductive currents (by convention) have a negative sign, the net current in SWV is actually a sum of the absolute values of both the current components (Figure 1.17.b). This method of measurement makes SWV the most sensitive electroanalytical technique. The net peak current in SWV, as in other pulse voltammetric techniques, is proportional to the analyte concentration, resulting often in detection limits in sub-nanomolar ranges. Besides, SWV provides an insight into both the half-electrode reactions, thus having a distinct advantage over cyclic voltammetry for studying the mechanisms of electrochemical reactions. SWV is a very fast technique, providing insight into the kinetics of fast electron transfer reactions, and into the kinetics of rapid chemical reactions coupled to the electroactive species. Although the theory of SWV is still developing, many excellent theoretical papers on SWV have appeared in last 30 years, providing criteria for recognition of many complex electrode mechanisms, and providing methods for measuring the kinetics and thermodynamics of various processes encountered in the investigated electrochemical systems [48]. During the last 25 years, this has led to SWV becoming one of the most explored voltammetric techniques for both quantitative applications and mechanistic studies, as well as for the determination of kinetics and thermodynamics in various electrochemical systems.

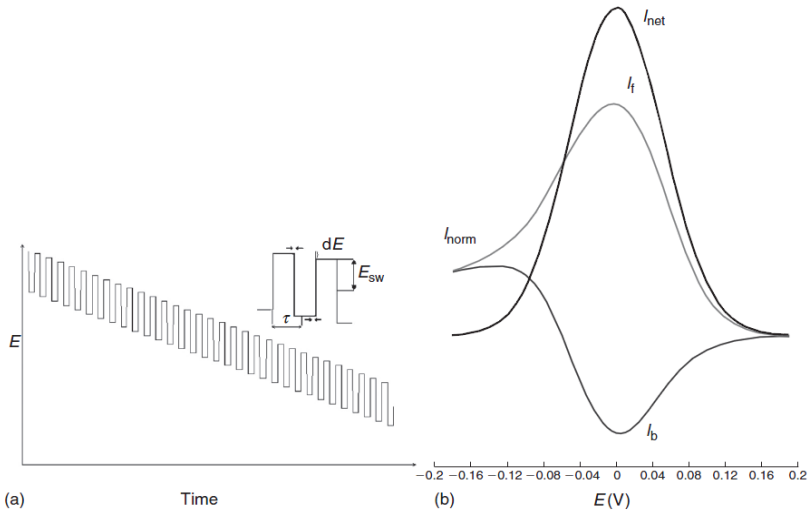

Figure 1.17: (a) Potential form in square-wave voltammetry: Esw, potential amplitude; dE, potential step; t, duration of a single pulse. The current is sampled twice in each pulse, in the time period between two arrows at the inset; (b) resulting simulated voltammogram in square-wave voltammetry: If, forward current, Ib, backward current, Inet, net current.

1.11. Sensor characterization

1.11.1. Scanning Electron Microscopy (SEM)

The scanning electron microscope (SEM) is a powerful and frequently used instrument, in both academia and industry, to study, for example, surface topography, composition, crystallography and properties on a local scale. The spatial resolution is better than that of the optical microscope although not quite as good as for the transmission electron microscope (TEM). The SEM has an extremely large depth of focus and is therefore well suited for topographic imaging. Besides surface topographic studies the SEM can also be used for determining the chemical composition of a material, its fluorescent properties, the formation of magnetic domains and so on. The specimen is bombarded by a convergent electron beam, which is scanned across the surface. This electron beam generates a number of different types of signals, which are emitted from the area of the specimen where the electron beam is impinging (Figure 1.18).

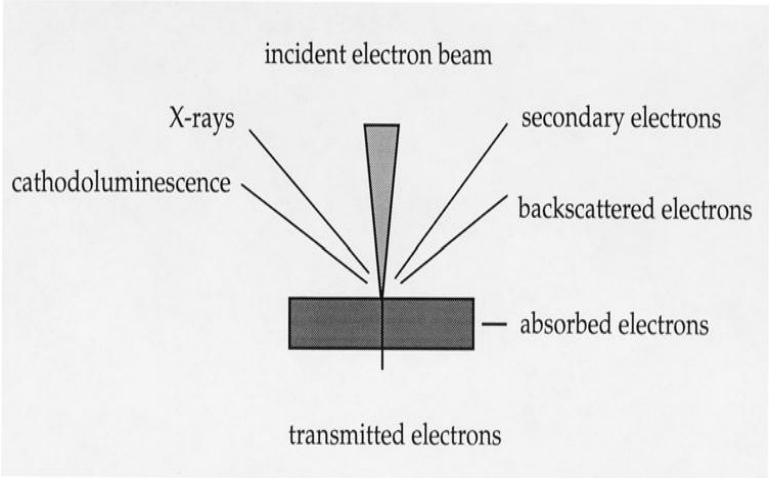

Figure 1.18: Different types of signals produced when high-energy electron impinges on a material.

The induced signals are detected and the intensity of one of the signals (at a time) is amplified and used to as the intensity of a pixel on the image on the computer screen. The electron beam then moves to next position on the sample and the detected intensity gives the intensity in the second pixel and so on.

The working principle of the SEM is shown in Figure 1.19. For improved signal-to-noise ratio in the image, one can use a slower scan speed. This means that the electron beam stays a longer time at one position on the sample surface before moving to the next. This gives a higher detected signal and increased signal-to-noise ratio.

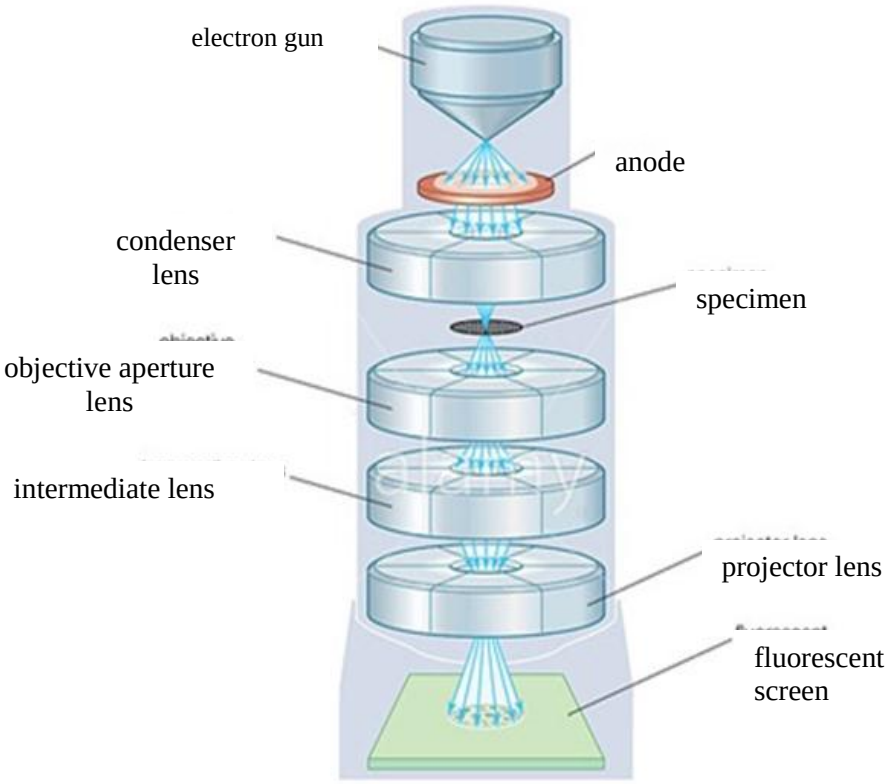

Figure 1.19: Schematic diagram of a SEM [49].

1.11.2. X-ray diffraction (XRD)

X-ray diffraction (XRD) relies on the dual wave/particle nature of X-rays to obtain information about the structure of crystalline materials. A primary use of the technique is the identification and characterization of compounds based on their diffraction pattern.

The dominant effect that occurs when an incident beam of monochromatic X-rays interacts with a target material is scattering of those X-rays from atoms within the target material. In materials with regular structure (i.e. crystalline), the scattered X-rays undergo constructive and destructive interference. This is the process of diffraction. The diffraction of X-rays by crystals is described by Bragg's Law, n(lambda) = 2d sin(theta). The directions of possible diffractions depend on the size and shape of the unit cell of the material. The intensities of the diffracted waves depend on the kind and arrangement of atoms in the crystal structure.

However, most materials are not single crystals, but are composed of many tiny crystallites in all possible orientations called a polycrystalline aggregate or powder. When a powder with randomly oriented crystallites is placed in an X-ray beam, the beam will see all possible interatomic planes. If the experimental angle is systematically changed, all possible diffraction peaks from the powder will be detected.

The parafocusing (or Bragg-Brentano) diffractometer is the most common geometry for diffraction instruments. This geometry offers the advantages of high resolution and high beam intensity analysis at the cost of very precise alignment requirements and carefully prepared samples. Additionally, this geometry requires that the source-to-sample distance be constant and equal to the sample-to-detector distance. Alignment errors often lead to difficulties in phase identification and improper quantification. A mis-positioned sample can lead to unacceptable specimen displacement errors. Sample flatness, roughness, and positioning constraints preclude in-line sample measurement. Additionally, traditional XRD systems are often based on bulky equipment with high power requirements as well as employing high powered X-ray sources to increase X-ray flux on the sample, therefore increasing the detected diffraction signals from the sample. These sources also have large excitation areas, which are often disadvantageous for the diffraction analysis of small samples or small sample features.

1.12. Objectives of the present work

The objective of this research is

i) To synthesis of WO_3 nanoparticles by hydrothermal method.

ii) To modify glassy carbon electrode with WO_3 nanoparticle.

iii) To characterize the sensor using electrochemical methods (Cyclic Voltammetry, Square Wave Voltammetry), X-ray Diffraction, Scanning Electron Microscope, Raman & Energy Dispersive X-ray microanalysis (EDX).

iv) To develop a pH sensor and also to study the sensitivity, selectivity, stability of this sensor using various electrochemical techniques.

Chapter II

Literature Review

2.1. Introduction

Sensors have currently become increasingly important in a world where technological advances demand precise information of numerous categories. They have been widely applied in fields such as industrial manufacturing, aerospace, ocean exploring, environmental protection, resources investigation, medical diagnosis, and bioengineering. Sensors can be made from various materials depending on the purposes they serve. High sensitivity, fast response, and good selectivity are the general requirements for a good sensor. For large-scale application, low material cost and easy fabrication are also required. With dramatic advances in nanotechnology, great progress has been made in recent years thanks to the newly developed nanomaterials for sensor application. Because of the inherent properties of nanomaterials, for example, super small size and large surface volume ratio, they can remarkably improve the sensitivity of the sensors as compared to traditional materials. By judiciously decorating the nanoparticle surface composition, unique target binding characters can be achieved to great selectivity. Furthermore, the robustness of nano semiconductor made it highly sustainable in various detection environments.

Over the last decade significant progress has been made in the development of immobilized electrochemical sensors for monitoring pH. This review discusses evolution of pH sensor based on micro and nanostructured sensor platforms for the biomedical and environmental applications.

2.2. Nanoparticle based pH sensor

Nanoparticles are nanometer size materials with unique physical and chemical properties and have been widely used for many years. Organic molecules, also in the nanometer size

range, possess functionalities that enable recognition and self assembly. The combination of nanoparticles and chemical or biological molecules is very attractive and has gained tremendous attention from academic and industry, because such combination could create new materials for electronics and optics and lead to new applications in genomics, proteomics, bio-medical and bio-analytical areas. For environmental application, nanometer size particles and their self assemblis offer the potential of novel functional materials, processes and devices with unique recognition activities, enhanced mobility in environmental and desired application flexibility.

Recently, Lidia *et al.* developed a nanoparticle based flexible pH sensor These flexible pH sensors based on WO_3 nanoparticles with a high surface area were produced by electrodeposition on gold electrodes with a sensing area of 1 mm^2. At first time the wax printed layer, here used as an insulator, was proven to be cytocompatible and therefore, a good alternative for sensor assembly. In open circuit voltage measurements, the pH sensitivity of these electrodes shows a near-Nernstain response of −56.7 ± 1.3 mV/pH and reversibility was confirmed for three complete cycles in a pH range of 9−5 [15].

S. Zaman *et al.* also reported a CuO NFs based pH sensor electrodes were fabricated to check the sensitivity of the CuO NFs for the pH in the range 2–11. The potentiometric response of this pH sensor appeared linear in a pH range between 2 and 11. The fabricated senor demonstrated good repeatability and reproducibility. This experiment paves the way for CuO nanostructures to find applications in biological fluids [50].

Feng Gao *et al*. [51] developed on A novel Rhoda mine-*b*-Isothiocyanate Doped Silica fluorescent core-shell nanoparticle based pH sensor using reverse micro-emulsion technique. The fluorescent core-shell nanoparticles are pH-sensitive, and the pH dynamic range of the sensing nanoparticles is between 5.0–10.0. The method offers the advantages of adequate sensitivity, accuracy and rapid detection of pH. The results are in good agreement with those using the standard glass electrode method. They show excellent stability and high reproducibility when used as pH sensors.

Milica Jovica *et al.* developed a Flexible potentiometric pH sensor based on iridium oxide nanoparticles. The sensor was fabricated using the simple layer-by-layer (LbL) deposition

technique, where alternate layers of the oppositely charged iridium oxide nanoparticles and the poly(diallyldimethylammonium chloride) (PDDA) polymer were deposited on the flexible indium tin oxide foil (ITO/PET).sensitivity of 74 mV/pH (14-bilayer)and using the ink-jet printing technology [52].

Zhenhua Bai *et al.* recently developed a fluorescent pH sensor based Ag@SiO2 Core−Shell Nanoparticle. The shell thickness of 8 nm, maximum fluorescence enhancements of 4 and 9 times were achieved when excited by 405 and 455 nm, respectively. The ratio of emission intensity at 513 nm excited at 455 nm to that excited at 405 nm is correlated well with the pH value of aqueous solution, over the pH range of 5−9. The pH sensitivity and linearity are demonstrated over the physiological region. The excellent structural and optical properties make these core−shell nanoparticles promising in application as intracellular pH sensor [53].

A recent application of a nanoparticle based pH sensor fabrication method is complex and multi-step process.

2.3. Metal/metal oxide-based pH sensor

A considerable amount of study has been focused on the development, fabrication, and characterization of metal/metal oxide pH electrodes. Typically, the pH electrodes employing metal/metal oxide as sensing materials are all-solid-state, and have several advantages in comparison to conventional glass electrodes. Unlike the glass pH electrodes, they require a high input impedance pH meter; the metal oxide-based pH sensor has low electrode impedance. In contrast to the sluggish response of glass pH electrodes, the solid-state metal oxide pH sensor presents a faster pH response. The method to prepare a metal/metal oxide-based pH electrode is compatible with thin film and MEMS manufacturing technologies and provides capability of mass production and miniaturization. A variety of metal/metal oxide materials show ideal or near-ideal Nernstian responses; these materials have been explored for use as pH sensing layers [54]. Some examples are IrO_x [55], RuO_2 [56], nanoporous PtO_2 [57], RuO_2 ßTiO_2 [58], TiO_2 ß PVC [59], PaO_2 [60], Sb/Sb_2O_3 [61], WO_3 [62], PbO_2 [63], Co_3O_4 [64], and SnO_2 [65, 66]. Among these many pH sensitive oxides, iridium oxide (IrO_x) shows high conductivity,

good chemical stability, and most importantly superior biocompatibility, making it the most popular material for the fabrication of all-solid-state pH microelectrodes. In addition to IrO_x, antimony has received renewed interest recently. Antimony has been used as a pH sensing material in commercially available pH catheters for esophageal pH monitoring. Fabrication methods and conditions that determine the structure and composition of iridium oxide affect pH response characteristics of resultant pH sensors. A comparison of some typical iridium oxide-based pH electrodes with respect to the fabrication method and pH sensing characteristics has been made by Madou's group [67]. Marzouk [68] described a modified method to prepare the iridium oxide layer on etched titanium substrate to enhance the stability of the pH sensitive layer. Micro-tip pH electrodes based on iridium oxide on a tapered glass micropipette with a tip of 3–10 μm in diameter [69] and on a carbon fiber [70] have been reported.

In a recent study on planar thin film iridium oxide-based pH sensor, Ges *et al.* [55] reported aging effects of IrO_x plating solution on the sensor's sensitivity. Iridium oxide films deposited from fresh plating solution showed maximum sensitivity, while those from a one-month-old solution showed decreases of 10–15% in sensitivity. Two properties of biocompatibility and corrosion resistance of iridium oxide electrodes are noticeable [71, 72]. This fact made iridium oxide electrodes as a potential candidate for Microbial induced corrosion investigation.

Ryan *et al.* for first time used atomic layer deposition (ALD) for iridium oxide (IrOx) fabrication as the pH sensitive layer with an average sensitivity of ~ 67 mV/pH at 22 °C. They could coat 110 nm IrOx layer on a glass substrate consists of 300 nm thick titanium eletrodes. Their pH sensor was able to detect pH in a range from pH 4 to pH 10 [73].

Yao *et al.* [67] reported a pH electrode based on lithium carbonate melt-oxidized iridium oxide film with the composition of $Li_xIrOy.\ nH_2O$. The electrode based on this oxide film exhibits promising pH sensing performance and high chemical stability, with an ideal Nernstian response 58.9 mV/pH over the pH range of 1 to 13. The electrode also shows a fast potential response with a 90% response time less than 0.2 s, and a low open-circuit potential drift 0.1 mV/day measured in pH 6.6 solution. The reproducibility in terms of the Nernst slopes and the apparent standard electrode potentials has been improved among

electrodes within the same batch. However, the biocompatibility due to inclusion of lithium salt was not assessed. The iridium oxide-based solid-state micro-pH electrodes have been used in many clinical research studies, such as measuring extracellular pH in ischemic hearts [74], in biofilms [75] and in esophagus tubes [76].

As Lu *et al.* [77] reported there is an optimum thickness for IrO_2 electrodeposited coating. Coating electrochemical performance increase when it's CSCc and thickness increase, but when CSCc approach to ~45mC/cm^2 delamination of IrO_2 coating was detected. Their demonstarated iridium oxide electrode showed a pH sensitivity -75.51 mV/pH in broad pH range of 1-13. A surface renewable IrO2 pH sensor or hydrogen ion-selective electrode can be made by using composite electrode technique. Quan *et al.* [78] used carbon black, polyvinyl chloride and ammonium hexachloroiridate to fabricate an IrO_2 based composite electrode. Increasing IrO2 content up to 40% showed an increasing on the pH response. They also investigated the effect of different ions on pH electrode efficiency that resulted that Fe (CN) $_6^{3-}$, Fe (CN) $_6^{4-}$, I^-, and H_2O_2 affected by electrode result. Similar results for IrO_2 pH sensor were also reported in other research [79].

Park *et al.* [80, 81] fabricated an iridium oxide-glass composite electrode by mixing ammonium hexachloroiridate and glass powder, pressing, and sintering under oxygen atmosphere. The mention electrode was renewable by using 2000 grit SiC emery paper whenever it becomes fouled or deactivated. They observed many microscopic voids in the electrode surface after sintering at high temperature. pH response in these electrodes was dependent on the size and population of voids. Surface voids can be reduced by hot press sintering technique.

Grant *et al.* [82] evaluated an electrochemical pH sensor along with a fiber optic sensor to monitor brain tissue *in vitro* as well as *in vivo*. The electrochemical pH sensor was based on sputtered iridium oxide thin films. The electrochemical sensor was fabricated on a flexible kapton substrate with sputter coating of 200 A titanium for adhesion, followed by 2000–4000 A of iridium, and then finally 2000–4000 A iridium oxide. The Ag/AgCl reference electrode was also fabricated on kapton substrate with a sputtered silver layer, and then the silver chloride top layer was formed electrochemically. The kapton substrates were sectioned into strips with 1 mm in width and 8 cm in length. The iridium oxide and

silver/ silver chloride electrodes were adhered back-to-back using an epoxy. Tests *in vitro* and *in vivo* indicated that the sensors showed a linear response of 57.9 ⁻0.3 (before) and 57.8 ⁻ 1.5 mV/pH (after 3 h *in-vivo* test) between pH 6.8 to 8.0. The *t*90 response time of the electrochemical sensor was less than 5 s. The potential drift was less than 0.4 mV/h in PBS; however, an increased drift was observed in *in-vivo* tests. Protein absorption may account for this increased drift in *in-vivo* tests. Although the redox reaction mechanisms of iridium oxide are still not clear, most researchers believe that the proton exchange associated with oxidation states of metal oxides is one of the possible pH sensing mechanisms [55-57]. During electrochemical reactions, oxidation state changes in the hydrated iridium oxide layer are accompanied by the injection/ejection of H^+. The possible reactions involved in the electrode processes are:

Hydration of iridium oxide

$$Ir_2O_3 + 3H_2O_2 \longrightarrow Ir(OH)_3$$

Charge transfer and injection/ejection of hydrogen ion

$$2Ir(OH)_3 \longleftrightarrow 2IrO_2.H_2O + 2H^+ + 2e^-$$

Depending on the fabrication techniques and deposition parameters, the pH sensitive slope of IrOx electrodes varies from near-Nernstian (about 59 mV/pH) to super-Nernstian (about 70 mV/pH or higher). Since the compounds in the oxide layers are possibly mixed in stoichiometry and oxidation states, most reported iridium oxide reactions use *x, y* in the chemical formulas, such as $Ir_2O_3 + xH_2O$ and $IrO_x(OH)_y$. Such mixed oxidation states in IrO_x compounds may induce more H^+ ion transfer per electron, which has been attributed to causing super-Nerstian pH responses [55].

Considering the H^+ dependent redox reaction between two oxidation states of the iridium oxide as the basis of the pH sensing mechanism, the electrode potential changes to the hydrogen ion concentration are expressed by Nernstian equation:

$$E = Eo + 2.303RT/F (\log [H^+]) = E^{o-} 61.54\ pH$$

Where E^o is the standard electrode potential with the value of 729 mV vs Ag/AgCl reference electrode. The potential/pH slope is expected to be 61.5 mV/pH at 37^{o}C.

2.4. Electrodes modified with pH-sensitive polymers

It has been shown that electromodified electrodes with conducting polymers could act as good candidates for replacement of popular glass pH electrodes [83]. The examples of pH chemical sensors using polymer-film-coated electrodes include electropolymerization of pyrrole, aniline, thiophene, or benzene derivatives [83]. However, the measurements of pH using the above-mentioned conductive polymers had poor reliability due to defects and pinholes present in the films structure.

Jamal *et al.* 2013 recently developed, A novel electrochemical pH sensor was fabricated through the use of an anthraquinone–ferrocene (AQ–Fc) complex based on a vertically aligned gold nanowire array electrode (AuNAE), in fig (2.2). In SWV measurments, the modified electrode was found to be linear over the range of pH 2-11, with a sensitivity of 1.38 $pH^{-1}cm^{-2}$ at 25 ^{0}C. The electrode was found to respond both in the presence and absence of oxygen, further expanding the potential applications to include de-oxygenated environments. Their sensor showed a potential drift of 1.0–3.3% after three hours and 95% of the signal was retained after one week [16].

Herlem *et al.* [83] reported a pH sensor, where a smooth Pt electrode was coated with an electrically insulating polymer, namely linear polyethylenimine (L-PEI). Platinum electrodes, modified by a coating of a thin L-PEI film, resulting from the anodic oxidation of pure ethylenediamine, exhibited a linear, reversible, and stable in time potential response sensitive to pH changes in aqueous media. The assembly of the electrode surface coated with electropolymerized ethylenediamine acted as a transducer of the electrode potential versus the pH value in aqueous solutions. A possible mechanism by which the linear polyethylenimine responds to pH changes could be due to the affinity of the numerous amino groups to the protons in solution. The reaction of H^+ with amino groups creates local charge density excess at the electrode surface. The potentiometric response can be considered as behaviour controlled by a surface reaction, which takes place on the

PEI film. Protonation and deprotonation of superficial amino groups of the PEI is symbolically described in Eq. shown in below [83]:

$$PEI + H^{+} \longrightarrow PEIH^{+}$$

When equilibrium is reached at the PEI/solution interface, then the equilibrium expression *K* of the surface reaction is determined by Eq. shown in below [83]:

$$K = [PEIH^{+}] / ([PEI]\ [H^{+}])$$

Herlem *et al.* [83] also reported that as the film thickness increases, the more amino groups are present, and thus the pH sensitivity of the modified electrode increases. These thick film modified electrodes give repeatable pH responses, independent of direction of pH change, and give consistent results when the pH value is varied in a random manner.

Another example of wire electrodes coated with pH-sensitive polymers, fabricated by galvanostatic electrochemical polymerization of monomers, namely, pyrrole (Py), 3-(2,5-dihydroxybenzyl) pyrrole (PyQH), aniline (An) and o-phenylenediamine (oPD) can be seen in [84]. The polymers were synthesized with perchlorate or bovine serum albumin (BSA) dopants in a propylene carbonate or universal buffer electrolytes, respectively. The potentiometric characteristics of the resulting films show sub- to near-Nernstian responses. The range of electrode sensitivities (at a temperature of 25 °C) for the four polymers used are -43.2 mV/pH for PPy, -46.0 mV/pH for PPyQH, -42.1 mV/pH for Pan and -50.7 mV/pH for PoPD [84]. All have a linear working range of pH 3 to pH 10 and an average response time of 3 to 5 min. The doping and supporting electrolyte anions' effect on the potentiometric sensitivity and response time of polypyrrole (PPy) electrodes towards changes of solution pH were studied in [85]. It was found that the response of PPy doped by easily exchangeable common anions (Cl^{-}, NO_3^{-}, and $ClO4^{-}$) in their solutions (KCl, KNO_3, $NaClO_4$) is slow. In contrast, polypyrrole films deposited in the presence of weak acid anions, such as phthalates, oxalates and salicylates, were characterised by instantaneous pH responses in these solutions.

The redox and charge transport properties of an electropolymerized N-substituted phenazine, polyphenosafranin (PPS) polymer film was interpreted as the diffusion-migration of electrons and ions. Electron transport occurs via a process of sequential electron self-exchange between neighbouring redox sites. The theory for the faradaic impedance of redox polymers was proposed by Mathias and Haas [86]. Electron transfer at the electrode-film interface is accompanied by the ingress of charge-compensating counter-ions to or from the film. When polymers including electroactive nitrogen atoms are reduced, either anions are released from the polymer, or protons are incorporated into it. Electron transport occurs via a process of sequential electron self-exchange between redox sites. Because it is accompanied by intermolecular proton transfer, deprotonation of the polymer may reduce the homogeneous electron-transfer rate constant. A pH sensor utilizing a redox-active copolymer has been reported by Robinson and Lawrence [87], where the response of vinylanthracene, vinylferrocene, and poly (vinylferrocene) has been analyzed and compared with the response of the p (VA-co-VF) copolymer. The results showed the presence of both poly (vinylferrocene) and poly (vinylanthracene) within the copolymer. The voltammetric response of p (VA-co-VF) has been analyzed over the pH range 4-9 and over a wide temperature scale.

2.5. Solid-state pH sensors

The miniaturized pH sensors are of great importance in biomedical and clinical applications. By taking advantage of all-solid-state configurations, the sensor size can be greatly reduced and the sensors can be mass produced with improved reproducibility. An all-solid-state pH sensor uses direct electrical contact between the pH sensitive membrane and the inner metal contact. Among pH sensitive membranes used in the fabrication of all-solid-state pH sensors, metal and metal oxides show clear advantages over other membranes, such as glass membranes [88] and polymer membranes [89], due to their well-defined metal/metal oxide interface and compatibility with micro fabrication techniques. As an all-solid-state pH sensor, ISFET has an insulator/metal interface.

Poor adhesion of membrane to metal is the leading cause of failure in solid-state potentiometric sensors [90]. For glass membranes, the mismatch of thermal coefficients of expansion between thin glass membrane and metal (mostly Pt) has been attributed to

premature failure due to hairline crack formations in the glass layer [88]. For polymer-based membranes, water vapor penetration was reported to compromise the membrane–metal interface, therefore affecting the sensor's performance.

M. Glance.Gostkiewicz *et al.* recently reported a miniaturized thick-film solid state pH sensor. It was fabricated through, the use of a metal oxide (RuO_2) on Thick Film.In potentiometric measurments the thick film pH sensor resulting in a device with a sensitivity of approximately 30mV/pH at ambient temperature [91].

Yoon *et al.* [89] also reported an all-solid-state sensor for blood analysis. The sensor consists of a set of ion-selective membranes for the measurement of H^+, K^+, Na^+, $Ca^{2+,}$ and Cl^-. The metal electrodes were patterned on a ceramic substrate and covered with a layer of solvent-processible polyurethane (PU) membrane. However, the pH measurement was reported to suffer severe unstable drift due to the permeation of water vapor and carbon dioxide through the membrane to the membrane–electrode interface. For conducting polymer-modified electrodes, the adhesion of conducting polymer to the membrane has been improved by introducing an adhesion layer. For example, polypyrrole (PPy) to membrane adhesion is improved by using an adhesion layer, such as Nafion [88] or a composite of PPy and Nafion [92].

Another problem that is common for all membrane-based solid-state sensors is the ill-defined membrane–metal interface. A large exchange current density is required to produce a reversible interface for a stable potentiometric sensor response. One approach to improving this interface is to use conducting polymers. Conducting polymers are electroactive π-conjugated polymers with mixed ionic and electronic conductivity. They are able to transduce an ionic signal into an electrical signal. Such polymers provide an interface between pH selective membranes and metallic transducers, which replaces the internal electrolyte of a conventional pH sensor. Research efforts have been made to utilize conducting polymers in a number of designs of all-solid-state miniaturized sensors [93-95]. Electroactive π-conjugated polymers, like polyaniline (PANI) and polypyrrole (PPy), are most commonly used in sensor fabrications.

2.6. Potentimetric pH sensors

Routinely used ion-selective electrodes (ISEs) for the determination of blood electrolytes have a market size comparable to that of glass electrodes. The lower detection limit and the discrimination of interferingions (the selectivity coefficients) have been improved during the past decade by factors up to $10^6$and 10^{10}, respectively, thus allowing their application in fields such as environmental trace analysis and potentiometric biosensing [96]. ISEs and their optical counterparts, ion-selective bulk optodes, have the unique capability of sensing free ion activities instead of the total concentration. Bulk optodes belong to a newer class of sensors and are usually based on the competitive or cooperative extraction of the analyte ion with protons between the polymeric and aqueous phase [97]. This two-phase sensing mechanism has advantages in reaching a lower detection limit dictated by the thermodynamics ion extraction, and may lead to the mass production of monodisperse ion sensing microbeads that can be flexibly coupled with analytical flow cytometry or optical-fiber based micro sensor arrays [98-100]. The unique ion-sensing capabilities of ISEs and bulk optodes make them very useful for clinical diagnosis, drug analysis and environmental monitoring.

Various materials have been considered suitable for potentiometric pH sensors [101-104]. Potentiometric pH sensors based on linear polyethylenimine (L-PEI) and linear polypropylenimine (L-PPI) (two synthetic enzymes and biocompatible polymers) films were prepared by electro polymerization of three different monomers: ethylenediamine (EDA), 1, 3 diaminopropane (1, 3-DAP) and diethylenetriamine (DETA) in order to be used in clinical, dermatological and biological applications, such as *in vivo* analysis [122 102]. These polymers are considered good candidates for pH biosensors due to their strong bonding to the electrode surfaces during the electro polymerization step.

Flavia E. Galdino *et al.* 2015 recently developed a reagent less pH sensor based upon disposable and economical graphite screen-printed electrodes (GSPEs.The potentiometric pH sensor utilizes GSPEs which are chemically pretreated to form surface immobilized oxygenated species that, when their redox behavior is monitored, give a Nernstian response over a large pH range (1−13). An excellent experimental correlation is observed

between the voltammetric potential and pH over the entire pH range of 1−13 providing a simple approach with which to monitor solution pH [105].

Potentiometric pH measurement using a neutral carrier membrane placed on a conducting polymer was employed by [106]. Conducting polymer coatings of 0.5 μm thickness were deposited on a Pt electrode by electro polymerization from a solution consisting of 120 mg $LiClO_4$ and 10 μl Pyrrole dissolved in 5 ml acetonitrile. Electro polymerization was carried out in the galvanostatic mode with a current density of 5 μA mm-2 and a polymerization time of 10 s. Finally, a drop of solution of PVC based neutral carrier membrane solution with trin-dodecylamine as proton carrier was put on the electrode with the aid of a micro-dispensing unit. The response of this pH sensor followed Nernstian law with a response time of less than 1 s. The potential drift was 250 μV per day, which corresponds to a pH drift of 5/1000 pH units per day [106]. This device was one of the earliest tested *in vivo* pH and glucose sensors, manufactured using thin film technology on flexible polymer substrate. The research towards integration of multi-sensor head for simultaneous *in vivo* monitoring is ongoing. Poly(vinylbenzylchloride-co-2,4,5-trichlorophenyl acrylate) (VBC-TCPA) spheres, approximately 725 nm in diameter, were prepared by dispersion polymerization then derivatized with diethanolamine to realize a mass changing pH-responsive polymer [107]. While the pH-responsive polymer spheres are suitable for use with any mass-sensitive sensor platform, in this work, the polymer spheres are combined with magnetoelastic thick films to achieve a remote query pH sensor. The magnetoelastic pH sensors were fabricated by spin-coating of aminated polymer spheres onto the surface of a magnetoelastic ribbon. The pH response of these sensors was examined by monitoring changes in sensor resonance frequency as a function of test-solution pH. The sensors demonstrated a linear pH response from pH 3.0 to pH 9.0, with a change in resonance frequency of 0.2% per pH unit for a 1.5- μm thick polymer layer [107].

Recently published research [97] demonstrated a strategy for covalent grafting of fluorophores into a self-plasticized polymer matrix, and a plasticizer-free bulk optode microsphere sensor for sodium using the polymer–fluorophore composite. Two types of Nile Blue derivatives were synthesized by covalently grafting the Nile Blue structure into self-plasticized poly (n-butyl acrylate) via urea (NBurea) or amide (NB-amide) linkers. Modification of n-butyl acrylate with a suitable functional group into the polymer

backbone for polymerization was followed by the reaction with Nile blue. The grafted NB-urea and NB-amide polymers prepared using this method can be used as fluoroionophore in ion selective optodes in the same way as commercial chromoionophores, but with improved lifetimes [108]. Plasticizer-free fluorescent ion-sensing microspheres were prepared using the two polymer–fluorophore composite for sodium, and showed good selectivity toward potassium, calcium and magnesium. The measuring ranges of sodium ions were found as 10^{-1}–10^{-4}M and 1–10^{-3}M, for NB-urea and NB-amide–PnBA, respectively, at physiological pH.

2.7. Calibration curve

The principle of pH electrode sensing mechanisms which are based on glass or polymer membranes is well investigated and understood. Common to all potentiometric ion selective sensors, a pH sensitive membrane is the key component for a sensing mechanism. When the pH sensitive membrane separates the internal standard solution with a constant pH from the test solution, the potential difference *E*a cross the membrane is determined by the Nernst equation:

$$E = \text{constant} + (RT/F) \ln [H^+]$$

where *R* is the gas constant, *T* is the absolute temperature (K), *F* is the Faraday constant, and $[H^+]$ is the hydrogen ion concentration in mol/L. Replaced with $pH = -\log[H^+]$,the equation has a form as follows:

$$E = \text{constant} - (2.303RT/F)\ pH = \text{constant} - (\text{slope})\ pH$$

Where 2.303*RT/F* is the slope of the line plot of *E*vs pH (also known as the slope factor), which is the basis of the pH electrode calibration curve. Strictly speaking, the activity of hydrogen ions should be used in the Nernst equation. However, in dilute solutions, activity of H^+ almost equals its molar concentration. In *in-vivo* and clinical applications, the molar concentration is used rather than the activity of H^+. Using a series of calibration solutions, the response curve or calibration curve of a pH electrode can be experimentally determined by plotting the cell voltage vs. the pH of the calibration solution. The linear range of the calibration curve is applied to determine the pH in any unknown solution. The slope of the

calibration curve within the linear range is used to determine the response slope or electrode sensitivity in mV/pH. This response slope is an important diagnostic characteristic of the electrode; generally, the slope gets lower as the electrode gets old or contaminated [109].

For a pH sensor with a Nerstian response, the slope, calculated from 2.303*RT/F*, is 59.16 mV/pH at 298 K. A useful slope range can be regarded as 50–70 mV/pH. Super Nerstian slopes are mostly reported from electrodes based on metal/metal oxide sensing materials. It has been reported that some electrodes present two linear response ranges. For example, IrOx microelectrodes prepared by Wipf *et al.* [110] have shown two linear slopes in the range of pH 2–6 and 6–12. It is clear from the Nernst equation that the temperature of the solution affects the response slope (2.303*RT/F*) of the calibration curve. The electrode voltage changes linearly in relationship to changes in temperature at a given pH; therefore, the pH of any solution is a function of its temperature. For example, the electrode response slope increases from 59.2 mV/pH at 25 ºC to 61.5 mV/pH at a body temperature of 37ºC.Formodern pH sensing systems, a temperature probe is normally combined with the pH electrode.

2.8. Analytical performance of the pH sensor

Sensitivity of the pH sensor: The sensitivity of a pH electrode is determined by the linear response slope of the pH electrode as defined by the Nernst equation. Typically, the electrode calibration curve exhibits a linear response range between a pH of 2 and 9. At very high and very low pH, there are deviations from linearity. The high detection end (high $[H^+]$, low pH) of most pH sensors is limited by the so-called acid error. The electrode reads higher than the actual pH in very acidic solutions. The mechanism of such an error is not well understood. The lower detection limit (low $[H^+]$, high pH) is often governed by the selectivity of the sensor. At high pH, alkaline interfering ions such Na are about 8 to 9 orders of magnitude higher than H^+ in the solution. Electrodes respond slightly to Na^+ or K^+, giving a lower reading than the actual pH. This deviation from the actual pH is often referred to as alkaline error [111].

Reproducibility/accuracy of the pH sensor: Accuracy is a measure of how close the result is to the true value; while reproducibility or precision is a measure of how close a series of measurements on the same sample are to each other. The accuracy and reproducibility of pH measurements can be highly variable and are dependent on several factors: electrode stability (drift and hysteresis), response slope/calibration curve, and accuracy of the pH meters. While some of these factors are determined by the properties of electrodes, some measures can be taken to improve measurement accuracy and reproducibility. The concentration is proportional to the measured voltage and so any error in voltage measurement will cause an error in the solution concentration. The measured voltage is the cell voltage including different potentials generated at all-solid–solid, solid–liquid and liquid–liquid interfaces of both sensing and reference electrodes. The potential of the electrochemical cell, *E*cell, is mainly given.

$$E_{cell} = E_{pH} - E_{ref} + E_j + E_{xy}$$

Where E_{pH} is the half-cell potential of the pH electrode, E_{ref} is the half-cell potential of the reference electrode, E_j is the liquid-junction potential, and E_{xy} is the interfering ions induced potential which affects the electrode's selectivity. Any variations in these potentials will cause changes in the overall cell voltages. Frequent recalibration can minimize potential drift, while using protection membranes can reduce the effect from interfering ions. Liquid-junction potentials develop at the interface between two electrolytes because of the differences in the migration rates of charged species across the interface. By using reference filling solutions with nearly equitransferrent electrolytes such as KCl, in which both ions have similar mobility when diffusing through the liquid junction, E_j can be minimized. E_{pH} is more strongly dependent on temperature in most cases than *E*ref and E_j are. Calibrations and measurements should therefore be carried out under temperature controlled conditions [112].

The error from pH measurement systems depends on the slope of the calibration line. For a pH sensor with a slope of 59 mV / pH, an error of 1 mV in measuring the electrode potential will cause a 0.017 pH change in the concentration. The lower the slope, the higher the errors are on the sample measurements [109]. Several factors need to be

considered to reduce the pH measurement error. First, an electrode with a high response slope should be used. Second, it is important to use a meter that is capable of measuring the millivolts or microvolts accurately and precisely. With modern meter technology, this is not normally a limiting factor. The potential measuring devices regularly used generally have an accuracy of 0.1 mV or higher (0.01 mV).Third, the electrode should be calibrated in the pH range close to the intended applications.

Although the calibration curve may show a straight line over several decades of concentration with an average slope, it is unlikely that this will be exactly the same across the whole range. For example, when multi-points (five points) calibrations are made, there may be a variation of several millivolts between the individual slopes calculated from two adjacent points at different concentration ranges or between the individual slopes and the overall slope. Therefore, for the most accurate results, it is recommended that the electrode slope be determined by using two-point calibration (also called bracketing) using two standard buffer solutions. These two buffer solutions are often selected that closely cover the expected range of the samples. This is especially important for some *in-vivo* measurements, where the pH variation is within a very narrow range. In some *in-vivo* applications, one-point calibration is used. Although a one-point calibration is insufficient to determine both the slope and one-point pH value, by assuming that the slope of prior calibration is unchanged, the electrode's performance *in vivo* can be assessed during operation. For example, in measuring esophageal acid exposure, since pH 4 is accepted as a cut-off value, one-point calibration was carried out during *in-vivo* ambulatory pH monitoring in which patients swallowed a juice with a predetermined pH close to 4 [113].

Stability and reliability: Poor operational stability due to drift has largely limited the long-term or implantable application of pH sensors. Some oxide-based electrodes present very high initial potential drift but their stability is improved after soaking for a certain amount of time ranging from hours to days [114,115]. Shelf-life also affects the storage stability of some sensors, such as glass electrodes. When all or most of the above properties are optimized, a reliable pH sensor system can be achieved for *in-vivo* measurements.

Biocompatibility: Biomaterials are inert substances that are used in contact with living tissue, resulting in an interface between living and non-living substances [116].

Biocompatibility of this interface is achieved by using such biomaterials for encapsulation in the construction of sensor devices. The interaction in an interface of device/tissue is limited by two factors. There is the corrosive environment, such as biological fluid, which contains salts and proteins among other cellular structures in which the sensor device must survive [117]. Second, there is the encapsulation material which may induce a toxic reaction due to poor biocompatibility and hemocompatibility [118]. It is crucial to use a biomaterial that can overcome both limiting factors to maintain the lifetime of the sensor device and protect the body [119].

The review has highlighted some novel approaches to the fabrication of electrochemical pH sensors. Several methods for the detection and measurement of pH have been described and compared. These sensors are scientifically relevant because they can be used for monitoring pH in biological and environmental fields. Some method enables multiple measurements and great sensitivity, but has very poor lateral and temporal resolution. Therefore the measurement itself generates it sown measure and, which is very unfavorable.

Table 2.1: List of pH sensing materials for sensors

Material	Detection Method	Advantages	Disadvantages	Ref.
AQ-FC/AQ-Sulfonate	Conducting polymer based pH sensor	Good stability over a wide pH range and first response	No information	16
Poly ally amine hydrochloride (PAH) and poly(acrylic acid) (PAA)	Optical fiber (Optical fiber pH sensors based on layer-by layer electrostatic self assembled Neutral Red)	Fast response (10s) and high repeatability	There are still too many unknown n factors.	120
Polyaniline	Conducting polymer pH sensor	Hydrofluoric acid don't influence the response of electrode	No information	121
copolymer: HEMA+ DMAEMA (9:1),TEGDA cross linker (1.5%), DMPA photo initiator, MPS adhesion promoter. 8 um layer	Conductimetric pH sensor, conductivity, interdigitated electrodes, Pt interdigitated electrode arrays	No information	No information	122

$W/W_2O_3/WO_3$ CuO NFs	Metal oxide pH sensor	1) Good stability over a wide pH range even at high temperature, high pressure and aggressive environment 2) fast response	No information	50
IrO_2	Metal oxide pH sensor	1) Good stability over a wide pH range even at high temperature, high pressure and aggressive environment 2) fast response	No information	123
Poly (meth acrylic acid)(PMAA) with poly(ethylene glycol) diamethacrylate	Nano-Constructed Cantilever based pH sensor	Highly sensitive, low power, and compact transduces	No information	124
Boron-doped silicon nano-wires (SiNWs)	ISFET based pH sensors	Small size and capability of nanowires for sensitive, label free and the real time detection of a wide range of bio-chemical species	No information	125
pAA-IOA, PEGD cross linker, AIBN initiator	Magnetoelastic pH sensor	Cheap fabrication	No information	126
Amorphous boron carbon nitride (a-BCxNy)	ISFET based pH sensors	The drain current which is an indicator of pH, remained stable over a period of 10 min in the phosphate solution with varied pH	Difficult to control, varying time to time	17

In this study, we developed a WO_3 nanoparticle based pH sensor. We choose WO_3 for sensing material because, tungsten oxide (WO_3) is a very promising material regarding its low cost and availability, improved stability, good morphological and structural control of the synthesized nanostructures, reversible change of conductivity, high sensitivity, selectivity, and biocompatibility. Furthermore, WO_3 is a well-studied wide band gap semiconductor (~2.75 eV) used for several applications as chromogenic material, sensing material, and catalyst. In conclusion, the development of novel pH sensors is still essential for their use in biological and environmental field.

Chapter III

Experimental

The electrochemical behavior of tungsten oxide nanoparticle modified glassy carbon electrode (WO_3/GCE) has been observed using cyclic voltammetry (CV) square wave voltammetry (SWV) and zero current potentiommetry (OCP) at glassy carbon electrode. The sensitivity of electrode reactions has been improved by modifying the electrode with WO_3 nanoparticle. WO_3 nanoparticle was prepared by hydrothermal method. It has been characterized by XRD, Raman, SEM and EDX. Details of the instrumentations are given in the following sections. The source of different chemicals, the instruments and brief description of the methods are given below.

3.1. Reagent and materials

Sodium tungsten (Na_2WO_4), sodium chloride (NaCl), hydrochloric acid (HCl), were purchased from E. Merck, Germany. Disodium hydrogen phosphate (Na_2HPO_4), sodium dihydrogen phosphate ($NaH_2PO_4.2H_2O$), sodium bicarbonate ($NaHCO_3$), disodium carbonates (Na_2CO_3), NaOH pellets, Nafion and chitosan were purchased from Sigma-Aldrich, India. All chemical were of analytical grade with high purity and were used as received.

3.2. Equipments

SWV and OCP measurements were performed with a potentiostat/ galvanostat (model: µStat 8400, Drop Sens, Spain). Three electrode cells has been used, where Tungsten oxide modified glassy carbon electrode (WO_3/GCE) was employed as a working electrode with Ag/AgCl and Pt wire as reference and counter electrodes, respectively. Morphology of the nanoparticle was examined using SEM (model: FEI Quanta 650 HRSEM) instrument operating at an acceleration voltage of 1000 kV). The crystal structures of nanoparticle were characterized by XRD (Oxford Instruments INCA energy system) and Raman spectra

(model: Renishaw (RA100) via confocal Raman Microscope at 514.5 nm excitation). For the sysnthesis of crystal, steel autoclaves has been used.

3.3. Electrochemical Techniques

Cyclic Voltammetry

Cyclic voltammetry is one of the most exploited techniques in electrochemical studies. Its primary advantage comes from the fact that it gives insight into both the half-reactions taking place at the working electrode, providing at the same time information about the chemical or physical phenomena coupled to the studied electrochemical reaction . Hence cyclic voltammetry is often considered as electrochemical spectroscopy. Although its usage is relatively minimal in quantitative food analysis, it is important to elaborate the principles of cyclic voltammetry, since every electroanalytical study almost inevitably commences with this technique. In cyclic voltammetry, starting from an initial potential Ei, a staircase (Figure 3.1) potential sweep (or linear sweep in older potentiostat) is applied to the working electrode. After reaching a switching potential Ef, the sweep is reversed the potential returns to its initial value. The main instrumental parameter in the cyclic voltammetry is the scan rate (v¼dE=t), since it controls the timescale of the voltammetric experiment. The useful scan rates range from 1 to 1000 mV=s, although scan rates of over 10 V=s are technically achievable. The instrumental output in cyclic voltammetric techniques is a current–potential curve, a cyclic voltammogram. The main features of the cyclic voltammogram are the cathodic and anodic peak potentials, the cathodic and anodic peak currents, and the formal (or half-peak) potential. While the half-peak potential (defined simply as a median between the cathodic and the anodic peak potentials) provides mainly thermodynamics information, the magnitudes of the peak currents reveal the kinetics involved in the electrochemical reaction. The shape of the cyclic voltammogram gives information about the type of the electrode reaction, the number of electrons involved in the elementary step of electrochemical transformation, as well as about the additional phenomena coupled to the electrochemical reaction of interest, like those for coupled chemical reactions or adsorption and crystallization. If the electron transfer process is much faster than the kinetics of the mass transport processes (diffusion), then

the electrode reaction is electrochemically reversible. In this case, the peak separation DEp is defined as follows:

$$\Delta E_{\mathrm{p}} = |E_{\mathrm{p,c}} - E_{\mathrm{p,a}}| = 2.303 \frac{RT}{nF}$$

For example, in a simple reversible and diffusion-controlled electrochemical reaction, where one electron is exchanged in an elementary act, the peak separation should be about 59 mV (at 258C). Moreover, the peak potential separation should not vary by increasing the scan rate, while both cathodic and anodic peak currents should be a linear function of the square root of the scan rate. Every breach of these criteria means deflection of the electrochemical reversibility, caused either by the slow electron transfer (quasi-reversibility or irreversibility) or by additional involvement of the electroactive species in chemical reactions or adsorption phenomena. For an electrochemically reversible reaction, the concentration of the electroactive species is linked to the peak current Ip by the Randles–Sev_cik expression [46] , and at 258C it reads as follows:

$$I_{\mathrm{p}} = 2.69 \times 10^5 \; n^{3/2} A c_0 \sqrt{Dv}$$

where

A is the active electrode surface area

C_0 is the initial concentration of the electroactive species in the solution

D is its diffusion coefficient

n is the number of the electrons exchanged

v is the scan rate

This equation enables exploration of cyclic voltammetry for quantitative determination purposes.

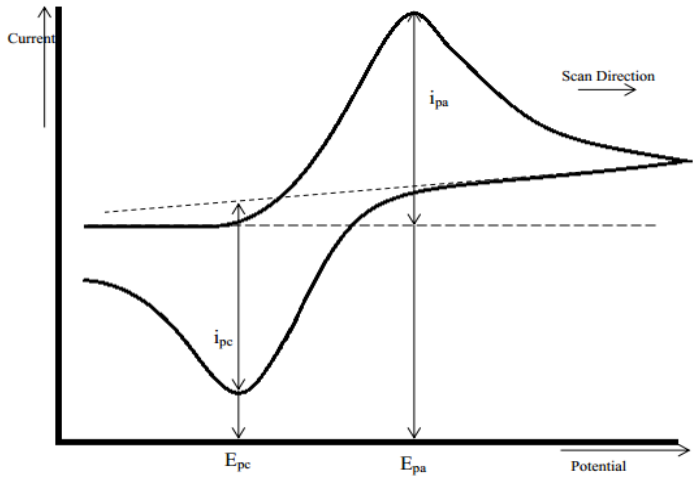

Figure 3.1: Cyclic Voltammogram response for a reversible redox couple.

Square Wave Voltammetry

The excitation signal in SWV consists of a symmetrical square wave pulse of amplitude E_{sw} superimposed on a staircase waveform of step height ΔE, where the forward pulse of the square wave coincides with the staircase step. The net current, i_{net}, is obtained by taking the difference between the forward and reverse currents ($i_{for} - i_{rev}$) and is centered on the redox potential. The peak height is directly proportional to the concentration of the electroactive species and detection limits as low as possible.

SWV has several advantages. Among these are its excellent sensitivity and the rejection of background currents. Another is the speed. This speed, coupled with computer control and signal averaging, allows for experiments to be performed repetitively and increases the signal to noise ratio. Applications of SWV include the study of electrode kinetics with regard to preceding, following, or catalytic homogeneous chemical reactions, determination of some species at trace levels, and its use with electrochemical detection in HPLC.

The important parameters for pulse techniques are as follows:

- Pulse amplitude is the height of the potential pulse. This may or may not be constant depending upon the technique.
- Pulse width is the duration of the potential pulse.
- Sample period is the time at the end of the pulse during which the current is measured.
- For some pulse techniques, the pulse period or drop time must also be specified. This parameter defines the time required for one potential cycle, and is particularly significant for polarography (i.e., pulse experiments using a mercury drop electrode), where this time corresponds to the lifetime of each drop (i.e., a new drop is dispensed at the start of the drop time, and is knocked off once the current has been measured at the end of the drop time - note that the end of the drop time coincides with the end of the pulse width).

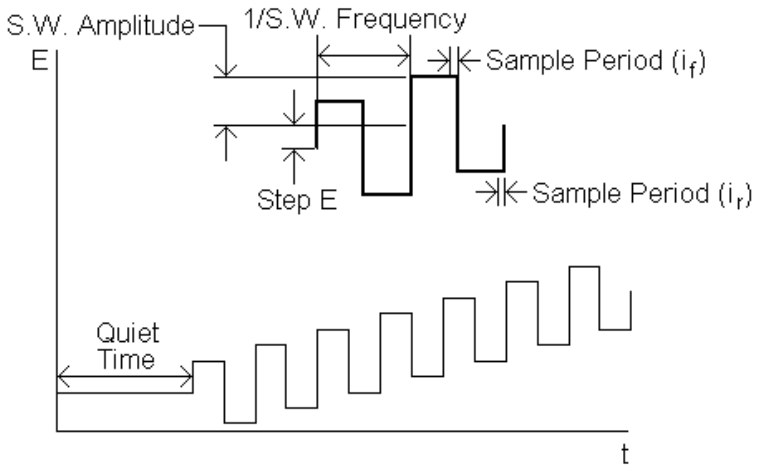

Figure 3.2: Potential form in square-wave voltammetry (SWV).

3.4. Preparation of WO_3 nanocrystal

Hydrothermal method

For the hydrothermal synthesis of WO_3 nanoparticles, 0.4 g of $Na_2WO_4 \cdot 2H_2O$ (Merck, Germany) were first dissolved in 8 g of deionized water with 0.15 g of NaCl (Merck, Germany) (as structure directing agent) and then acidified with 1 g of 6 M HCl solution .The final solution was transferred to 40 mL Teflon-lined stainless steel autoclave and installed in a oven (YCo-010 searies, GeMMY 888). The synthesis conditions were set at 180 °C for 1 h followed by a cooling period to room temperature inside the oven. The synthesis product was collected by centrifugation at 3000 rpm for 2 min (model: EBA 21) and washed three times with water. The final powder was finally dried in the oven (YCo-010 searies, GeMMY 888) at 60 °C for at least 8 h [127].

3.5. Modification of working electrode

GCE is used in this study for electrode modification using WO_3 nanoparticle obtained using hydrothermal methods. The modified electrode was prepared by a simple casting method (Fig. 3.1).

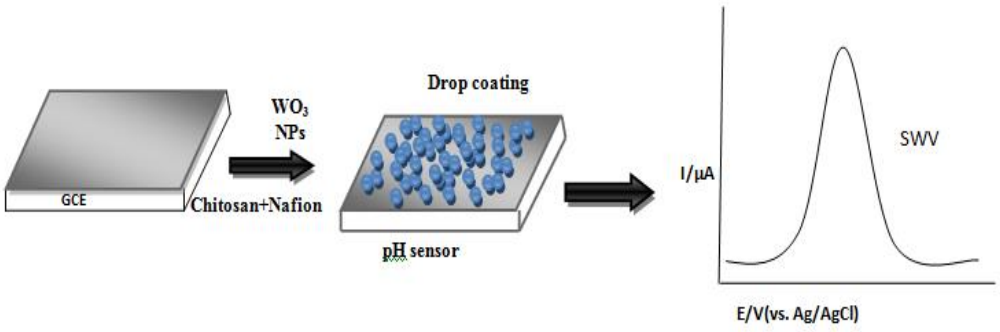

Figure 3.3: Schematic diagram of Modification of Working Electrode.

Prior to the surface coating, the GCE was polished with 1.0 and 0.3 µm alumina powder, respectively, and it was rinsed with water, followed by sonication in ethanol solution and water successively. Then, the electrode allowed drying in a stream of nitrogen. After that, 10 µL of WO_3 nanoparticle and 5 µL of 1% chitosan and 1% nafion was dropped on the clean surface of GCE, and it was dried at room temperature for overnight.

3.6. Preparation of pH Solution

Various pH solution were prepared using Phosphate buffer: 1.41 g disodium Hydrogen phosphate (0.01M), 1.56 g sodiumdihydrogen phosphate (0.1M), 0.84 g sodium hydrogen carbonate (0.1M), 0.4 g sodium hydroxide (0.1M), 13.6 g sodium acetate (0.5 M), 2.9 ml of acetic acid (0.5 M) and made to 100 ml with distilled water, the solution was adjusted to the appropriate pH with Orion 2 Star pH meter.

3.7. Standardization of the System

The whole electrochemical set-up was tested using a standard experiment. In the standard experiment we have studied the following redox couple at a GC electrode.

$$[Fe\ (III)\ (CN)_6]^{3-} + e^- \rightleftharpoons [Fe\ (II)\ (CN)_6]^{4-}$$

The reaction above was studied electrochemically by pumping electrons into the system from a GC electrode and by measuring the change in the flow of current during the reaction. This is done most conveniently by scanning the potential of the electrode at a constant rate.

In general, the peak current of diffusion controlled reversible or quasi-reversible electro - chemical reaction follows Randles–Sevcik equation

$$Ip = 0.4463nF\sqrt{\frac{nFD}{RT}}AC\sqrt{v}$$

Where ip: the peak current, n: the number of electrons, F: Faraday constant, T: the temperature in Kelvin, R: the gas constant, A: the surface area of the working electrode, D: the diffusion coefficient of the electro active species, C: the bulk concentration of the electro active species and *v*: the scan rate of voltammograms.

3.8. Electrochemical pH measurements

Cyclic voltammograms were performed over the definite potential range vs. Ag/AgCl in a cell containing 20.0 mL of 0.1 M buffer solution. The surface of the electrodes is completely immersed. The cell is deaerated for 5 minutes with high purity nitrogen gas. The solution has been kept quiet for 10 seconds. To determine the potential window, electrochemical scanning is carried out with the supporting electrolyte to obtain the background voltammogram.

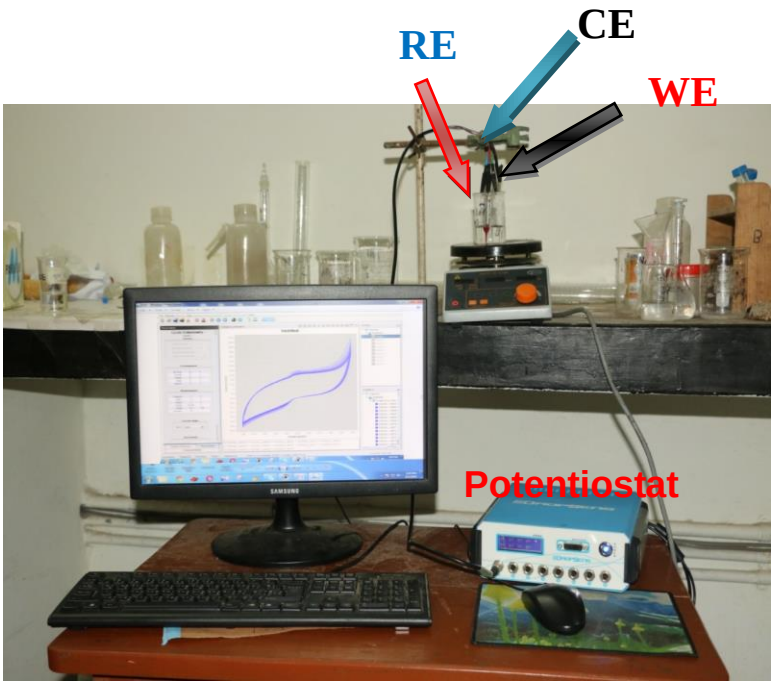

Figure 3.4: Electrochemical experimental setup

For SWV and OCP experiments, the voltage was switched directly from open circuit to the appropriate applied potential (vs. Ag/AgCl). Initially, studies were carried out with the

modified electrode in 0.1 M buffer solutions containing pH in order to determine whether the performance is suitable for the subsequent monitoring of the pH response. Square wave and OCP, were performed by applying a potential to the electrode immersed in a 20 ml of 0.1M buffer solution. The resulting real time potential responses were recorded over a period of time.

3.9. Removing Dissolved Oxygen from Solution

Dissolved oxygen can interfere with observed current response so it is needed to remove it. Experimental solution was indolent by purging for at least 5-10 minutes with 99.99% pure and dry nitrogen gas (BOC, Bangladesh). By this way, traces of dissolved oxygen were removed from the solution.

3.10. Reproducibility and repeatability measurements

To check the output response, stability, and repeatability of the electrode, the sample was tested three to four times in a PBS with pH ranging from 3 to 11. It was observed that the WO_3 NPs showed stable potentiometric response, excellent reproducibility, and good sensor stability.

3.11. Drift and stability measurements

To determine the contribution the signal drift played, a SWV was recorded every 30 min for two hours in three buffer solutions with a pH of 5, 7 and 9. These solutions were chosen as representatives of the three states of the solutions: acidic, basic and neutral. This shows that the signal may take between 0 and 30 minutes to stabilize, depending on the pH. To measure the stability, the signal was recorded up to 7 days.

3.12. Real sample test

As it is evident from the previous work that new electrode which are proposed by different researchers for the sensing of pH usually avoid applying them for the sensing pH in real unbuffered samples. However, in this work, we have validated our sensor against the laboratory standard glass pH electrode in the real sample: malt vinegar and antacid.

The next chapter we will describe more about result and discussion on the development of a novel pH sensor.

Chapter IV

Results and discussion

4.1. Electrochemical setup standardization

Cyclic voltammograms (CVs) of ferricyanide at glassy carbon electrode were performed at concentration of 2mM of ferricyanide 0.1 M KCl as supporting electrolyte, each solution was scanned at different scan rate equal to 20, 40, 60, 80, 100, 120, 140, 160 mV/s. The resultant CV curves and the electrochemical parameters are shown respectively in Figure 4.1 and Table 4.1.

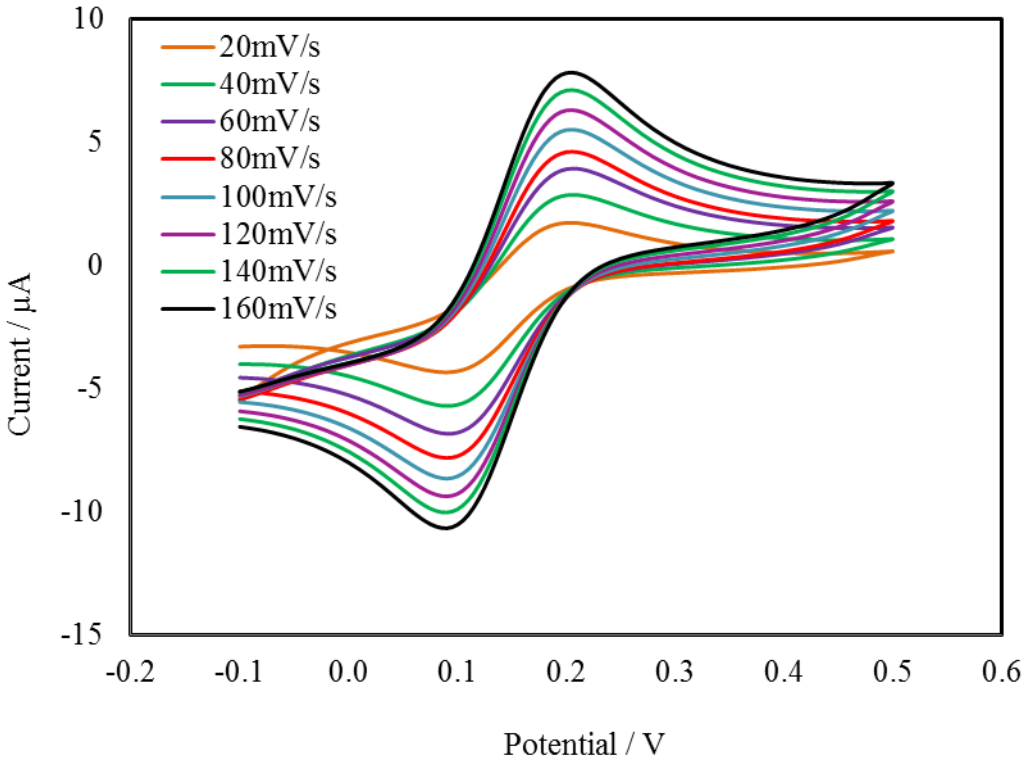

Figure 4.1: CVs of ferricyanide at glassy carbon electrode were performed at concentration of 2mM of ferricyanide 0.1 M KCl as supporting electrolyte, different scan rate 20, 40, 60, 80, 100, 120, 140, 160 mV/s.

Table 4.1: Electrochemical parameters obtained from voltammograms of Figure 4.1

scan rate Vs^{-1}	SQRT of scan rate ν1/2	anodic peak potential (Epa)	cathodic peak potential (Epc)	anodic peak current (i_{pa})	cathodic peak current (i_{pc})	i_{pa}/i_{pc}
0.02	0.141421	0.19	0.10	2.198	2.098	1.0476
0.04	0.20	0.19	0.11	3.224	3.013	1.0700
0.06	0.244949	0.19	0.10	4.201	3.830	1.0698
0.08	0.282843	0.19	0.11	4.903	4.781	1.0251
0.10	0.316228	0.19	0.11	5.700	5.191	1.0980
0.12	0.34641	0.19	0.11	6.389	6.105	1.0465
0.14	0.374166	0.19	0.10	7.060	6.838	1.0324
0.16	0.4	0.19	0.11	7.686	7.081	1.0854

ν = scan rate; ν1/2= SQRT of scan rate; Epa= anodic peak potential; Epc= cathodic peak potential; ipa= anodic peak current; ipc= cathodic peak current.

In general, the peak current of diffusion controlled reversible or quasi-reversible electro - chemical reaction follows Randles–Sevcik equation

$$Ip = 0.4463nF\sqrt{\frac{nFD}{RT}}\,AC\,\sqrt{v}$$

Where ip: the peak current, n: the number of electrons, F: Faraday constant, T: the temperature in Kelvin, R: the gas constant, A: the surface area of the working electrode, D: the diffusion coefficient of the electro active species, C: the bulk concentration of the electro active species and *v*: the scan rate of voltammograms. Thus, if we know the value of diffusion coefficient of ferricyanide at 298K the surface areas for ferricyanide are calculated from the slope of the plot of ip versus √v (Figure 4.2).

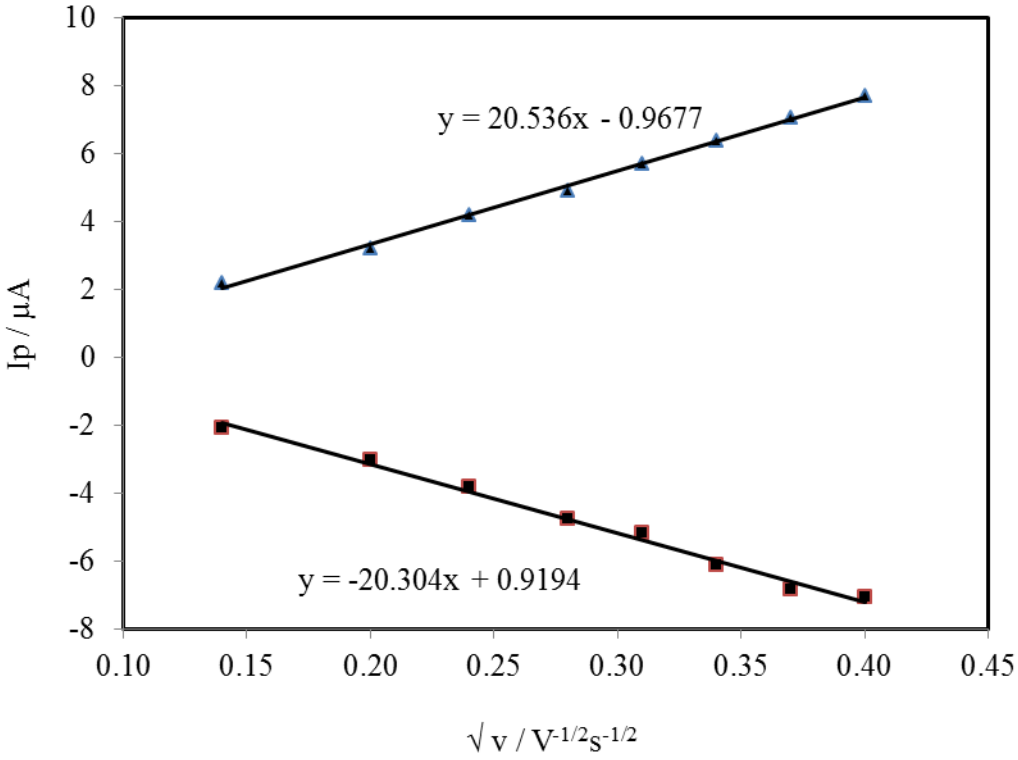

Figure 4.2: The anodic and the cathodic peak heights as function of the square root of the scanning rate for platinum electrode.

From Equation (1) we get,

$$\text{Slope} = 0.4463nF\sqrt{\frac{nFD}{RT}}AC$$

$$A = \frac{Slope}{0.4463nF\sqrt{\frac{nFD}{RT}}C}$$

From the curve (Figure 4.2) the value of slope is 20.536×10^{-6} and the standard value of diffusion coefficient for ferricyanide in GCE is 1.52×10^{-6} cm^2/s. where concentration C = 2×10^{-6} mol/cm^3 so we get,

$$A = \frac{20.536\times10^{-6}}{0.4463\times1\times96500\sqrt{\frac{1\times96500\times1.52\times10^{-6}}{8.314\times298}}\times2\times10^{-6}}$$

$$A = 0.0285\ cm^2$$

From the theoretical value the surface area of GC electrode i.e. used for experiment is $0.03cm^2$. We show that the experimental value of surface area is very close to theoretical value. This calculated result has been used in further studies. Also it proves that the electrochemical work station uses with minimum interferences.

4.2. Synthesis of nanoparticle and its physical characterizations

The morphology of the hydrothermally synthesized WO_3 nanoparticles was observed by SEM with a magnification of (20000X to 80000X) (Figure 4.3). The particle size was estimated to be approximately 100 nm, resulting in agglomerated nano globular type shape. The WO_3 crystalline structure was verified by XRD. The peaks all can be indexed to the planes of different tungsten oxide sample (Figure 4.4). Due to the peak position and intensity, the WO_3 and $WO_{2.92}$ are the main component of tungsten oxide nanoparticles. According to the EDX results (Figure 4.5), the average content of tungsten (W) and oxygen (O) is 24.5% (atomic percentage) and 75.5%, which confirm the tungsten oxide (W: O=1:3) component, also verified that the all the peaks corresponds to tungsten oxide. As shown in Raman spectra (Figure 4.6), the strong peaks at 643 and 820 cm^{-1} correspond to O-W-O stretching band. The peak at 235 and 307 cm^{-1} represent the bending vibration δ (O–W–O). The bond at 432 cm^{-1} assigned to W-O. The peak at 946 cm^{-1} can be attributed to the terminal -W=O bond. These bonds further confirm the formation of tungsten oxide nanoparticle [128]. Therefore, from all the characterization results, it can be concluded that the hydrothermally synthesized WO_3 nano particle is formed by agglomerates of globular type shape with average particle size of less than 100 nm. The reduced nano particle size has higher surface area that exposed to the test environment and better response to pH changes [127].

$$2Na^+ + WO_4^{2-} \longrightarrow WO_2(OH)_2 + 2NaCl$$

$$2[WO_2(OH)_2 + 3H_2O \longrightarrow [WO(OH)_3.H_2O]_2$$

$$[WO_3.H_2O]_n \longrightarrow [WO_3]_n + nH_2O$$

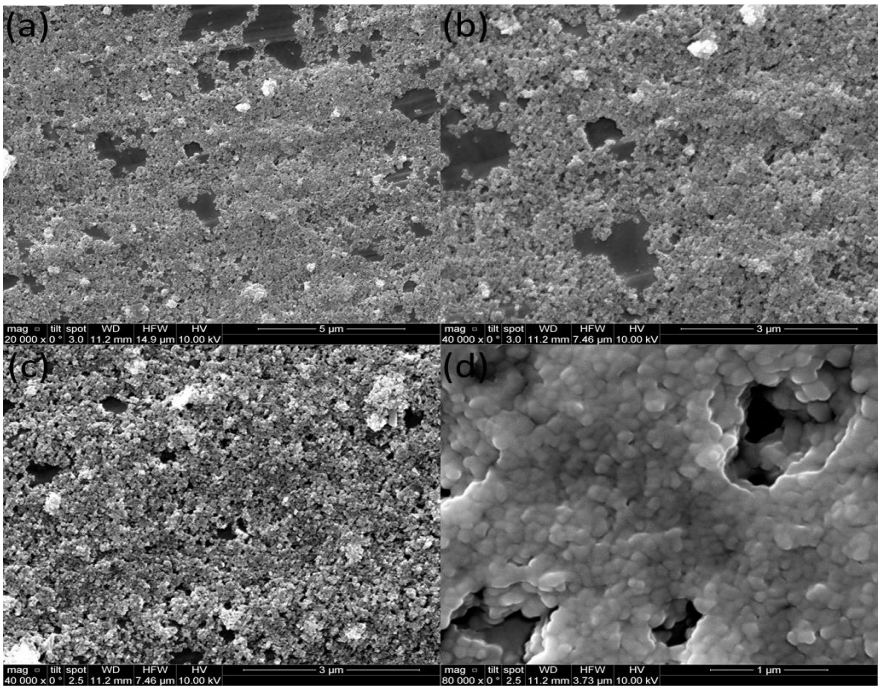

Figure 4.3: (a-d) Scanning electron microscopy (SEM) images of WO_3 nanoparticles at different magnifications (20000 to 80000X)

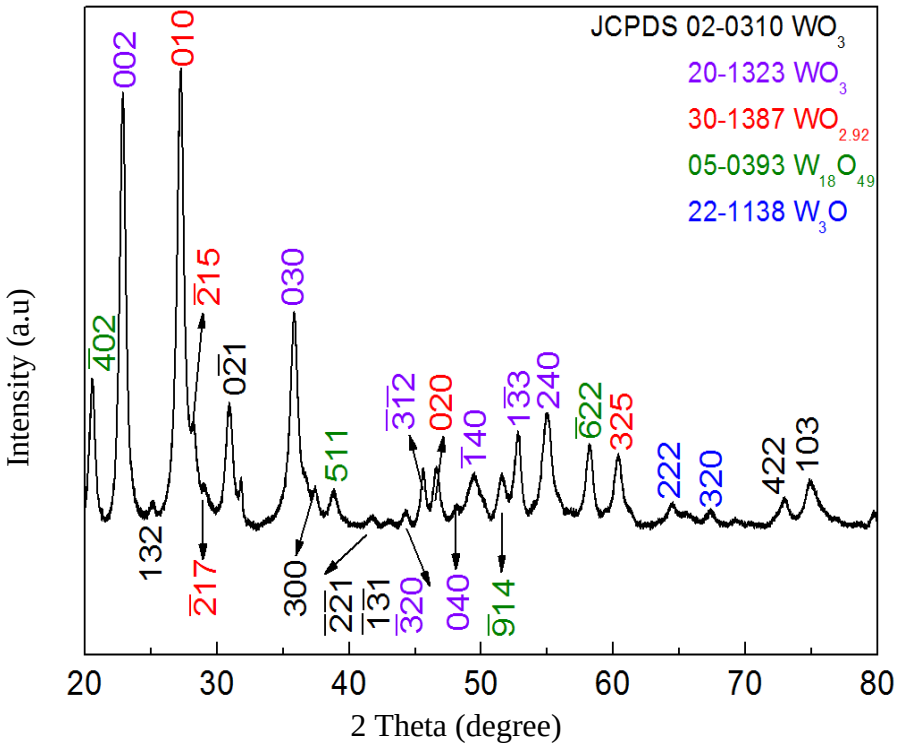

Figure 4.4: X-ray diffraction (XRD) patterns of WO_3 nanoparticles

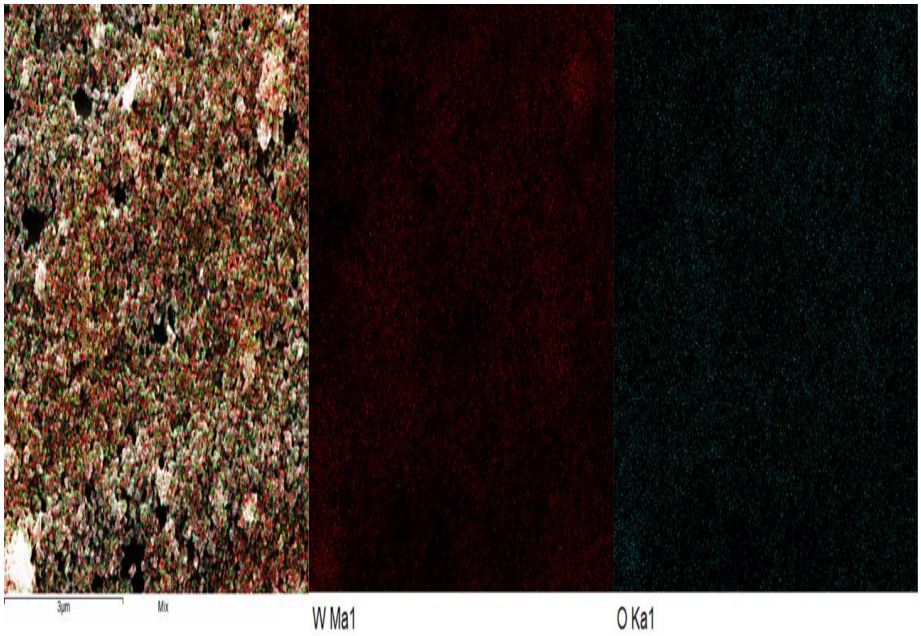

Figure 4.5: Energy Dispersive X-ray spectroscopy (EDX) images of WO_3 nanoparticles

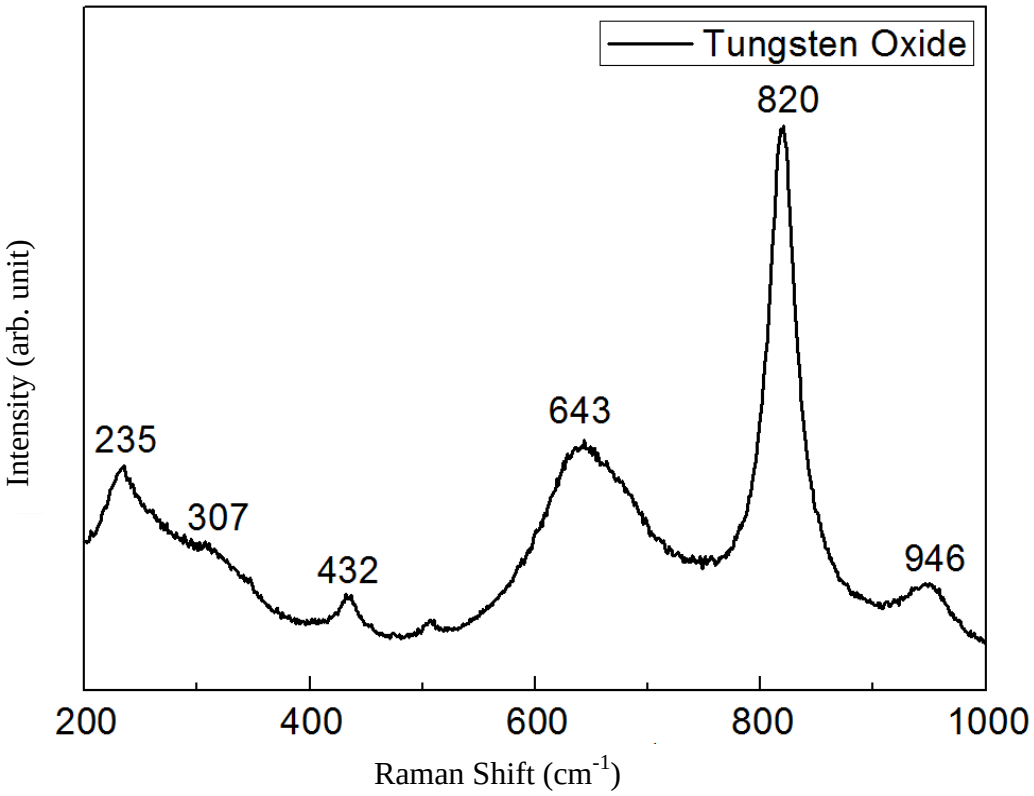

Figure 4.6: Raman spectra of WO_3 nanoparticles

4.3. Sensor fabrication

GCE is used in this study for electrode modification using WO_3 nanoparticle. The modified electrode was prepared by a simple casting method [129]. Prior to the surface coating, the GCE was polished with 1.0 and 0.3 µm alumina powder, respectively, and was rinsed with water, followed by sonication in ethanol solution and water successively. After that, 10 µL of WO_3 nanoparticle and 5 µL of 1% chitosan and 5 µL of 1% nafion mixture was dropped on the clean surface of GCE, and was dried at room temperature for overnight (Figure 4.7).

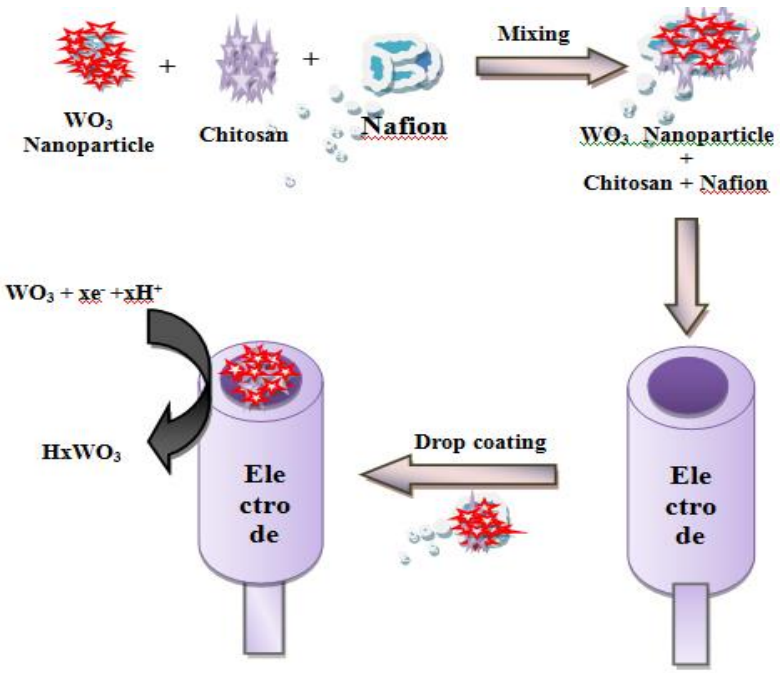

Figure 4.7: Schematic diagram of stepwise fabrication of the pH sensor

4.4. Electrochemical characterization of WO_3 nanoparticle modified GCE

To demonstrate the sensing application of WO_3 nanoparticle, a novel pH sensor was constructed by deposition of the aqueous dispersion of WO_3 nanoparticle on to GCE surface in the presence of chitosan and Nafion. CVs were recorded for WO_3/GCE at 0.1M

PBS, pH 7 at different scan rates, in the range of 60-160 mVs^{-1}. Both the anodic and cathodic currents increases linearly with the scan rate (Figure 4.8), indicating that the electrochemical reaction is surface control. The current increases with scan rate for the sensor shows no significant resistance on the electrode surface [130].

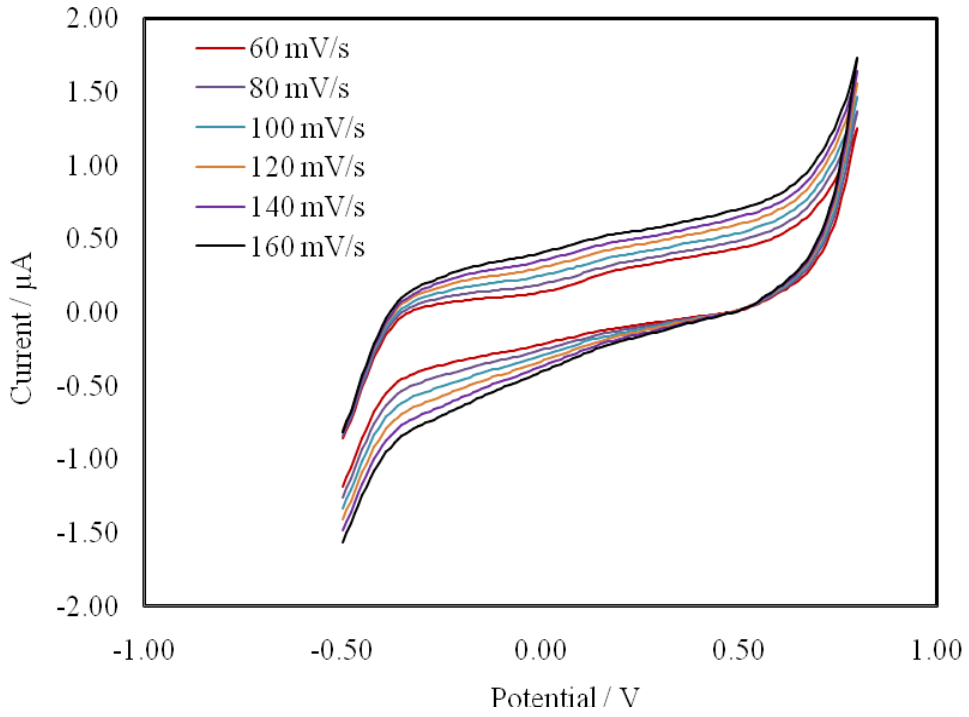

Figure 4.8: CVs detailing the effect of scan rate (60 - 160) mV / s using WO_3/GCE at 0.1M PBS.

4.5. Electrochemical characterization of WO_3 nanoparticle modified AuE

At first, we investigated the electrochemical behavior of WO_3 modified gold (WO_3/AuE) using CV (Figure 4.9) and SWV (Figure 4.10) in 0.1 M buffer solution with pH ranging 3 to 11 at a scan rate of 0.05 Vs^{-1}. It is seen that AuE exhibits peak potential with different pH value, but their potential change is randomly. That's why the total potential change is irregular and no potential change is linearly (Figure 4.11) obtained for gold electrode. It can be concluded that the AuE is not good for sensing pH.

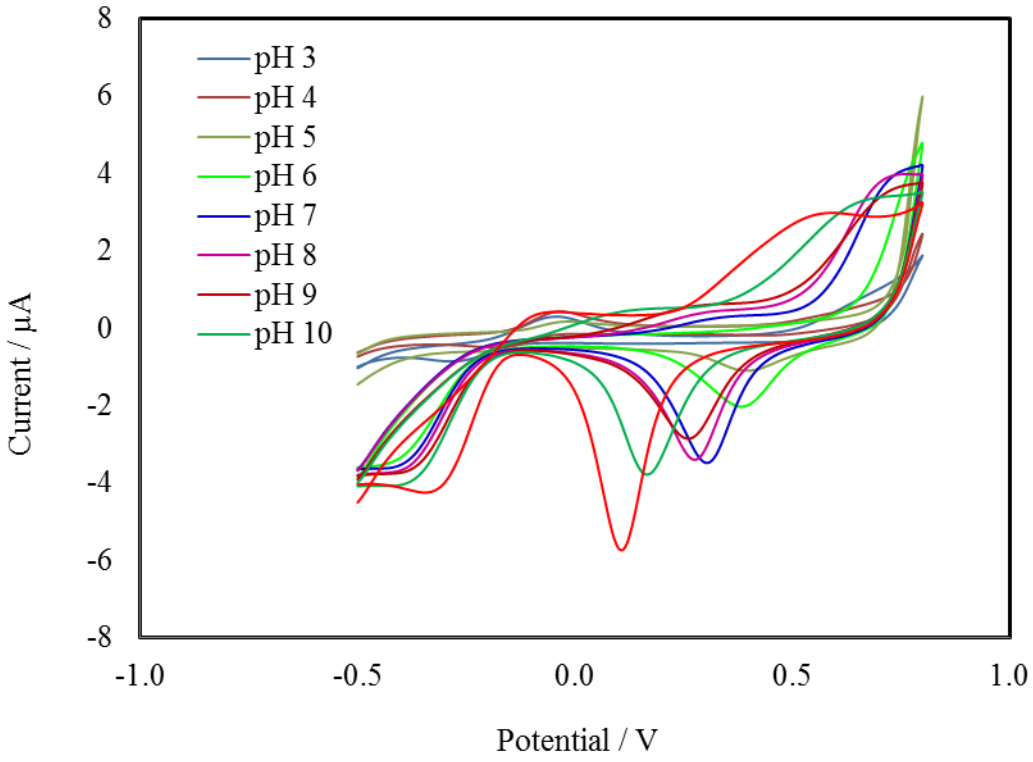

Figure 4.9: CVs of 0.1 M buffer at different pH values in the presence of WO_3/AuE (scan rate 0 .05 V / s).

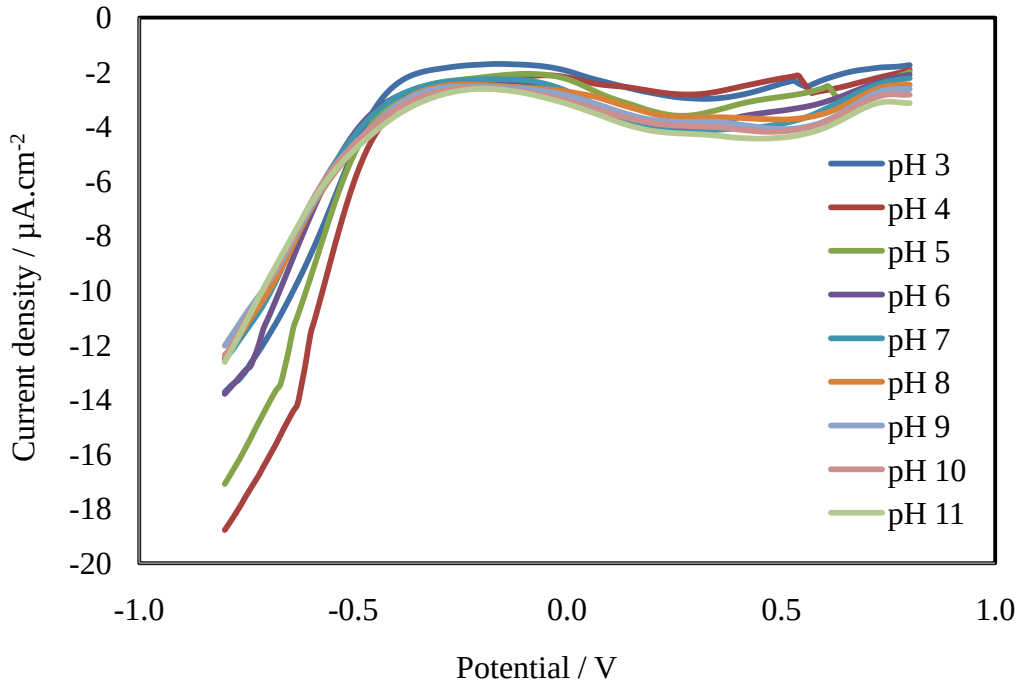

Figure 4.10: SWV of 0.1 M buffer at different pH values in the presence of WO_3/AuE.

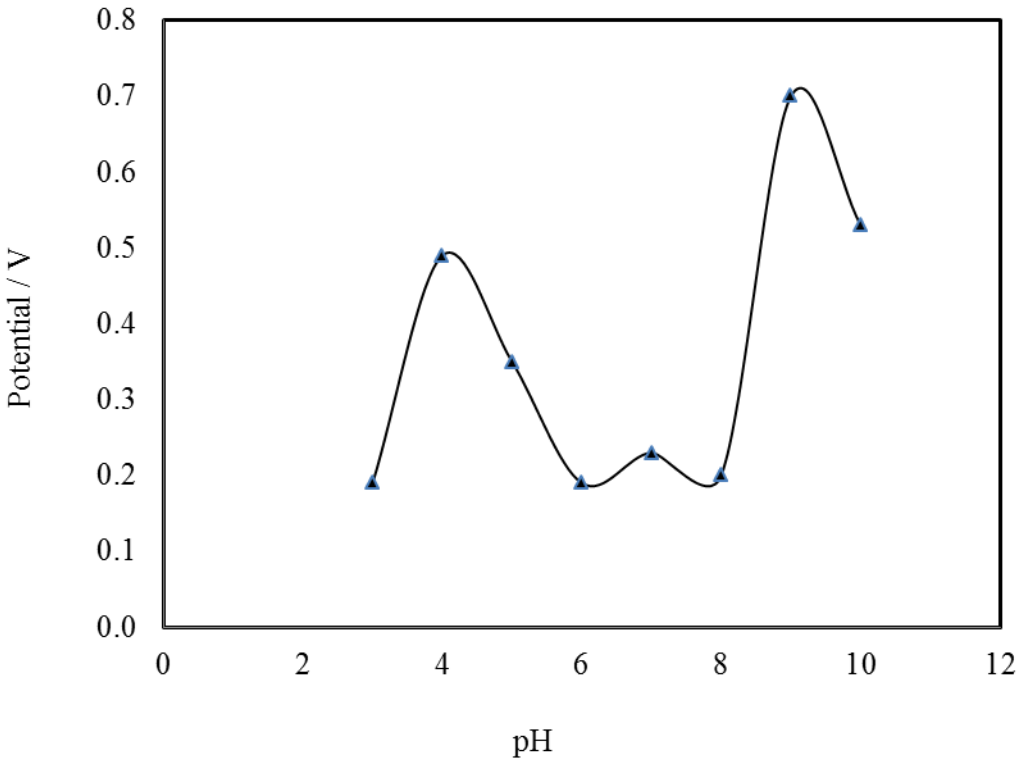

Figure 4.11: pH sensitivity measured from pH 3 to 11 using WO_3/AuE.

4.6. Electrochemical characterization of Bare GCE

Then, we investigated the electrochemical behavior of bare GCE using CV (Figure 4.12) and SWV (Figure 4.13) in 0.1 M buffer solution with pH ranging 3 to 11 at a scan rate of 0.05 Vs^{-1}. It is seen that bare GCE exhibits peak potential with different pH value, but their potential change is randomly. That's why the total potential change is irregular and no potential change is linearly (Figure 4.14) obtained for bare GCE. It can be concluded that the bare GCE is not good for sensing pH.

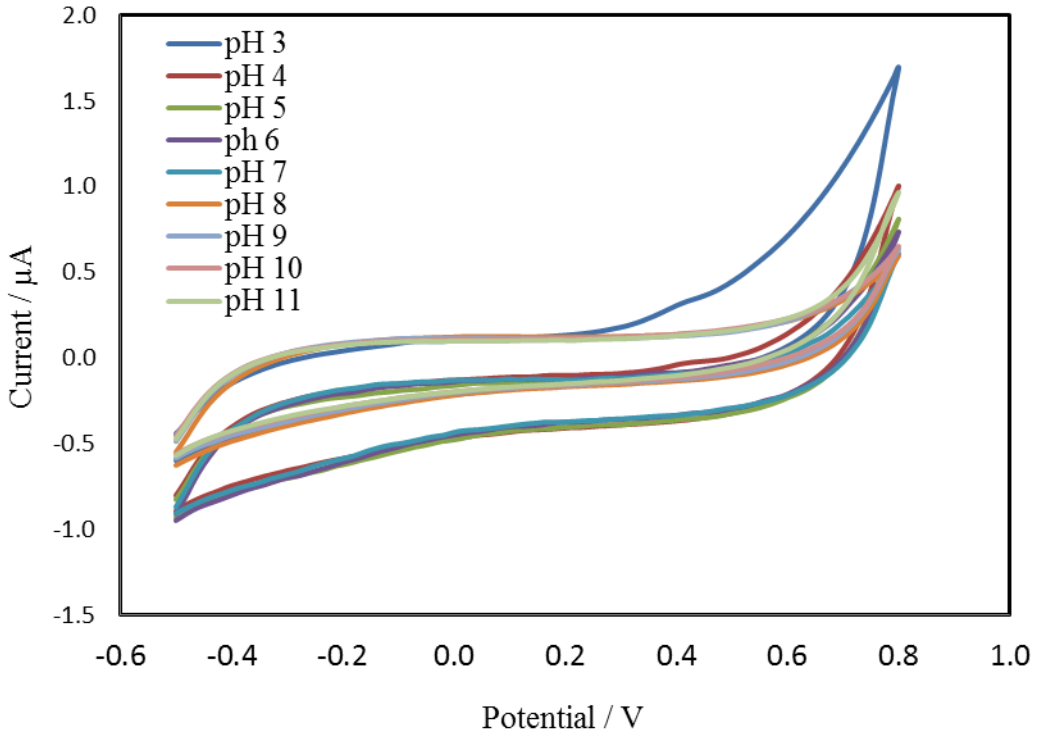

Figure 4.12: CVs of 0.1 M buffer at different pH values on bare GCE.

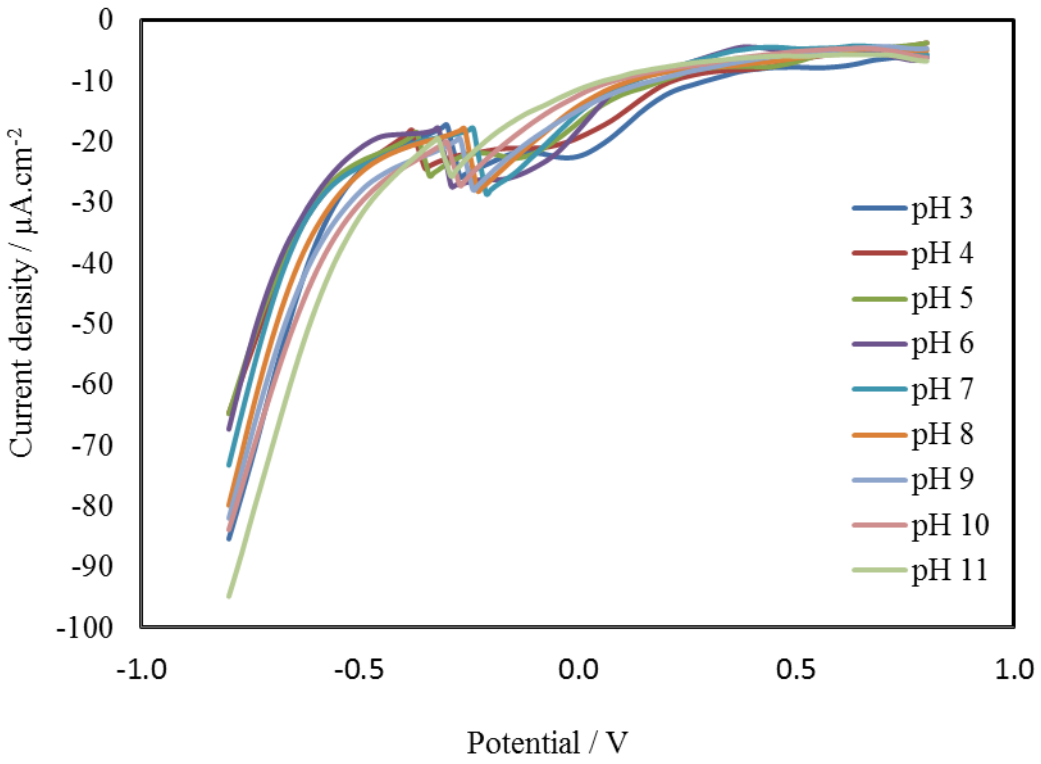

Figure 4.13: SWV of 0.1 M buffer at different pH values (3-11) on bare GCE.

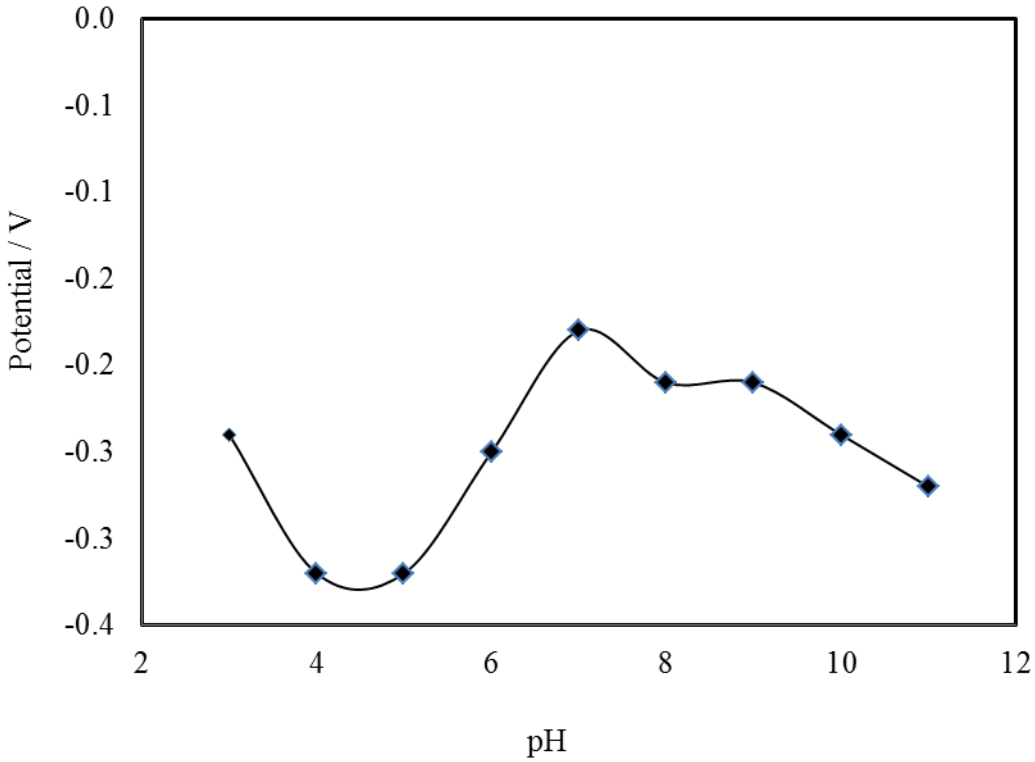

Figure 4.14: pH sensitivity measured from pH 3 to 11 at bare GCE.

4.6.1. Electrochemical characterization of NiO/GCE using SWV

Previously we discuss the electrochemical behavior of modified gold electrode and bare GCE, now we discuss the electrochemical behavior of NiO nanoparticle modified GCE. At first NiO nanoparticle was modified on GCE, that's collected from my group and then their electrochemical behavior was investigated using CV (Figure 4.15) and SWV (Figure 4.16) of NiO modified GCE in 0.1M different pH value at scan rate of 0.05 VS^{-1}.

It is seen that the modified NiO/GCE exhibits weak peak potential shifts in different pH value and these potential change is randomly. That's why the total potential change is irregular for modified NiO/GCE and no potential change is linearly obtained shown in (Figure 4.17). It can be concluded that NiO nanoparticle cannot sensing pH.

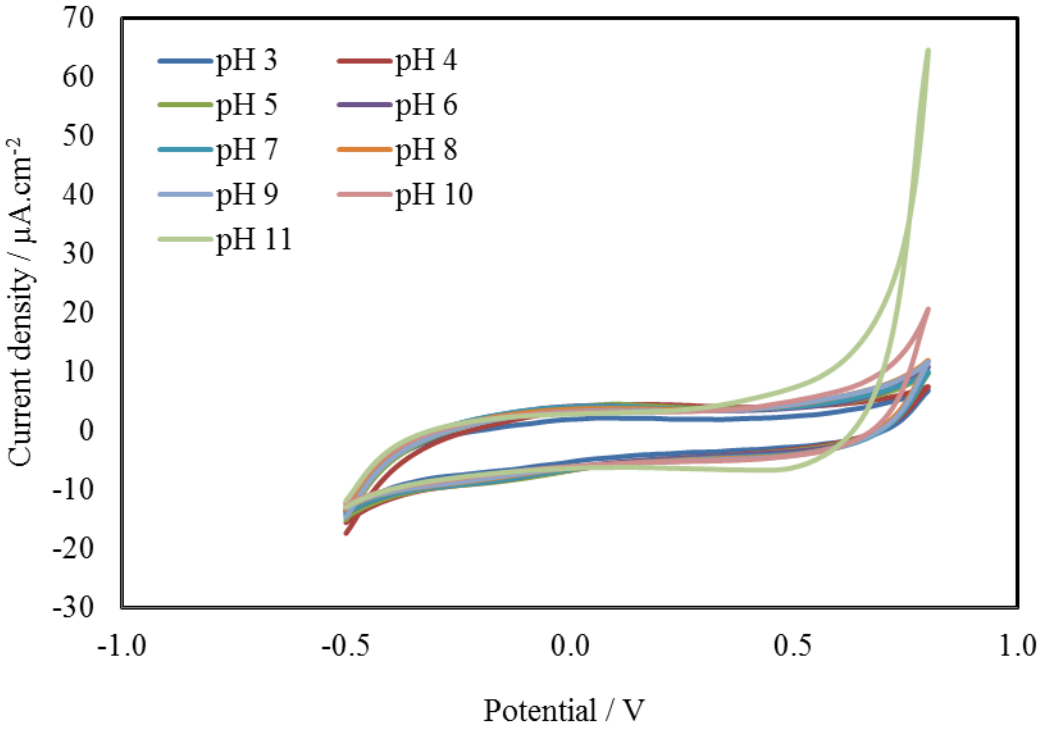

Figure 4.15: CVs of 0.1 M buffer at different pH values in the presence of NiO/GCE.

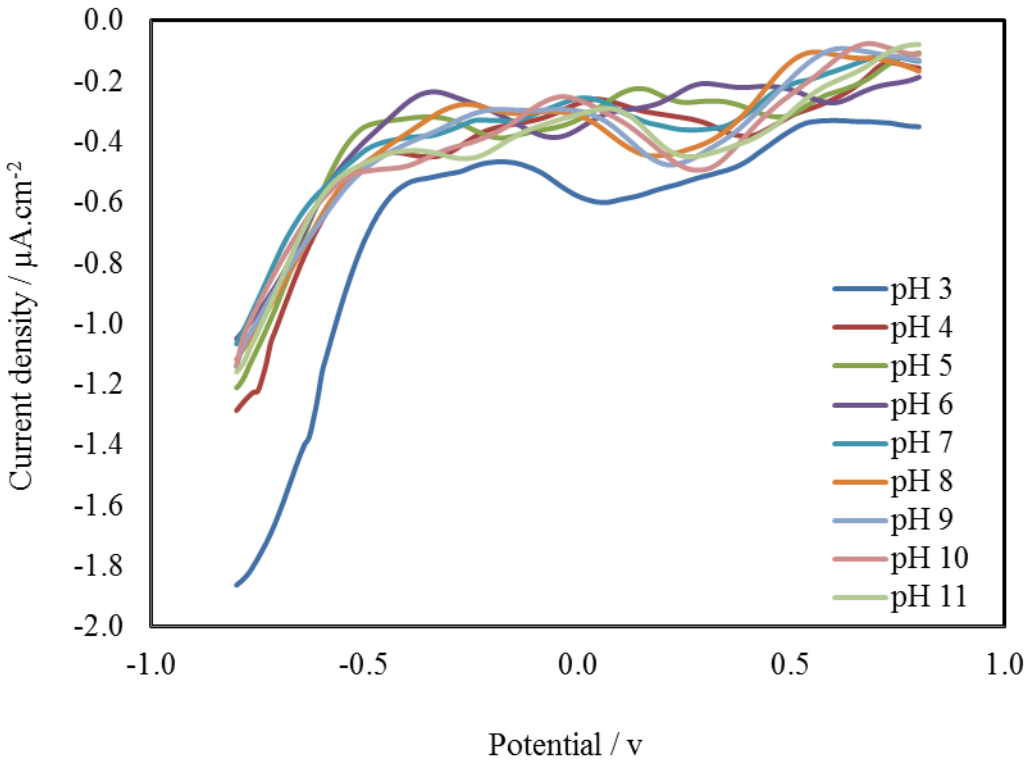

Figure 4.16: SWV of 0.1 M buffer at different pH values (3-11) in the presence of NiO/GCE.

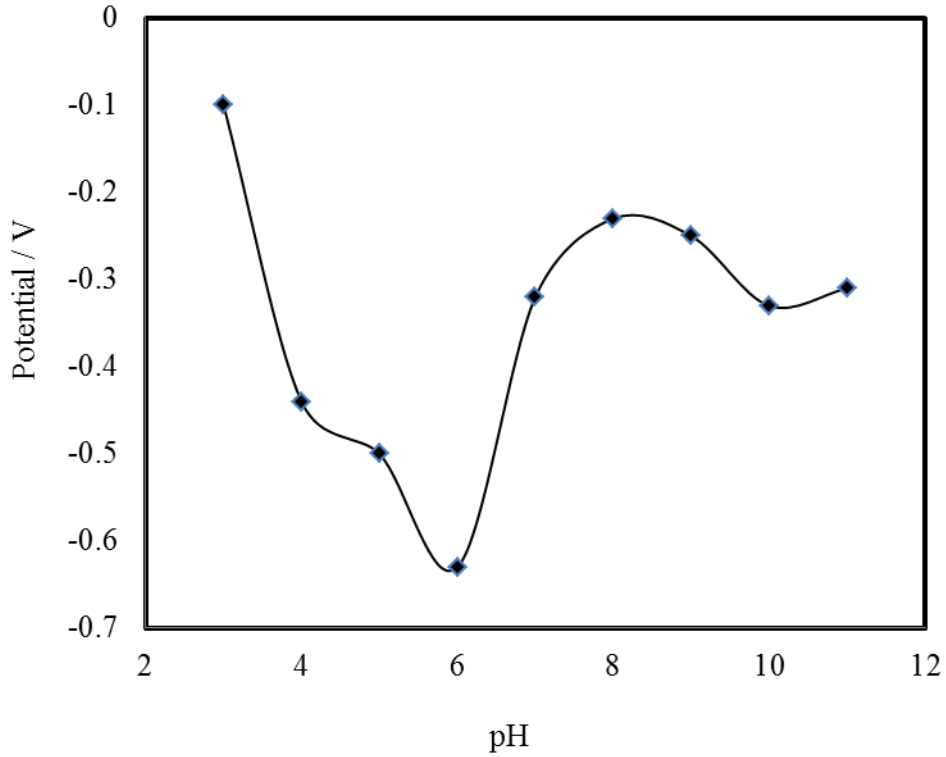

Figure 4.17: pH sensitivity measured from pH 3 to 11 using NiO/GCE.

4.6.2. Electrochemical characterization of WO_3 /GCE using SWV

Since the principal focus of this paper is on the fabrication of a pH sensor, the SWV response of the WO_3 modified GCEs was recorded in a series of aqueous buffer solutions ranging from pH 3 to pH 11. SWV was chosen since it can be swept at much faster speeds and was found to be more sensitive compared to other voltammetric methods [131].

Several different accurately measured 0.01M buffer (HCl, PBS) [132] ranging from pH 3-11 were electrochemically tested with SWV using GCE and WO_3/GCE, scanning catholically from positive to negative potentials, a clear single reduction peak is realized. As can be observed from (Figure 4.18, 4.19), increasing the pH results more negative over potentials as well as their being peaks with lower intensity. This observation attributes to less proton available while pH increases, limiting the amount of species that can be reduced.

The sensing mechanism for this material is possibly due to the redox reaction involving the double injection of cations and electrons to the structure. Thus forming a tungsten oxide bronze with higher conductivity than tungsten oxide.

$$WO_3 + xe^- + xH^+ \longrightarrow HxWO_3$$

x corresponds to the number of protons (H^+); and electrons (e^-) involved in the reaction and $HxWO_3$ represents the tungsten bronze. The reaction mechanism is explained by means of small polaron transition (formation of W^{5+} sites) for amorphous film and drude-like free electron scattering for crystalline films. The measured difference between these two mechanisms for amorphous and crystalline tungsten oxide film is the electron localization or delocalization [133-135]. The measured potential is therefore dependent on the pH and if there is a linear relation between these two parameters, then it is described to have a Nernstian behavior. The sensitivity of the sensor can in that case be obtained by the slope of the linear regression according to the equation [136].

$$E = E^0 - (2.303RT/F)\ pH = E^0 - 0.05916pH$$

Where E^0 corresponds to the standard electrode potential, R is the gas constant, T is the temperature, and F is the faradays constant. The resulting theoretical maximum sensitivity is -59 mV /pH. In this situation all space charges are formed, owing to the redox reaction, indicating a good performance of the sensor. The pH sensor produced in this work (Figure 4.20) demonstrated a mean sensitivity value of 60 ± 0.01 mV/pH which is close to the theoretical value. The correlation coefficient of R^2 values of about 0.999. This confirms the good sensitivity of the WO_3 nano particle to the variation of proton concentration in solution due to the redox reaction involved in the process.

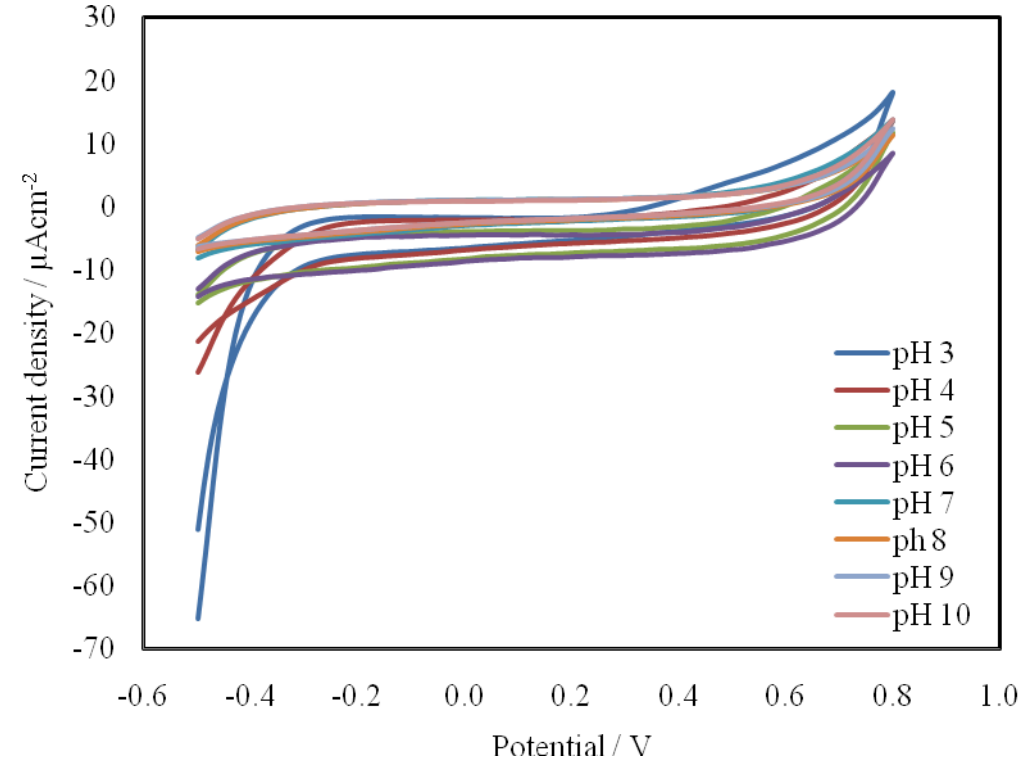

Figure 4.18: Cyclic voltammetry of 0.1 M buffer at different pH values (3-11) on WO_3/GCE.

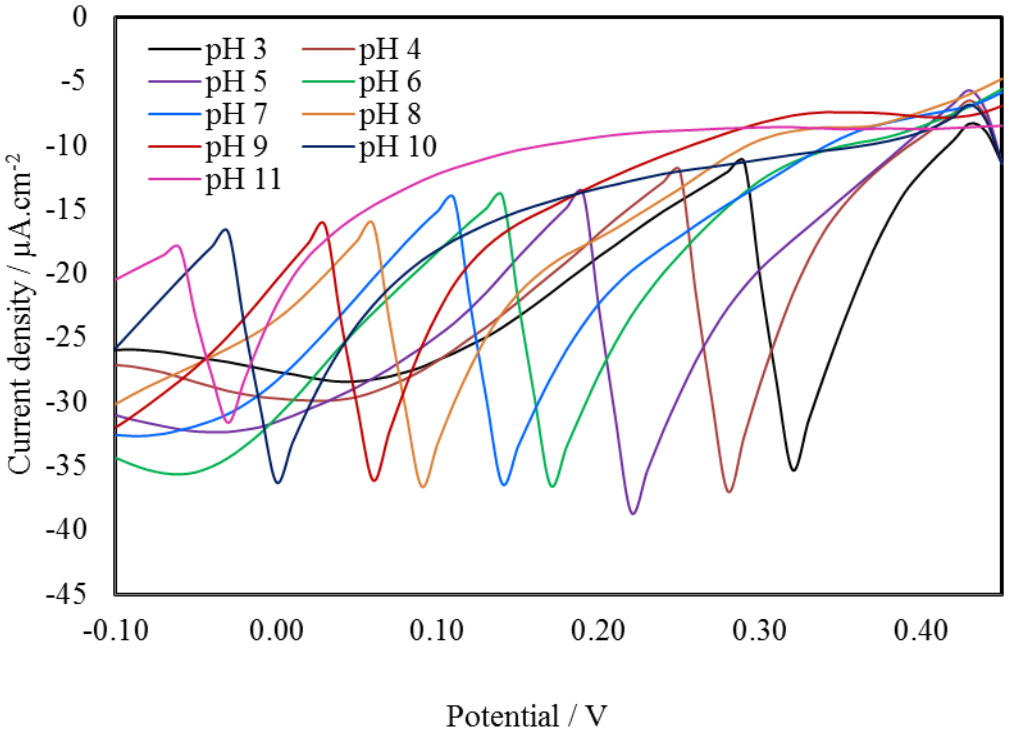

Figure 4.19: SWV of 0.1 M buffer at different pH values (3-11) on WO_3/GCE.

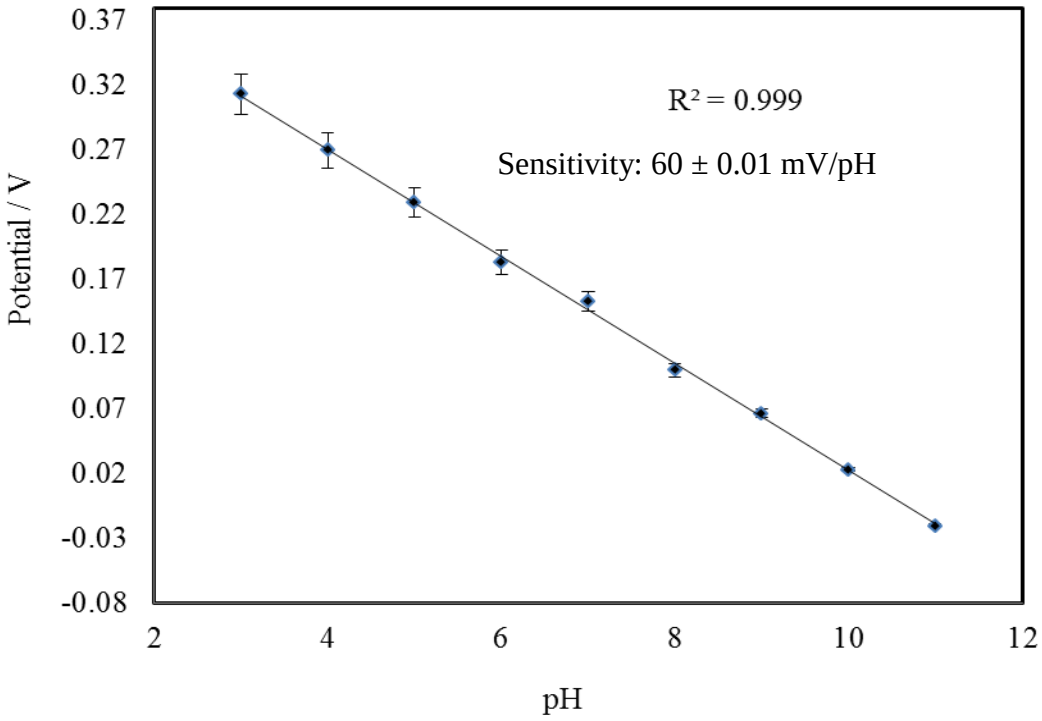

Figure 4.20: pH sensitivity measured from pH 3 to 11 usingWO_3/GCE.

4.6.3. Zero current potentiometric (OCP) sensing and analytical performance of pH sensor.

The pH sensitivity was also confirmed by measuring the OCP when dipping the electrode in buffer solution for 120 s. Figure 4.21- 4.22 shows electrodes OCP as a function of time to step pH changes of buffer solution between pH 3-11. The pH changes were realized by changing pH buffer solutions. The calibration of the electrode was carried out in both directions, from pH 3-11 and vice versa. It is apparent that the electrodes provide an excellent reversibility and the potential response was independent against pH value or direction of pH changes. The potential response of the prepared electrode demonstrates pH sensitivity of 65 mV/pH. By measuring both SWV and OCP, it has been found that WO_3/GCE can successfully sense the pH ranging from 3 – 11.

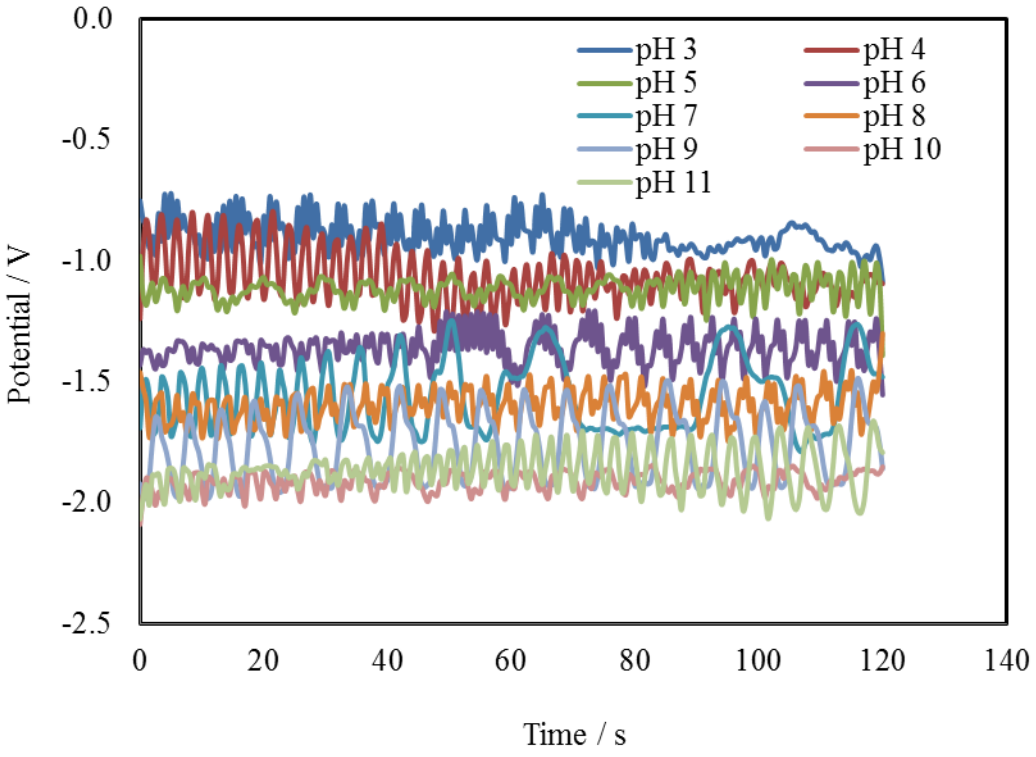

Figure 4.21: Zero current potentiometry (OCP) of 0.1 M buffer at different pH values in the presence of WO_3/GCE.

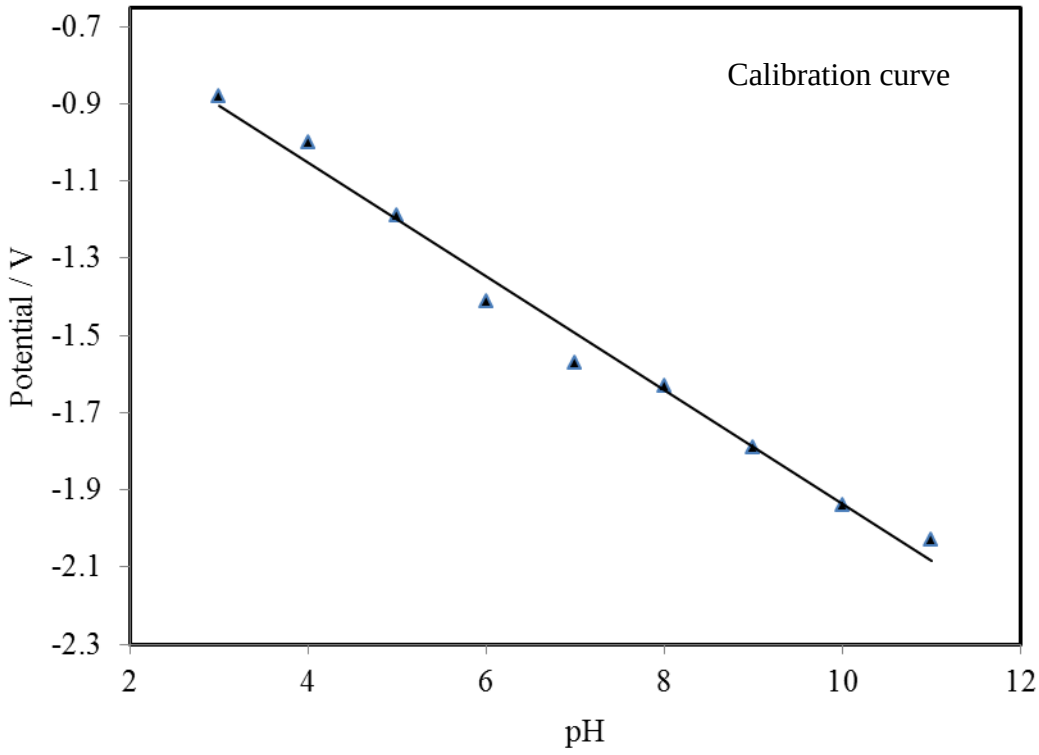

Figure 4.22: pH sensitivity measured from pH 3 to 11 using WO_3/GCE.

4.7. Electrochemical characterization of WO_3 /GCE in the presence and absence of oxygen

The possibility of the WO_3/GCE to be utilized in both an oxygenated and de-oxygenated environment was evaluated. (Figure 4.23) shows the voltametric response of the WO_3 immobilized GCE, when the electrode was placed in buffer solution both in the presence and absence of oxygen. This oxygen-free environment can then be compared to the same measurement under ambient conditions, when oxygen is naturally present in the atmosphere. It can be clearly seen that the only difference is slight increase in the reductive current in the presence of oxygen. It can therefore be concluded that this sensor can be utilized to measure the pH of solutions, irrespective of the O_2 concentration. Similar tests have been obtained by Jamal et al. [16] work where author have modified anthraquinone–ferrocene (AQ–Fc) complex based on a vertically aligned gold nanowire array electrode (AuNAE).

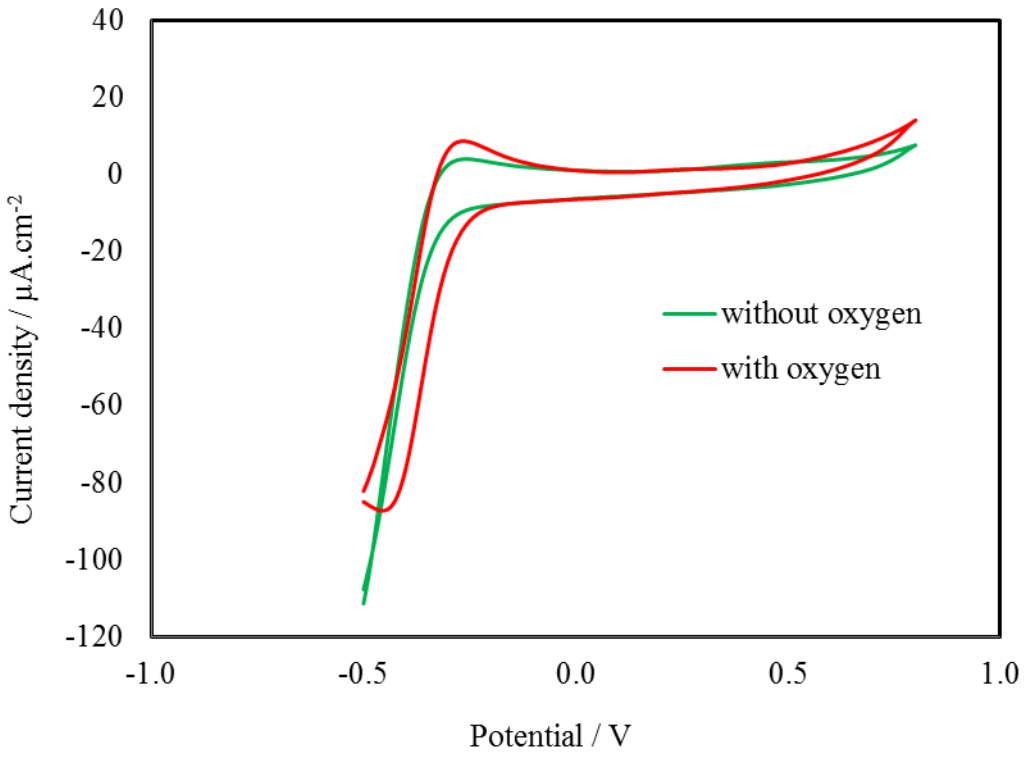

Figure 4.23: CVs showing the response of the WO_3 immobilized layer to the presence and absence of oxygen at pH 6 PBS buffer.

4.8. Real sample test

As is evident from the literature, new electrodes that are proposed for the sensing of pH mostly neglect to apply them to the sensing of pH in "real" unbuffered samples [137, 138]. Consequently, the proposed analytical pH sensing protocol herein is validated against the laboratory standard glass probe pH sensor in the "real" unbuffered samples: a commonly available antacid and malt vinegar. The electro analytical SWV and OCP signals gained are visible in Figure (4.24 - 4.27) and comparable values of pH was obtained, with an antacid a pH value of 9.00 and malt vinegar a pH value of 4.00 from the WO_3/GCE. This demonstrates there is potential for this approach to be developed into a portable, hand-held, voltammetric pH sensor using WO_3 nanoparticle modified GCE.

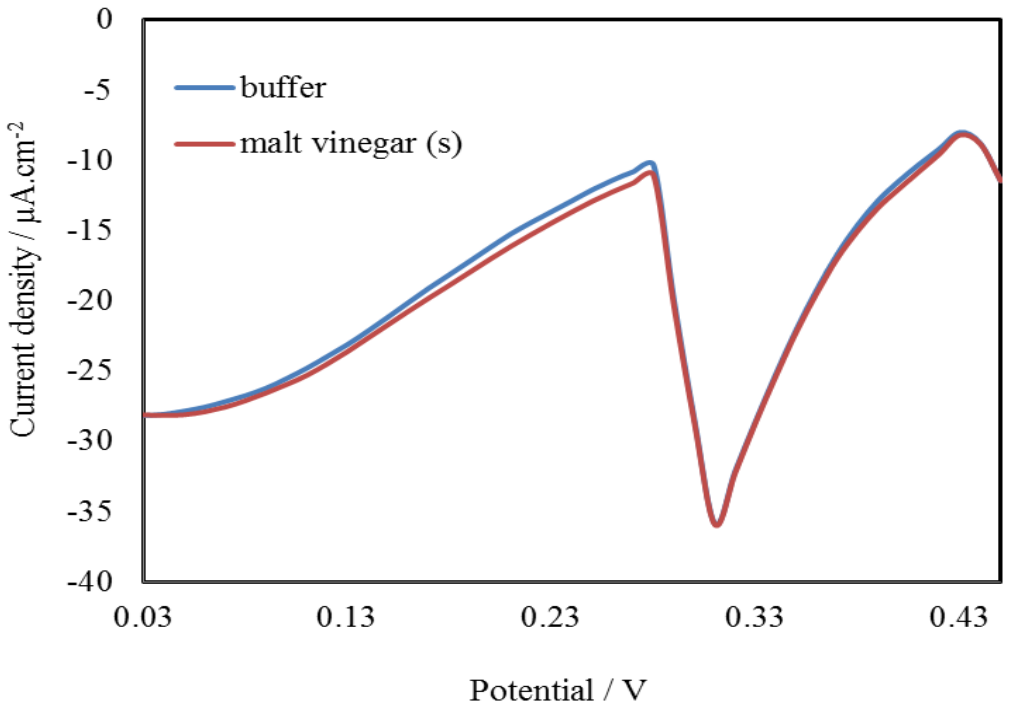

Figure 4.24: Electrochemical signal (SWV) obtained in "real" unbuffered samples for malt vinegar using WO_3 / GCE.

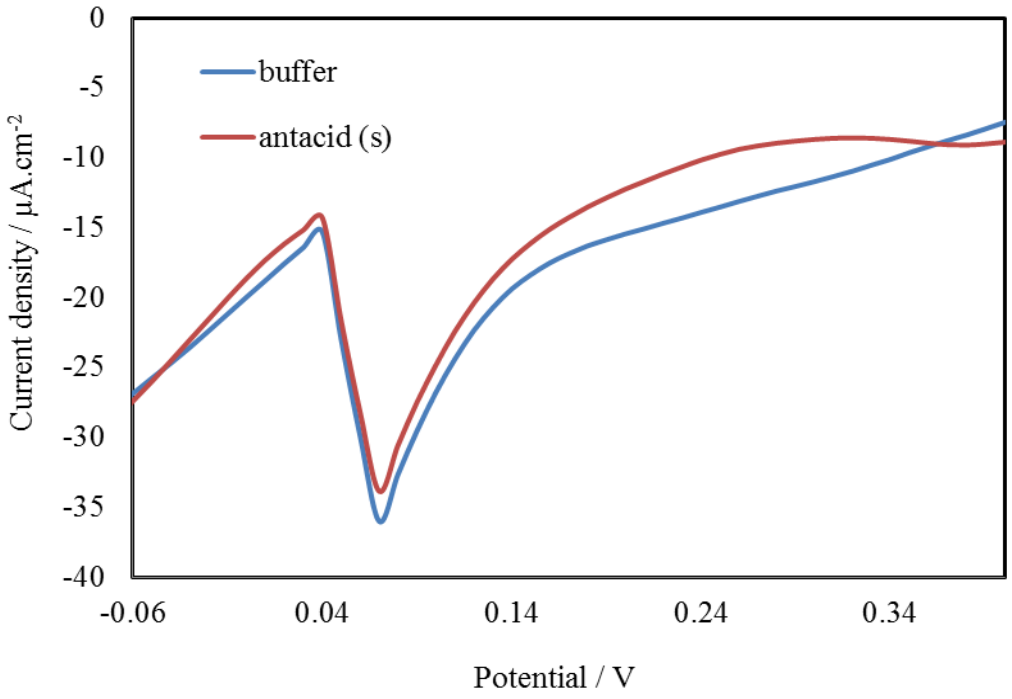

Figure 4.25: Electrochemical signal (SWV) obtained in "real" unbuffered samples for antacid using WO_3/GCE.

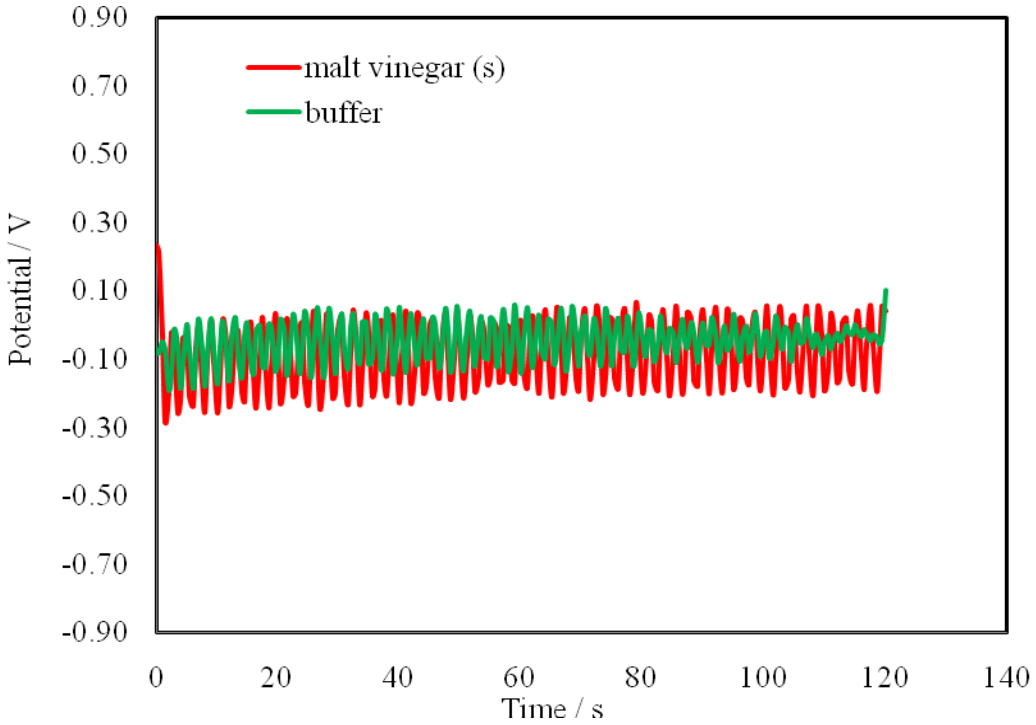

Figure 4.26: Electrochemical signal (OCP) obtained in "real" unbuffered samples for malt vinegar using WO_3/GCE.

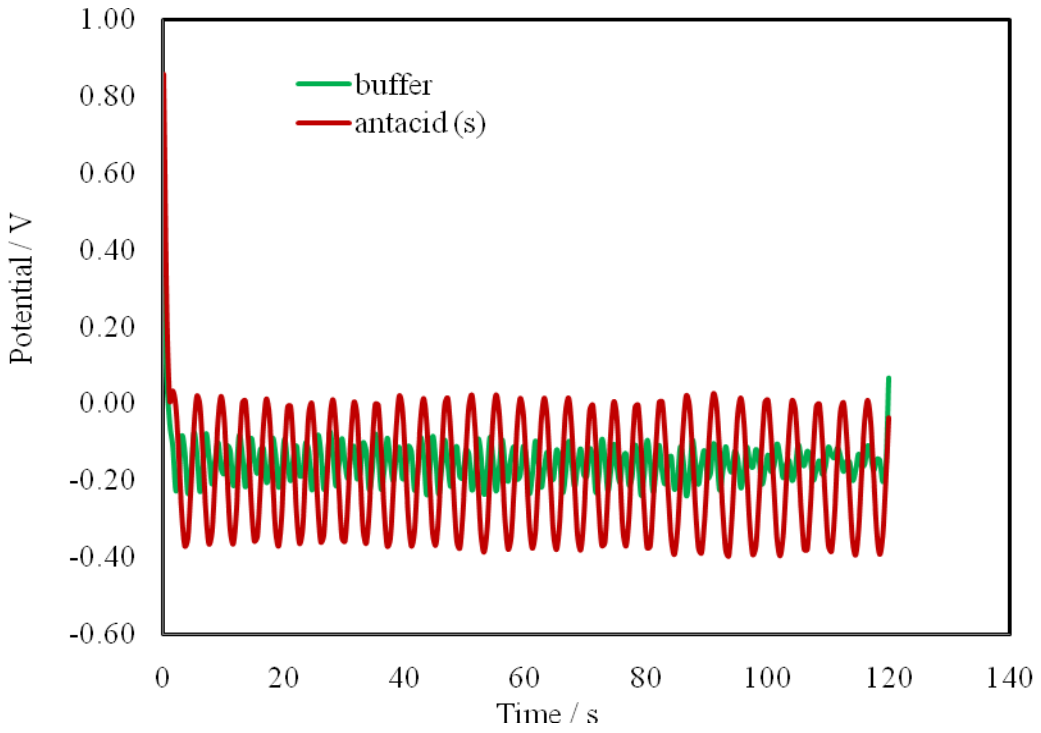

Figure 4.27: Electrochemical signal (OCP) obtained in "real" unbuffered samples for antacid using WO_3/GCE.

4.9. Repeatability and reproducibility measurement

To check the output response, stability, and repeatability of the electrode, the sample was tested three to four times in a PBS buffer solution with pH ranging from 3 to 11; the result is shown in (Figure 4.28). It was observed that the WO_3 NPs showed stable potentiometric response, excellent reproducibility, and good sensor stability. Similar tests have been obtained by Zaman et al. [50] work where author have modified CuO NFs on gold electrode.

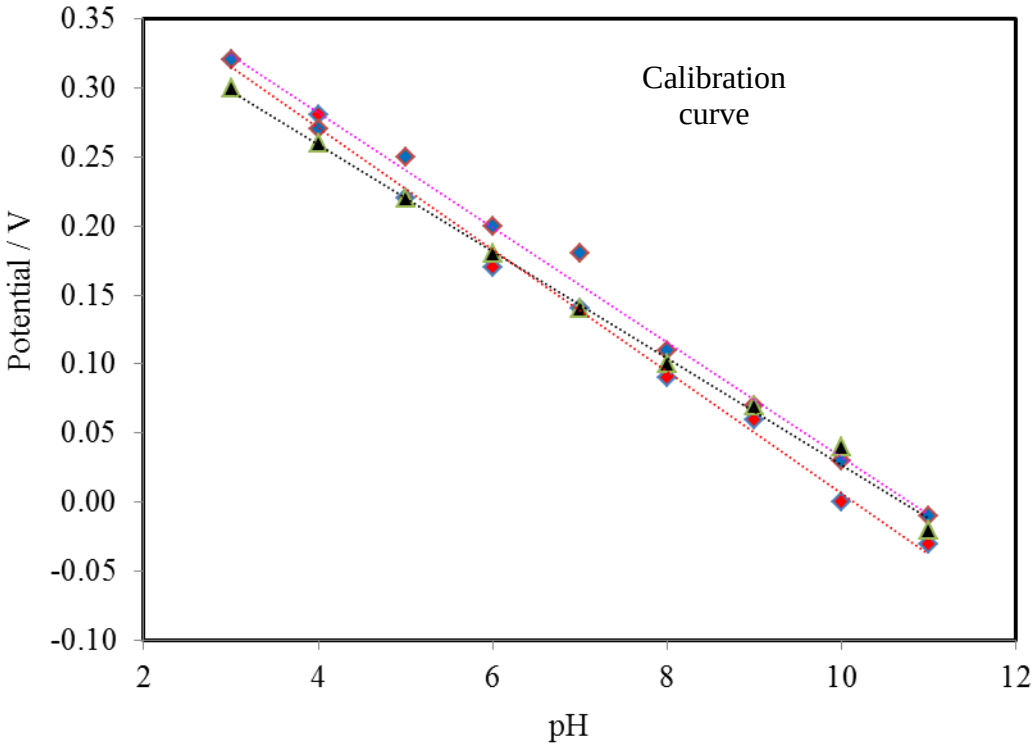

Figure 4.28: Repeatability and reproducibility test of three WO_3 NPs pH sensor electrodes at various pH buffer solutions.

4.10. Drift and stability measurement:

To determine the contribution the signal drift played, a SWV was recorded every 30 min for three hours in three buffer solutions with a pH of 5, 7 and 9. These solutions were chosen as representatives of the three states of the solutions: acidic, basic and neutral. The results are detailed in (Figure 4.29) which shows that the signal may be taken between 0 and 30 minutes to stabilize, depending on the pH. There was excellent precision thereafter. The drift of the potential reading in a neutral pH buffer was 33 mV within 3 hours. Similarly a potential drift of 24 mV was recorded in an acidic solution and 50 mV for a basic media. However even the response in pH 9 buffer, which exhibited the largest drift, only represents a 5 % deviation from the peak potential. To measure the stability, the signal was recorded up to 7 days thereafter, where sensitivity retained up to 95%.

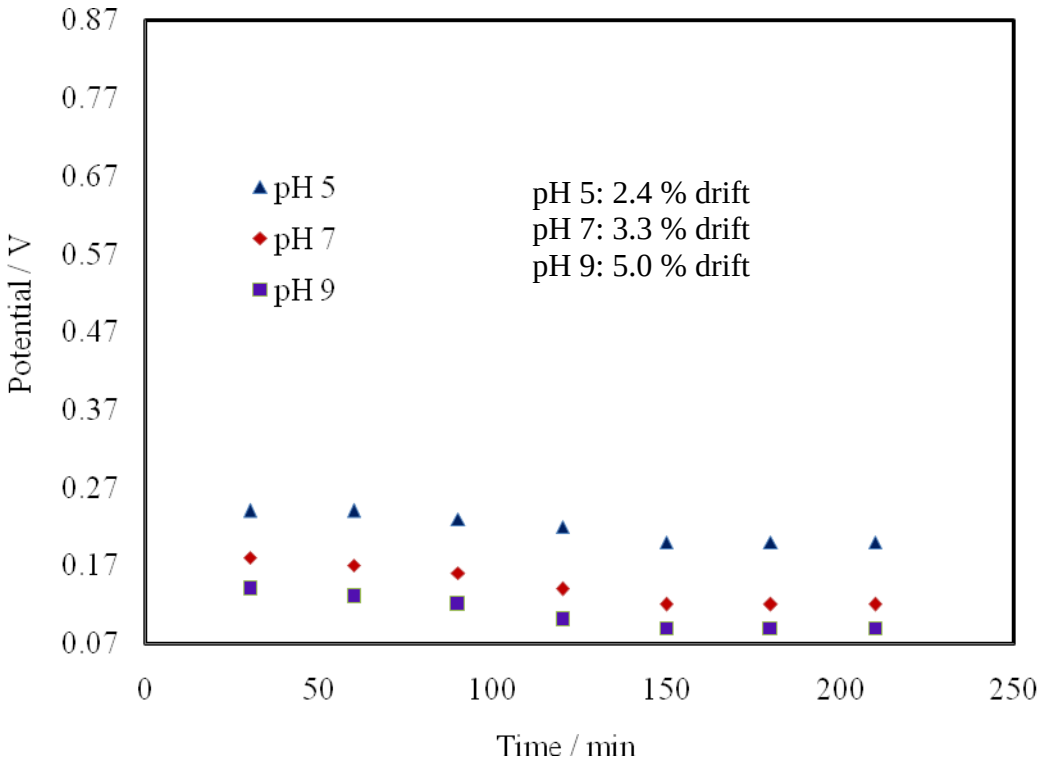

Figure 4.29: Electrode drift of WO_3 nanoparticle immobilized on the GCE; potential readings of pH 5, 7 and 9, signals have been taken every 30 min over period of 3 hours

Similar results have been obtained by Lidia et al. work, where author have modified WO_3 nano particle on gold electrode. However, the drift of this sensor has not been tested, along with oxygenated and deoxygenated environment. It is to note that, working on glassy carbon instead of gold may open up the door to develop WO_3 modified pH sensor based on graphite electrode [132], which is much cheaper compare to other electrodes. Sensitivity in this work compares favorable with recent reports tabulated in Table 1. To the best of our knowledge, no articles have demonstrated the use of WO_3 based GCE as sensing platform for detecting pH. We also have demonstrated stability, drift study on this system for pH detection. In addition, we would like to demonstrate in our further work pencil graphite and graphite electrode based on WO_3 for detecting pH.

Table 4.2: A comparison of different pH sensors

Electrode	Sensitivity V/pH	Drift %	pH range	Reference
GCE/WO_3 NPs	60 ± 0.01	2.4 - 5	3 - 11	This work
Gold /WO_3 NPs	−56.7 ± 1.3	_	5 - 9	[15]
AQ–Fc/AuNAE	70	1-3 %	2-11	[16]
Gold /CuO NFs	28	_	2-11	[50]
Thick Film/RuO_2	30	_	4-10	[91]
AQ–Fc/GCE	52	< 5	3 - 8	[139]
AQ–CNT/GCE	51	1.4	3 - 10	[140]
AQ– Sulfonate/GCE	38	2 – 3 mV	2 - 10	[141]

To the best of our knowledge no articles have demonstrated the use of GCE, using WO_3 nanoparticle as the sensor platform. The method described herein demonstrates how the WO_3/GCE could be utilized as a pH sensor with good stability and excellent sensitivity over a large pH range. The arrangement we described a low cost pH sensor than the cost of the nearest anthraquinone modified electrode. Although the use of AQ-FC on AuNAE exhibited more sensitivity but, there cost is very high.

In this study, we have developed a sensitive, selective and cost effective pH sensor using WO_3 nanoparticle. The results of electrochemical detection of pH indicate WO_3 nanocrystal exhibit high selectivity and sensitivity toward the redox reaction with pH solution. Our present study is important because it provides us a novel method for detection of pH by using metal oxides nanocrystal as sensing materials. The fabrication method and sensing material is very cheap and easy compares to the previously reported some sensing platform.

Chapter V

Conclusions

In summary, a novel pH sensor has been successfully fabricated using WO_3 nanoparticle as sensing materials in presence of chitosan and nafion. We have described a new, cost effective and sensitive sensor platform to detect pH.

In the present work, WO_3 nanoparticle has been synthesized using hydrothermal method. The resulting WO_3 nanostructures have been used here for the development of a pH sensor. The synthesized WO_3 nanocrystals obtained diffraction peaks are in accordance with the reported standard spectrum JCPDS, No. 02-0310. SEM-EDX, XRD and Raman spectra is used for the study of the morphology of the prepared WO_3 nanostructures. It can be inferred that the nanostructures appeared like as nanocrystal having an average particle size of 100 nm.

Excellent linearity has been found for pH detection using WO_3/GCE. The sensitivity of WO_3/GCE has been found to be 60 mV/pH and a potential drift of 2.4 – 5.0 % after three hours of continuous use. The sensor showed linearity range of pH 3 -11 and could retain 95% of its initial sensitivity after 1 week of use. We have also tested our sensor in the real samples and found to have excellent co-relation with the standard method. The electrode was found to respond both in the presence and absence of oxygen, further expanding the potential applications to include de-oxygenated environments.

Recommendations

Further work is needed to improve the pH sensor. Recommendations are as follows

- To enhance the stability and sensitivity.
- Fixing nanoparticle on GC electrode.
- Extensive fundamental electrochemical properties will be investigated.
- To drift free pH measurement.
- Check on pencil graphite electrode.

References

[1] Skoog, D. A., West, D. M., Holler, F. J., and Crouch, S. R., 2014, *"Fundamentals of Analytical Chemistry*", Belmont: Brooks/Cole, Cengage Learning. p. 1. ISBN 0-495-55832-X.

[2] Martin, C. R. and Mitchell, D. T., 1998, *"Nanomaterial's in* analytical *chemistry*". Anal. Chem., vol. 70, pp. 322-327.

[3] Nalwa, H. S., 1999, "*Handbook of nanostructured materials and nanotechnology".* San Diego Academic Press, vol. IV, pp. 621-629.

[4] Chang, S. Y., Liu, L. and Asher, S. A., 1994, *"Preparation and Properties of Tailored Morphology."* J. Am. Chem. Soc., vol.116 pp.6739-67344.

[5] Chan, W. C. W. and Nie, S., 1998, *"Quantum dot bio conjugates for ultrasensitive nonisotopic detection."* Science, vol. 281, pp. 2016-2018.

[6] Santra, S., Wang, K., Tapec, R. and Tan, W., 2001, *"Development of novel dye-doped silica nanoparticles for biomarker application."* J Biomed Opt., vol.6, pp. 160-166.

[7] Couvreur, P., Dubernet, C. and Puisieux, F., 1995, *"Polymeric drug nanoparticles prepared by an aerosol flow."* J. Eur. Pharm Biopharm., vol. 41, pp. 2-13.

[8] Tadros, T. F., 1993, *"Polymer lattices, Science and technology."* (Second Edition), Adv. Colloid Interface Sci. vol. 461, pp. 47-69.

[9] Jing, M., Li, W., Zhuang, Z. X., Chen, X. and Wang, X. R., 2002, *"Molecular Imprinting Science and Technology."* J. Chin. Sens. Act. vol. 5, pp. 263-275.

[10] Zhou, D. D., 2008, *"Microelectrodes for in-Vivo Determination of pH. In Electrochemical sensors, biosensors and their biomedical applications."* Academic Press, Inc. pp. 261-305.

[11] Fog, A. and Buck, R. P., 1984, *"Electronic semiconducting oxide as pH sensor."* Sens. Act. vol. 5, pp. 137 - 146.

[12] Bezbaruah, A. N. and Zang, T. C., 2002, *"Fabrication of anodically electrodeposited iridium oxide film pH microelectrodes for micro*

environmental studies." Anal. chem., vol. 74, pp. 5726.

[13] Vernardou, D., Drosos, H., Spanakis, E., Koudoumas, E., Savvakis, C. and Katsarakis, N., 2011, *"Electrochemical and Photo catalytic Properties of WO_3 Coatings Grown at Low Temperatures."* J. Mater. Chem., Vol. 21, pp.513.

[14] Natan, M. J., Mallouk, T. E. and Wrighton, M. S., 1987, *"pH-Sensitive WO_3-Based Micro electrochemical Transistors."* J. Phys. Chem., Vol. 91, pp. 648-654.

[15] Lidia, S., Joana, P. N., Ana, C., Daniela, N., Nuno, C., Isabel, M. F., Pedro, B., Luis, P., Jorge, S., Rodrigo, M. and Elvira, F., 2014, *"WO_3 Nanoparticle-Based Conformable pH Sensor."* ACS Appl. Mater. Interfaces, vol. 6, pp. 12226-12234.

[16] Louise, D., Mamun, J. and Kafil, M. R., 2013, *"Novel pH sensor based on anthraquinone-ferrocene modified free standing gold nanowire array electrode."* Anal. Methods, vol. 5, pp. 880-884.

[17] Miao, Y. and Chen, J. and Feng, K., 2005, *"New technology for the detection of pH."* J. Appl. Phys., vol. 44, pp. 4838-4832.

[18] Qing Y. cai, Craig A. Grimes, 2000 "A remote query Magneto elastic pH sensor", Grimes. Actuators B vol.62, 2000, pp. 121 – 130.

[19] http://www. springerlink.com/content/vt5q5873550n5472/fulltext.pdf

[20] Wilson, G. S. and Gifford, R., 2005, *"Biosensors for real-time in vivo measurements."* Biosens. Bioelectron, vol. 20, pp. 2388 - 2403.

[21] Eggins, B.R., 2008, *"Chemical Sensors and Biosensors (Google eBook),"* John Wiley & Sons

[22] Palchetti, I. and Mascini, M., 2012, *"Electrochemical Nanomaterial Based Nucleic Acid Aptasensors."*Anal. Chem., vol. 402, pp. 3103-3114.

[23] Adibi, M., Pirali, M. H. and Norouzi, P., 2011, *"Copper Nano-composite Potentiometric Sensor."* Int. J. Electrochem. Sci., vol. 6, pp.717-726.

[24] Silvester, D. S., 2011, *"Recent Advances in the use of Ionic Liquids for Electrochemical Sensing."* Analyst, vol. 136, pp. 4871-4882.

[25] Ni, Y. N. and Kokot, S., 2008, *"Does Chemometrics Enhance the Performance of Electro analysis."* Anal. Chim. Acta, vol. 626, pp. 130-146.

[26] Hernandez-Velez, M., 2006, *"Nanowires and 1D arrays fabrication: An overview."* Thin Solid Films, vol. 495, pp. 51-63.

[27] Yogeswaran, U. and Chen, S. M., *"Multi-walled carbon nanotubes with poly (methylene blue) composite film for the enhancement and separation of electro analytical responses of catecholamine and ascorbic acid."* Sens, Act. vol. 128, pp. 1016.

[28] Shie, J. W., Yogeswaran, U. and Chen, S. M., 2008, *"Electro analytical properties of cytochrome by direct electrochemistry on multi-walled carbon nanotubes incorporated with DNA bio composite film."* Talanta, vol. 74, pp. 1659-1669.

[29] Murray, R. W., 1984, *"Chemically Modified Electrodes,"* Electro anal. Chem., vol. 13, pp.191-368.

[30] Scott, S. N. S., Oyama, N. and Anson, F. C., 1980, J. Electro anal. Chem. vol. 110, pp. 303-307

[31] Wang, J. and Taha, Z., 1990, *"Catalytic oxidation and flow detection of carbohydrates at ruthenium dioxide modified electrodes."* Anal. Chem., vol. 62, pp. 1413-1416.

[32] Ugo, P. and Moretto, L. M., 1995, *"Environmental technology and green economy."* Electro anal. Chem., vol. 7, pp. 1105-1113.

[33] Oliveira, M. F., Mortimer, R. J. and Stradiotto, N. R., 1991, *"Electro oxidation and Determination of Dopamine Using a Nafion-Cobalt Hexacyanoferrate Film Modified Electrode."* J. Microchem., Vol. 64, pp.155-159.

[34] Alkire, R., Kolb, D. and Lipkowski, J., 2009, *"Chemically modified electrodes."* Germany: Wiley-VCH, Weinheim.

[35] Murray, R. W. and Albery, W. J., 1981, *"Modified Electrodes: Chemically Modified Electrodes for Electro catalysis."* The Royal Society, vol.302, pp.253-265.

[36] Orazio, D., 2003, *"Biosensors in clinical chemistry."* Clin. Chim. Acta, vol. 334, pp. 41-69.

[37] Durst, R., Baumner, A., Murray, R., Buck, R. and Andrieux, C., 1997, *"Chemically modified electrodes: Recommended terminology and*

definitions." IUPAC, pp. 1317-1323.

[38] Colorado State University Fort Collins Department of Chemistry, 1994, *"Chemically modified electrodes."* vol. 98, pp.5714-5720.

[39] Sanghav, B. and Srivastava, A., 2010. *"Simultaneous voltammetric determination of acetaminophen, aspirin and caffeine using an in situ surfactant-modified multiwalled carbon nanotube paste electrode."* Electrochim. Act. vol. 55, pp. 8638-8648.

[40] Krajewska, B., 2004, *"Application of chitin- and chitosan-based materials for enzyme immobilizations: a review,"* Enzyme Microbe. Technol., vol. 35, pp. 126-139.

[41] Heitner, W. C., 1996, *"Recent advances in perfluorinatedionomer membranes: structure, properties and applications.*" J. Membrane Science. vol. 120, pp. 1-33.

[42] https://en.wikipedia.org/wiki/Double layer (surface science).

[43] J. Wang, 2000, Anal. Electrochem. 2nd ed., Wiley-VCH, New York.

[44] Bagotsky, V. S., 2005, *"Fundamentals of Electrochemistry."* John Wiley & Sons.

[45] www.electrochemistry.co.kr/mall1/m mall detail. Php? Ps goid=259.

[46] Kissinger, P. T. and Heineman, W. R., 1983, *"Cyclic voltammetry,"* J. Chem. Educ., vol. 60, pp. 702-706.

[47] Kahlert, H., 2001, *"Reference electrodes, in Electro analytical Methods."* Scholz, F. (Ed.), Springer, AQ14Berlin=Heidelberg=New York, chap. III.

[48] Lovric, M., 2001, *"Square-wave voltammetry, in Electro analytical Methods,"* Scholz, F. (Ed.), Springer, Berlin=Heidelberg=New York, chap. II.

[49] http://www.gettyimages.com/detail/illustration/the-components-of-a-transmission-electron-microscope-stock-graphic/141483581.

[50] Zaman, S., 2011, *"CuO Nano flowers as an electrochemical pH sensor and the effect of pH on the growth."* J. Electro anal. Chem. vol. 662, pp. 421-425.

[51] Feng, G., Lun, W., Lijuan, T. and Changqing, Z., 2005, Springer-Verlag.

[52] Milica, J., Jonnathan, C. H. A. and Hubert, H., 2013, Giraulta, envirobot RTD.

[53] Zhenhua, B., Rui, C., Peng, S., Youju, H., Handong, S. and Dong, K. H., 2013, ACS Appl. Mater. Interfaces vol. 5, pp. 5856-5860.

[54] Kreider, K.G., Tarlov, M.J. and Cline, J. P., 1995, *"Sputtered thin-fi lm pH electrodes of platinum, palladium, ruthenium, and iridium oxides."* Sens. Act. vol. 28, pp. 167-172.

[55] Ges, I.A., Ivanov, B.L., Schaffer, D.K., Lima, F.A., Werdich, A.A. and Baudenbacher, F.J., 2005, *"Thin-film IrOx pH microelectrode for microfluidic-based microsystems. Biosens."* Bioelectron. vol. 21, pp. 248-256.

[56] Vonau, W., Enseleit, U., Gerlach, F. and Herrmann, S., 2004, Conceptions, materials, *"processing of miniaturized electrochemical sensors with planar membranes.''* Electrochim. Acta. vol. 49, pp. 3745-3750.

[57] Park, S., Boo, H., Kim, Y., Han, J., Kim, H.C. and Chung, T.D., 2005, *" pH-sensitive solid-state electrode based on electrodeposited nanoporous platinum.''* Anal. Chem. vol. 77, pp. 7695-7701.

[58] Pocrifka, L.A., Goncalves, C., Grossi, P., Colpa, P.C. and Pereira, E.C. 2006, *"Development of RuO_2ßTiO$_2$ (70ß30) mol% for pH measurements.''* Sens. Actuators B. vol. 113, pp. 1007-1012.

[59] Gac, A., Atkinson, J.K., Zhang, Z., Sexton, C.J., Lewis, S.M., Please, C.P. and Sion, R., 2004, "*Investigation of the fabrication parameters of thick film titanium oxide-PVC pH electrodes using experimental designs."* Microelectronics Int. vol. 21, pp. 44-53.

[60] Liu, C.C., Bocchicchio, B.C., Overmeyer, P.A. and Neuman, M.R., 1980, *"A palladium oxide miniature pH electrode."* Science. vol. 207, pp.188-192.

[61] Jones, R.D., Neuman, M.R., Sanders, G. and F.T. Cross, 1982, *"Miniature antimony pH electrodes for measuring gastro esophageal reflux."* Ann. Thoracic Surg., vol. 33, pp. 491-495.

[62] Yamamoto, K., Shi, G.Y., Zhou, T.S., Xu, F., Zhu, M., Liu, M., Kato, T., Jin, J.Y. and Jin, L.T. 2003, *"Solid state pH ultra micro sensor based on a*

tungstic oxide film fabricated on a tungsten nanoelectrode and its application to the study of endothelial cells." Anal. Chim. Acta. vol. 480, pp. 109117-109122.

[63] Eftekhari, A., 2003, *"pH sensor based on deposited fi lm of lead oxide on aluminum substrate electrode."* Sens. Actuators B. vol. 88, pp. 234-238.

[64] Li, Q., Luo, G. and Shu, Y. 2003, *"Response of nanosized cobalt oxide electrodes as pH sensors."* Anal. Chim. Acta. vol. 409, pp. 137-142.

[65] Pan, C.W., Chou, J.C., Sun, T.P. and Hsiung, S.K., 2005, *"Development of the real-time pH sensing system for array sensors."* Sens. Actuators B. vol. 108, pp. 870-876.

[66] Tsai, C.N., Chou, J.C., Sun, T.P. and Huiung, S.K., 2005, *"Study on the sensing characteristics and hysteresis effect of the tin oxide pH electrode."* Sens. Act. B, vol. 108, pp. 877-882.

[67] Yao, S., Wang, M. and Madou, M., 2001, *"A pH electrode based on melt-oxidized iridium oxide."* J. Electrochem. Soc. vol. 148, pp. 29-36.

[68] Marzouk, S.A., 2003, *"Improved electrodeposited iridium oxide pH sensor fabricated on etched titanium substrates."* Anal. Chem. vol. 75, pp. 1258-1266.

[69] Bezbaruah, A. and Zhang, T., 2002, *"Fabrication of anodically electrodeposited iridium oxide film pH microelectrodes for micro environmental studies."* Anal. Chem. vol. 74, pp.5726-5732.

[70] Wipf, D., Ge, F., Spaine, T. and Baur, J., 2000, *"Microscopic measurement of pH with iridium oxide microelectrodes."* Anal. Chem. vol. 72, pp. 4921-4927.

[71] Song, I., Fink, K. and Payer, J., 1998, *"Metal oxide/metal pH sensor: Effect of anions on pH measurements."* Corrosion. vol. 54.

[72] Arikawa, T., Takasu, Y., Murakami, Y., Asakura, K. and Iwasawa, Y. 1998, *"Characterization of the structure of RuO_2-IrO_2/Ti electrodes by exafs."* J. Phy. Chem. vol. 102(19), pp. 3736-3741.

[73] Ryynanen, T., Nurminen, K., Hamalainen, J., Leskela, M. and Lekkala, J., 2010, *"pH electrode based on ALD deposited iridium oxide, Procedia Engineering."* vol. 5, pp.548-552.

[74] Marzouk, S., Buck, R., Dunlap, L., Johnson, T. and Cascio, W., 2002, *"Measurement of extracellular pH, K (⁻), and lactate in ischemic heart."* Anal. Biochem. vol. 308, pp. 52- 60.

[75] VanHoudt, P., Lewandowski, Z. and Little, B., 1992, *"Iridium oxide pH microelectrode."* Biotechnol. Bioeng. vol. 40, pp. 601-608.

[76] Papeschi, G., Merigliano, S., Zaninotto, G., Baessato, M., Ancona, E. and Larini, M., 1984, *"The iridium/iridium oxide electrode for in vivo measurement of esophageal and gastric pH."* J. Med. Eng. Technol., vol. 8, pp. 221-227.

[77] Lu, Y., Wang, T., Cai, Z., Cao, Y., Yang, H. and Duan, Y.Y., 2009, *"Anodically electrodeposited iridium oxide films microelectrodes for neural micro stimulationandrecording",* Sens. Act. vol. 137, pp. 334-338.

[78] Quan, H., Kim, W., Chung, K. and Park, J., 2005, *"Surface renewable hydrogen ion-selective polymeric composite electrode containing iridium oxide",* Bulletin Korean Chemical Society, vol. 26, pp. 1565-1570.

[79] Bezbaruah, A.N. and Zhang, T.C., 2002, *"Fabrication of anodically electrodeposited iridium oxide film pH microelectrodes for micro environmental studies,"* Anal. Chem., vol. 74, pp. 5726-5733.

[80] Park, J., Kim, J. and Quan, H., 2010, *"A surface renewable iridium oxide-glass composite hydrogen ion electrode."* J. Micro. chem., vol. 95, pp. 102-106.

[81] Park, J. M., and Kim, J.Y., 2010, *"Surface Renewable Iridium Oxide-Glass or Ceramic Composite Hydrogen Ion Electrode."* US Patent App. vol. 12, pp. 791-795.

[82] Grant, S.A., Bettencourt, K., Krulevitch, P., Hamilton, J. and Glass, R., 2000, *"Development of fiber optic and electrochemical pH sensors to monitor brain tissue."* Crit. Rev. Biomed. Eng. vol. 28, pp. 159-163.

[83] Herlem, G., Lakard, B., Herlem, M. and Fahys, B., 2001, *"pH sensing at Pt electrode surfaces coated with linear poly ethylenimine from anodic polymerization of ethylenediamine."* J. Electrochem. Soc., vol. 148, pp.435-439.

[84] Santiago, K. S., Bartolome, A. J. and John, V. B. 1999, *"Electrochemically synthesized polymer-based pH sensors."* J. Philippine Sci., vol. 128, pp.

120-126.

[85] Michalska, A. and Maksymiuk, K., 2001, *"Counter-ion influence on polypyrrole potentiometric pH sensitivity."* Microchim. Acta, vol. 143, pp. 163-165.

[86] Mathias, M. F. and Haas, O., 1993, "*Effect of counter ion type on charge transport at redox polymer modified electrodes."* J. Phys. Chem., vol. 97, pp. 9217-9225.

[87] Robinson, K. L. and Lawrence, N. S., 2006, *"Redox-sensitive copolymer: A single-component pH sensor."* Anal. Chem., vol. 78, pp. 2450-2455.

[88] Vonau, W., Gabel, J. and Jahn, H. 2005, *"Potentiometric all solid-state pH glass sensors."* Electrochim. Acta, vol. 50, pp. 4981-4987.

[89] Yoon, H.J., Shin, J.H., Lee, S.D., Nam, H., Cha, G.S., Strong, T. D. and Brown, R.B., 2000, *"Solid-state ion sensors with a liquid junction-free polymer membrane-based reference electrode for blood analysis."* Sens. Actuators B. vol. 64, pp. 8-14.

[90] Martin, S., Ha, J., Kim, J., Strong, T., Cha, G. and Brown, R., 2004, *"ISE arrays with improved dynamic response and lifetime, in Tech. Digest of the Solid-State Sensor,"* Actuator, and Microsystems Workshop, pp. 396-399.

[91] Glance-Gostkiewicz, M., Sophocleous, M., Atkinson, J.K., Garcia-Breijo, E., 2012, *"Performance of miniaturized thick-film solid state pH sensors."* Published Elsevier Ltd.

[92] Kaden, H., Jahn, H. and Berthold, M., 2004, *"Study of the glass/polypyrrole interface in an all-solid-state pH sensor."* Solid State Ionics. vol. 169, pp. 129.

[93] Trojanowicz, M., 2003, *"Application of conducting polymers in chemical analysis."* Microchim. Acta. vol. 143, pp. 75-79.

[94] Zachara, J.E., Toczylowska, R., Pokrop, R., Zagorska, M., Dybko, A. and Wroblewski, W., 2004, *"Miniaturisedall-solid-state potentiometric ion sensors based on PVC-membranes containing conducting polymers."* Sens. Act. vol. 101, pp. 207-212.

[95] He, L. and Toh, C.S., 2006, *"Recent advances in analytical chemistry a material approach."* Anal. Chim. Acta. vol. 556, pp. 1-27.

[96] Bakker, E. and Pretsch, E., 2007, Modern potentiometry. Angewandte Chem. Int. Edition, vol. 46, pp. 5660-5664.

[97] Ngeontae, W., Xu, C., Ye, N., Wygladacz, K., Aeungmaitrepirom, W. and Tuntulani, T., 2007*, "Polymerized Nile Blue derivatives for plasticizer-free fluorescent ion optode microsphere sensors."* Anal. Chimica. Acta. vol. 599-605, pp. 124.

[98] Wygladacz, K. and Bakker, E., 2005, *"Imaging fiber microarray fluorescent ion sensors based on bulk optode microspheres."* Anal. Chimica. Acta. vol. 532, pp. 61.

[99] Wygladacz, K., Radu, A., Xu, C., Qin, Y. and Bakker, E., 2005, *"Fiber-Optic Micro sensor Array Based on Fluorescent Bulk Optode Microspheres for the Trace Analysis of Silver Ions."* Anal. Chem., vol. 77, pp. 4706.

[100] Xu, C., Wygladacz, K., Qin, Y., Retter, R., Bell, M. and Bakker, E., 2005, *"Microsphere optical ion sensors based on doped silica gel templates."* Anal. Chimica. Acta. vol. 537, pp. 135.

[101] Lakard, B., Herlem, G., Labachelerie, D. M., Daniau, W. and Martin, G., 2004*, "Miniaturized pH biosensors based on electrochemically modified electrodes with biocompatible polymers."* Biosensors and Bioelectronics, vol. 19, pp. 595-606.

[102] Lakard, B., Herlem, G., Lakard, S., Guyetant, R. and Fahys, B., 2005, *"Potentiometric pH sensors based on electrodeposited polymers."* Polymer, vol. 46, pp. 12233.

[103] Malkaj, P., Dalas, E., Viteratos, E. and Sakkopoulos, S., 2006, *"pH electrodes constructed from polyaniline/zeolite and polypyrrble/zeolite conductive blends."* J. Applied Polymer Sci., vol. 101, pp. 1853.

[104] Lakard, B., Segut, O., Lakard, S., Herlem, G. and Gharbi, T., 2007, *"Potentiometric miniaturized pH sensors based on polypyrrole films."* Sensors and Actuators B., vol. 122, pp. 101.

[105] Flavia, E. G., Jamie, P. S., Sophie, I. K., Dimitrios, K. K., Iniesta, I., Graham, C. S., Juliano, A. B. and Craig, E. B., 2015, *"Graphite Screen-Printed Electrodes Applied for the Accurate and Reagent less Sensing of pH."* Anal. Chem, vol. 87, pp. 11666-11672.

[106] Urban, G., Jobst, G., Keplinger, F., Aschauer, E., Tilado, O. and Fasching, R., 1992, *"Miniaturized multi enzyme biosensors integrated with pH sensors on flexible polymer carriers for in vivo applications." Biosensors & Bioelectronics,* vol. 7, pp. 733-739.

[107] Ruan, C., Ong, K. G., Mungle, C., Paulose, M., Nickl, N. J. and Grimes, C. A., 2003, *"A wireless pH sensor based on the use of salt-independent micro-scale polymer spheres."* Sen. Act., vol. 96, pp. 61-69.

[108] Mathison, S. and Bakker, E., 1999, *"Renewable pH cross-sensitive potentiometric heparin sensors within corporated electrically charged* H^+ *ionophores."* Anal. Chem., vol. 71, pp. 4614-4621.

[109] Rundle, C., 2005, *"A Beginner's Guide to Ion-Selective Electrode Measurements."* http://www.nico2000.net/ Book/Guide1.html

[110] Wipf, D., Ge, F., Spaine, T. and Baur, J., 2000*, "Microscopic measurement of pH with iridium oxide microelectrodes."* Anal. Chem. vol. 72, pp. 4921-4927.

[111] Ges, I.A., Ivanov, B.L., Schaffer, D.K., Lima, F.A., Werdich, A.A. and Baudenbacher, F.J., 2005, *"Thin-fi lm IrOx pH microelectrode for microfluidic-based microsystems."* Biosens. Bioelectron. vol. 21, pp. 248-256.

[112] Buck, R.P., Rondinini, S., Covington, A.K., Baucke, F.G., Brett, C.M., Camoes, M.F., Milton, M.J., Mussini, T., Naumann, R., Pratt, K.W., Spitzer, P. and Wilson, G.S., 2002, *"The measurement of pH definition, standards and procedures (IUPAC Recommendations 2002)."* Pure Appl. Chem., vol. 74, pp. 2169-2200.

[113] Pandolfino, J.E., Ghosh, S., Zhang, Q., Heath, M., Bombeck, T. and Kahrilas, P.J., 2006, Slimline vs. glass pH electrodes: what degree of accuracy should we expect? Alimentary Pharmacol. & Therapeutics, vol. 23, pp. 331-340.

[114] Park, S., Boo, H., Kim, Y., Han, J., Kim, H.C. and Chung, T.D., 2005, *"pH-sensitive solid-state electrode based on electrodeposited nonporous platinum."* Anal. Chem. Vol. 77, pp. 7695-7701.

[115] Li, Q., Luo, G. and Shu, Y. 2000, *"Response of nanosized cobalt oxide electrodes as pH sensors."* Anal. Chim. Acta. vol. 409, pp. 137-142.

[116] Yuen, T., Agnew, W., Bullara, L. and McCreery, D., 1990, "Biocompatibility of electrodes and materials in the central nervous system, in Neural Prostheses: Fundamental Studies (W. Agnew and D. McCreery, eds), pp. 171-321.

[117] Guth, U., Oelbner, W. and Vonau, W., 2001, *"Investigation of corrosion phenomena on chemical micro sensors."* Electrochim. Acta. vol. 47, pp. 201-210.

[118] Frost, M. C., Batchelor, M. M., Lee, Y., Zhang, H., Kang, Y., Oha, B., Wilson, G. S., Gifford, R., Rudich, S. M. and Meyerhoff, M. E., 2003, *"Preparation and characterization of implantable sensors with nitric oxide release coatings."* J. Microchem. vol. 74, pp. 277-288.

[119] W. Oelbner, J. Zosel, U. Guth, T. Pechstein, W. Babel, J. G. Connery, C. Demuth, M. G. Gansey, and J. B. Verburg, 2005, *"Encapsulation of ISFET sensor chips."* Sens. Act. 105, 104-117.

[120] Goicoechea, J., Zamarreno, C. R., Matıas, I. R. and Arregui, F. J. 2009, *"Optical fiber pH sensors based on layer-by-layer electrostatic self-assembled Neutral Red"*, Elsevier.

[121] Ayad, M. M., Salahuddin, N. A., Alghaysh., M. O. and Issa, R. M., 2010, *Phosphoric acid and pH sensors based on polyanniline films.*, Current App. Phy., vol. 10, pp. 235-240.

[122] Norman, F. S., Matthew, J. L., Phlip, M. N. and Shaun, A. F., 1994, *"Micro fabricated conductimetric pH sensor"*, Elsevier.

[123] Wen, D. H., Hung C., Sanchali, D., Mu, C and Chiao, J.C., 2011, *"A flexible pH sensor based on the iridium oxide sensing film."* Sens. Act. vol. 169, pp. 1–11

[124] Corres, J.M., Arregui, F.J., Matías, I.R. and Rodríguez, Y., 2013, "*High Sensitivity Optical Fiber pH Sensor using poly(acrylic acid) nanofibers.*" vol. 978, pp.4642-4673

[125] Andrej, D. Jamornmarn, G., Hayssam, E. H. and Kohn, E., 2007, "*pH sensor on O-terminated diamond using boron-doped channel*," Diamond and Related Materials., vol. 16, pp. 905-910

[126] Qingyun, C., Kefeng, Z., Chuanmin, R., Tejal, A. D. and Craig, A. G. 2004, *"A Wireless, Remote Query Glucose Biosensor Based on a pH-Sensitive Polymer."* Anal. Chem. vol. 76, pp. 4038-4043.

[127] Ahmadi, M., Younesi, R. and Guinel, M., *"Synthesis of Tungsten Oxide Nanoparticles using a Hydrothermal Method at Ambient Pressure."*

[128] Elizabeth, I., Ross, M. and Israel, E. W., 2007, *"Structural Determination of Bulk and Surface Tungsten Oxides with UV-vis Diffuse Reflectance Spectroscopy and Raman Spectroscopy."* J. Phys. Chem., vol. 111, pp. 15089-15099

[129] Liu, S., Yu, B. and Zhang, T., 2013, Corresponding pore volume distribution, Electrochim. Acta. vol. 102, pp. 104-107.

[130] Xingyou, L., Akihiko H., Takeshi F. and Mingwei, C., 2011, WPI Advanced Institute for Materials Research, Tohoku University, Sendai., vol. 309, pp. 980-8577.

[131] Harris, D. C., 2010, *"Quantitative Chemical Analysis,"* WH Freeman and Company, New York, 8th ed.

[132] Flavia, E. G., Jamie, P. S., Sophie, I. K., Dimitrios, K. K., Iniesta, I., Graham, C. S., Juliano, A. B. and Craig, E. B., 2015, *"Graphite Screen-Printed Electrodes Applied for the Accurate and Reagent less Sensing of pH."* Anal. Chem, vol. 87, pp. 11666-11672.

[133] Lee, S. H., Je, M., Cheong, H. M., Ozkan, E., Tracy, E. C. and Deb, S. K., 2003, *"Effect of crystallinity on Electrochromic Mechanism of LixWO_3 Thin Films."* Solid State Ionics, Vol. 156, pp. 447-452.

[134] Lampert, C. M., 1984, *"Electrochromic Materials and Devices for Energy Efficient Windows."* Sol Energy Mater, vol. 11, pp. 1-27.

[135] Hotchandani, S., Bedja, I., Fessenden, R. and Kamat, P., 1994, *"Electrochromic and Photoelectrochromic Behavior of Thin WO_3 Films Prepared from Quantum Size Colloidal Particles."*Langmuir, Vol. 10, pp. 17-22.

[136] Zhou, D. D., 2008, "*Microelectrodes for in-Vivo Determination of pH. In Electrochemical sensors, biosensors and their biomedical applications,"* Academic Press, Inc., pp. 261−305.

[137] Lu, M. and Compton, R. G., 2014, *"Voltammetric pH sensing using carbon electrodes: glassy carbon behaves similarly to EPPG."* Analyst, vol. 139, pp. 2397-2403.

[138] Lu, M., Compton, R. G., 2014, *Voltammetric pH sensing using carbon electrodes: glassy carbon behaves similarly to EPPGA.* Analyst, vol. 139, pp. 4599-4605.

[139] Lafitte, G. H., Wang, W., Yashina, A. S. and Lawrence, N. S., 2008, Electrochem. Commun, vol. 10, pp. 1831-1834.

[140] Kumar, A. S. and Swetha, P., 2011, "*Colloids and surfaces a physicochemical and engineering aspects."* Colloids Surf, A, vol. 384, pp. 597-604.

[141] Shiu, K. K., Song, F. and Dai, H. P., 1996, "*Potentiometric pH sensor with anthraquinone sulfonate adsorbed on glassy carbon electrodes."* Electro analysis, vol. 8, pp. 1160-1164.